



HÁSKÓLI ÍSLANDS

Geology and internal structure of Lambafell Quality assessment and volume of basaltic volcanic glass

Þóunn Kara Valdimarsdóttir, Ármann Höskuldsson, William M. Moreland, Børge Johannes Wigum, Björn Davíð Þorsteinsson, Birta Dís Jónsdóttir Blöndal, Lidia Stroganova, Jacqueline Grech Licari

Done for Hornsteinn ehf.



HÍ

JARÐVÍSINDASTOFNUN

Geology and internal structure of Lambafell

Quality assessment and volume of basaltic volcanic glass

Iðunn Kara Valdimarsdóttir, Ármann Höskuldsson, William M. Moreland, Børge Johannes Wigum, Björn Davíð Þorsteinsson, Birta Dís Jónsdóttir Blöndal, Lidia Stroganova, Jacqueline Grech Licari

Done for Hornsteinn ehf.

Institute of Earth Sciences, University of Iceland.

School of Engineering and Natural Sciences

2024

Geology and internal structure of Lambafell:
Quality assessment and volume of basaltic volcanic glass

Report done for Hornsteinn ehf.

Copyright © 2024 Iðunn Kara Valdimarsdóttir, Ármann Höskuldsson, William M. Moreland, Børge Johannes Wigum, Björn Davíð Þorsteinsson, Birta Dís Jónsdóttir Blöndal, Lidia Stroganova, and Jacqueline Grech Licari
This report is not to be copied without permission from authors.

All rights reserved.

Institute of Earth Sciences
School of Engineering and Natural Sciences
University of Iceland
Sturlugata 7
101 Reykjavík

Tel.: 525 4700

Orcid: <https://orcid.org/0009-0000-6785-0251>

Filing information:

Valdimarsdóttir, I. K., Höskuldsson, Á., Moreland, W. M., Wigum, B. J., Þorsteinsson, B. D., Jónsdóttir Blöndal, B. D., Stroganova, L., & Grech Licari, J. 2024. Geology and internal structure of Lambafell: Quality assessment and volume of basaltic volcanic glass

Institute of Earth Sciences, School of Engineering and Natural Sciences,
University of Iceland, 112 p.

ISBN 978-9935-9664-2-1

Publisher: University of Iceland, Institute of Earth Sciences
Reykjavík, February 2024

Contents

Contents.....	4
1 Introduction	11
Formation of subglacial hyaloclastite mountains	12
2 Methods	15
Aerial and Lidar mapping.....	15
3D modelling and volume estimations	15
Ground penetrating radar	16
Boreholes	17
Sample preparation	18
Microscopy	18
3 General geology.....	19
4 Composition of Lambafell.....	21
Microscopy	21
Borehole 4 – BH4 (0-87 m)	21
Borehole 5 – BH5 (0-51 m)	51
Borehole 6 - BH6 (0-60 m).....	70
5 Geological interpretations of Lambafell	92
Cross sections through Lambafell.....	96
Ground Penetrating Radar.....	99
Geological map of Lambafell	100
7 Volume estimates of geological units in Lambafell.....	102
8 Discussion and summary of results.....	104
References.....	106
Appendix	109
Drill logs.....	109

List of Figures:

Figure 1 Location of Lambafell	12
Figure 2 Solubility of water in basaltic magma at Reykjanes.....	13
Figure 3 Schematic figure of the five phases in a subglacial eruption	14
Figure 4 Location of boreholes four to six	17
Figure 5 Glass slides prepared for microscopy	18
Figure 6 Sample BH4-1, 1 mm	22
Figure 7 Sample BH4-1, <1 mm.....	22
Figure 8 Sample BH4-2, 1 mm	23
Figure 9 Sample BH4-2, <1 mm.....	23
Figure 10 Sample BH4-3, 1 mm.....	24
Figure 11 Sample BH4-3, <1 mm.....	24
Figure 12 Sample BH4-4, 1 mm.....	25
Figure 13 Sample BH4-4, <1 mm.....	25
Figure 14 Sample BH4-5, 1 mm.....	26
Figure 15 Sample BH4-5, <1 mm.....	26
Figure 16 Sample BH4-6, 1 mm.....	27
Figure 17 Sample BH4-6, <1 mm.....	27
Figure 18 Sample BH4-7, 1 mm.....	28
Figure 19 Sample BH4-7, <1 mm.....	28
Figure 20 Sample BH4-8, 1 mm.....	29
Figure 21 Sample BH4-8, <1 mm.....	29
Figure 22 Sample BH4-9, 1 mm.....	30
Figure 23 Sample BH4-9, <1 mm.....	30
Figure 24 Sample BH4-10, 1 mm.....	31
Figure 25 Sample BH4-10, <1 mm.....	31
Figure 26 Sample BH4-11, 1 mm.....	32
Figure 27 Sample BH4-11, <1 mm.....	32
Figure 28 Sample BH4-12, 1 mm.....	33

Figure 29 Sample BH4-12, <1 mm.....	33
Figure 30 Sample BH4-13, 1 mm.....	34
Figure 31 Sample BH4-13, <1 mm.....	34
Figure 32 Sample BH4-14, 1 mm.....	35
Figure 33 Sample BH4-14, <1 mm.....	35
Figure 34 Sample BH4-15, 1 mm.....	36
Figure 35 Sample BH4-15, <1 mm.....	36
Figure 36 Sample BH4-16, 1 mm.....	37
Figure 37 Sample BH4-16, <1 mm.....	37
Figure 38 Sample BH4-17, 1 mm.....	38
Figure 39 Sample BH4-17, <1 mm.....	38
Figure 40 Sample BH4-18, 1 mm.....	39
Figure 41 Sample BH4-18, <1 mm.....	39
Figure 42 Sample BH4-19, 1 mm.....	40
Figure 43 Sample BH4-19, <1 mm.....	40
Figure 44 Sample BH4-20, 1 mm.....	41
Figure 45 Sample BH4-20, <1 mm.....	41
Figure 46 Sample BH4-21, 1 mm.....	42
Figure 47 Sample BH4-21, <1 mm.....	42
Figure 48 Sample BH4-22, 1 mm.....	43
Figure 49 Sample BH4-22, <1 mm.....	43
Figure 50 Sample BH4-23, 1 mm.....	44
Figure 51 Sample BH4-23, <1 mm.....	44
Figure 52 Sample BH4-24, 1 mm.....	45
Figure 53 Sample BH4-24, <1 mm.....	45
Figure 54 Sample BH4-25, 1 mm.....	46
Figure 55 Sample BH4-25, <1 mm.....	46
Figure 56 Sample BH4-26, 1 mm.....	47
Figure 57 Sample BH4-26, <1 mm.....	47

Figure 58 Sample BH4-17, 1 mm.....	48
Figure 59 Sample BH4-27, <1 mm.....	48
Figure 60 Sample BH4-29, 1 mm.....	49
Figure 61 Sample BH4-29, <1 mm.....	49
Figure 62 Sample BH5-1, 1 mm.....	52
Figure 63 Sample BH5-1, <1 mm.....	52
Figure 64 Sample BH5-2, 1 mm.....	53
Figure 65 Sample BH5-2, <1 mm.....	53
Figure 66 Sample BH5-3, 1 mm.....	54
Figure 67 Sample BH5-3, <1 mm.....	54
Figure 68 Sample BH5-4, 1 mm.....	55
Figure 69 Sample BH5-4, <1 mm.....	55
Figure 70 Sample BH5-5, 1 mm.....	56
Figure 71 Sample BH5-5, <1 mm.....	56
Figure 72 Sample BH5-6, 1 mm.....	57
Figure 73 Sample BH5-6, <1 mm.....	57
Figure 74 Sample BH5-7, 1 mm.....	58
Figure 75 Sample BH5-7, <1 mm.....	58
Figure 76 Sample BH5-8, 1 mm.....	59
Figure 77 Sample BH5-8, <1 mm.....	59
Figure 78 Sample BH5-9, 1 mm.....	60
Figure 79 Sample BH5-9, 1 mm.....	60
Figure 80 Sample BH5-10, 1 mm.....	61
Figure 81 Sample BH5-10, <1 mm.....	61
Figure 82 Sample BH5-11, 1 mm.....	62
Figure 83 Sample BH5-11, <1 mm.....	62
Figure 84 Sample BH5-12, 1 mm.....	63
Figure 85 Sample BH5-12, <1 mm.....	63
Figure 86 Sample BH5-13, 1 mm.....	64

Figure 87 Sample BH5-13, <1 mm.....	64
Figure 88 Sample BH5-14, 1 mm.....	65
Figure 89 Sample BH5-14, <1 mm.....	65
Figure 90 Sample BH5-15, 1 mm.....	66
Figure 91 Sample BH5-15, <1 mm.....	66
Figure 92 Sample BH5-16, 1 mm.....	67
Figure 93 Sample BH5-16, <1 mm.....	67
Figure 94 Sample BH5-17, 1 mm.....	68
Figure 95 Sample BH5-17, <1 mm.....	68
Figure 96 Sample BH6-1, 1 mm.....	71
Figure 97 Sample BH6-1, <1 mm.....	71
Figure 98 Sample BH6-2, 1 mm.....	72
Figure 99 Sample BH6-2, <1 mm.....	72
Figure 100 Sample BH6-3, 1 mm.....	73
Figure 101 Sample BH6-3, <1 mm.....	73
Figure 102 Sample BH6-4, 1 mm.....	74
Figure 103 Sample BH6-4, <1 mm.....	74
Figure 104 Sample BH6-5, 1 mm.....	75
Figure 105 Sample BH6-5, <1 mm.....	75
Figure 106 Sample BH6-6, 1 mm.....	76
Figure 107 Sample BH6-6, <1 mm.....	76
Figure 108 Sample BH6-7, 1 mm.....	77
Figure 109 Sample BH6-7, <1 mm.....	77
Figure 110 Sample BH6-8, 1 mm.....	78
Figure 111 Sample BH6-8, <1 mm.....	78
Figure 112 Sample BH6-9, 1 mm.....	79
Figure 113 Sample BH6-9, <1 mm.....	79
Figure 114 Sample BH6-10, 1 mm.....	80
Figure 115 Sample BH6-10, <1 mm.....	80

Figure 116 Sample BH6-11, 1 mm.....	81
Figure 117 Sample BH6-11, <1 mm.....	81
Figure 118 Sample BH6-12, 1 mm.....	82
Figure 119 Sample BH6-12, <1 mm.....	82
Figure 120 Sample BH6-13, 1 mm.....	83
Figure 121 Sample BH6-13, <1 mm.....	83
Figure 122 Sample BH6-14, 1 mm.....	84
Figure 123 Sample BH6-14, <1 mm.....	84
Figure 124 Sample BH6-15, 1 mm.....	85
Figure 125 Sample BH6-15, <1 mm.....	85
Figure 126 Sample BH6-16, 1 mm.....	86
Figure 127 Sample BH6-16, <1 mm.....	86
Figure 128 Sample BH6-17, 1 mm.....	87
Figure 129 Sample BH6-17, <1 mm.....	87
Figure 130 Sample BH6-18, 1 mm.....	88
Figure 131 Sample BH6-18, <1 mm.....	88
Figure 132 Sample BH6-19, 1 mm.....	89
Figure 133 Sample BH6-19, <1 mm.....	89
Figure 134 Sample BH6-20, 1 mm.....	90
Figure 135 Sample BH6-20, <1 mm.....	90
Figure 136 A drone image of subglacial tuff in the Björgun quarry.....	93
Figure 137 Steeply dipping pillow breccia in Björgun quarry.....	94
Figure 138 A drone image of the Björgun quarry.....	94
Figure 139 A drone image of the Eden quarry.....	95
Figure 140 A drone image of the Eden quarry face.....	95
Figure 141 A drone image of the west side of Lambafell.....	96
Figure 142 A map showing the five profiles through Lambafell.....	97
Figure 143 A schematic showing a cross-section through borehole BH4.....	98
Figure 144 A schematic showing a cross-section through borehole BH5.....	98

Figure 145 A schematic showing a cross-section through borehole BH6	98
Figure 146 A schematic showing a cross-section through Björgun quarry.....	99
Figure 147 A schematic showing a cross-section through Eden quarry.....	99
Figure 148 A geological map of the studied area of Lambafell.....	101
Figure 149 A 3D model of the hyaloclastite and overlying breccia and lava.....	103

List of Tables:

Table 1 The main findings in BH4 in Lambafell	50
Table 2 The main findings in BH5 of Lambafell.....	69
Table 3 The main findings in BH6 of Lambafell.....	91
Table 4 Estimated volume of the geological units of Lambafell.....	103
Table 5 Drill log from BH4 in Lambafell	109
Table 6 Drill log from BH5 in Lambafell	111
Table 7 Drill log from BH6 in Lambafell	112

1 Introduction

Many volcanoes are either partially or entirely covered by glaciers. Eruptions at these volcanoes can be catastrophic due to explosive water-magma reaction and rapid melting of ice, forming devastating floods or “jökulhlaups”. During last century, at least 64 eruptions occurred associated with glaciers and/or thick snow cover, 20 of which occurred during the latter half of that century (Thorarinsson, 1975; Major and Newhall, 1989; Gudmundsson and Björnsson, 1991; Hoskuldsson and Sparks, 1997; Hoskuldsson et al., 2007). Volcan Hudson in southern Chile erupted in 1971 and 1991. In these eruptions, the glacier filling the Hudson caldera partly melted and caused flooding of the valley of Rio de los Huemules (Best, 1992). A thick glacier covers both the volcanoes Grímsvötn and Katla, in Iceland. Both volcanoes have erupted several times during the past 1000 years (Thorarinsson, 1974; Thordarson and Hoskuldsson, 2008), causing colossal jökulhlaups on the plains of Skeiðará and Mýrdalssandur.

In high latitudes, volcanic units entirely made of pillow lava and/or hyaloclastites (volcanic glass) are frequently observed. These units were erupted during periods of glaciation and display evidence of intrusion into ice and or reaction between erupted magma and meltwater (Noe-Nyegaard, 1940; Kjartansson, 1943; Sigvaldason, 1968; Baker, 1969; Hoskuldsson and Sparks, 1997; Hoskuldsson et al., 2007).

Landforms built during subglacial eruptions typically have much higher aspect ratios (H/L) than their subaerial equivalents. For example, fissure vents erupting under subaerial conditions form extensive thin lava flows, whereas subglacial eruptions typically pile up a linear ridge of pillow lava and/or hyaloclastites. Such subglacial ridges are tens to hundreds of meters high (H) and extend laterally (L) distances of some hundreds of meters to a few kilometers. Similarly, in a basaltic point-source eruption, steep-sided table mountains are results of subglacial eruptions, whereas gently sloping lava shields form in subaerial eruptions. The difference in the landforms relates to several factors. Factors such as restraining influence of ice, more effective cooling, creation of an ice-bounded water cavity or lake and explosive water–magma interactions (Pjetursson, 1900; Noe-Nygaard, 1940; Kjartansson, 1943; Carslaw and Jaeger, 1959; Sigvaldason, 1968; Jones, 1969; Solomon, 1969; Jones, 1970; Sæmundsson, 1970; Allen, 1980; Moore and Calk, 1991; Hoskuldsson and Sparks, 1997; Hoskuldsson et al., 2007).

This report analyzes the subglacial formation and building blocks in the Lambafell mountain in Reykjanes, Iceland (Figure 1). Detailed geological mapping of hyaloclastite mountains, such as Lambafell, is difficult due to a very dynamic emplacement environment and lack of internal exposure.

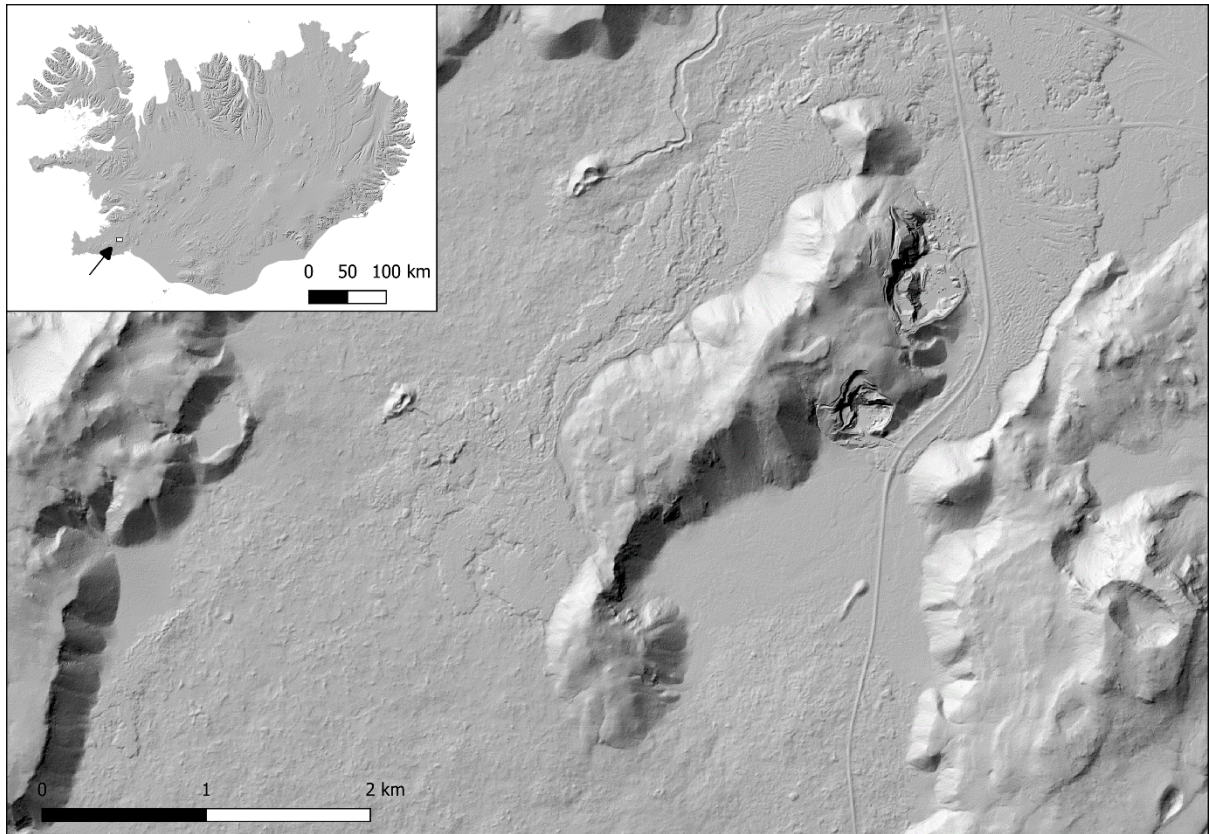


Figure 1 Location of Lambafell, in the area named Þrengsli, SW Iceland. The digital elevation model (DEM) is sourced from Landmælingar Íslands but is supplemented with our lidar data of the quarries (from summer 2022).

Formation of subglacial hyaloclastite mountains

The generation of the building blocks in hyaloclastite mountains depends on the type of magma being erupted. Magma erupted in Iceland has a composition from basalt to rhyolite. The amount of magmatic water is of prime importance, independent of the magma composition. Thus, magma that is undersaturated in magmatic water will form solid lava units, while magma that is saturated with magmatic water, will start releasing water and fragmenting once in contact with the melt water. That process forms volcanic glass, that these mountains take their name from, hyaloclastite (meaning glassy particles). Water saturation of magmas is pressure dependent (Figure 2). Basaltic magmas generally contain less water than rhyolitic magmas. Therefore, the fragmentation process takes place closer to the surface in basaltic eruption, than in rhyolitic eruptions.

Solubility of H₂O in Reykjanes basalt at 1150°C

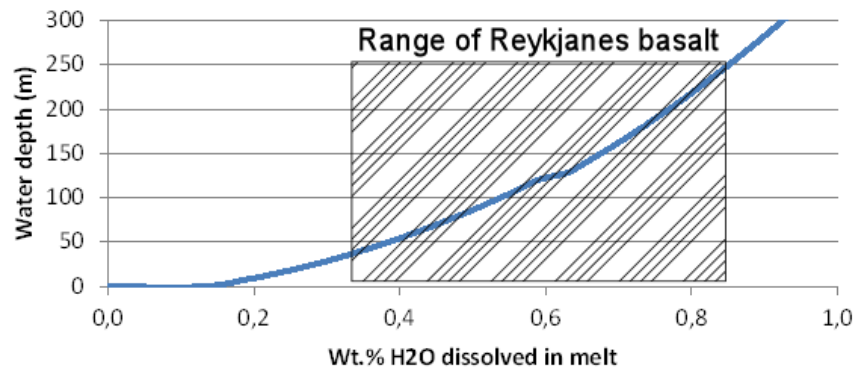


Figure 2 Solubility of water in basaltic magma at Reykjanes, Iceland. Magma with water concentrations above the line does not engage in explosive water-magma interaction, those magmas form pillow lava, but below the line indicates that explosive water-magma interaction takes place. In case of an eruption the descending line would be straight down. Hence, when magma crosses the pressure threshold indicated by the line, explosive interactions begin. The diagram gives an idea of what should be the minimum thickness of the glassy/tuffaceous material.

An idealized subglacial eruption is composed of five main building blocks (Figure 3). The first unit to form is pillow lavas and melt water, however, the pressure conditions need to be such that the magmatic water does not escape from the magma. In basaltic eruption at Reykjanes the confining pressure ranges from the equivalent of 200 to 300 m of water. Once magma reaches water saturation, explosive water magma interaction begins. During this phase glassy fragments form. This second phase in the eruption will last until the accumulations of the erupted material have reached well above the water table. At the water-atmosphere intersection the basaltic glassy material will travel through the atmosphere before coming to rest. This third phase will form well-layered tephra sequences, composed of material falling through the air and material flowing along the surface, of the mountain in making. Once water insulates from the magma, in this steadily growing mountain, explosive activity ceases and effusive lava forms. This is the fourth phase in the eruption, during which lava covers the top of the formation. During this phase, lava that flows off the top, forms lava deltaic breccia on the slopes of the mountain and can increase its areal coverage considerably. In fissure eruptions geological formation formed in phases three and four are interlayered, since not all eruptive vents dry out at the same time. The final fifth phase, in the mountain building, forms after the eruption ceases and the glacier comes back to the newly built mountain. At that time, erosion begins, and glacial deposition takes place, leaving behind glacial sediments on the sides and top of the formation.

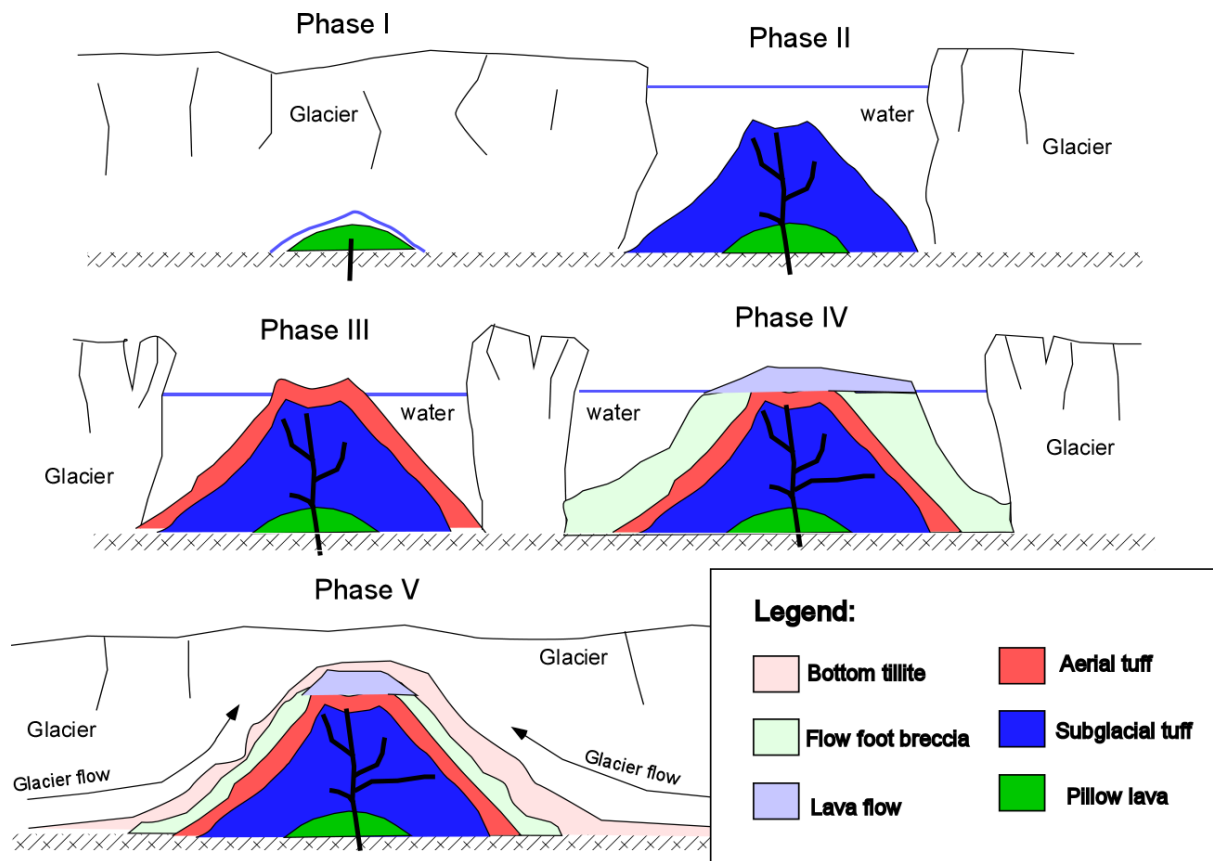


Figure 3 Schematic figure of the formation of the five phases in a subglacial eruption. Phase I is represented by pillow lava formation if the confining pressure is high enough. Phase II marks the onset of explosive magma water interaction, controlled by pressure decrease as the pillow lava piles up. Phase III represents the time when the volcano begins to break the water table and emit ash into the atmosphere. Phase IV represents the time when magma does not encounter water and effusive activity begins. At this time, the flow foot breccia is formed and the lava on top of the mountain. Phase V begins once the eruption is over, and the glacier covers the volcano. At this time extensive bottom sediments from the glacier encounter the volcano and are deposited on its sides (modified after Jónsdóttir Blöndal, 2022)

2 Methods

To achieve the goal of this study several methods are used. Standard geological mapping methods are composed of visiting in the field and noting the different geological successions, their position within the mountain and internal relationship. A detailed topographic map of the mountain was generated by LIDAR and aerial photogrammetry, thus giving higher precision of volume estimates and internal relations of the geological units. Ground penetrating radar was used to achieve the internal relations of the geological units along drill holes. The composition and quality of the material was done through microscopy.

Aerial and Lidar mapping

Aerial mapping was carried out using a DJI Matrice 300 RTK quadcopter unmanned aerial vehicle (UAV or drone) together with a DJI L1 lidar module. The L1 module captures both RGB photographs and lidar (light detection and ranging) point clouds. Additionally, a DJI D-RTK 2 GNSS mobile station was used to provide real-time differential positioning data to the Matrice, enabling centimeter-level accuracy of the point cloud.

Lidar data was initially processed using DJI Terra to reconstruct and colorize the point cloud. A 2-dimensional digital surface model was created using CloudCompare by rasterizing the point cloud at a resolution of 50 cm.

3D modelling and volume estimations

Estimates of the shape and position of hyaloclastite within Lambafell were made through a combination of field observations, borehole data, and theoretical cross-sections drawn of the internal stratigraphy of the mountain through each of the three boreholes. As a large part of the western slopes of Lambafell are seemingly free of flow foot breccia and almost entirely made of hyaloclastite, the slope angles of those hyaloclastite slopes were used as a guide to estimate the configuration of the internal boundary between the hyaloclastite and the flow foot breccia that lies on top in other areas of the mountain. This was aided by the borehole data. From these cross-sections and the contours of the hyaloclastite hills, the contours of the hyaloclastite-flow foot breccia contact were drawn on a 2D map.

The contours of the hyaloclastite subsurface were interpolated into a 3-dimensional surface using the program Maptek Vulcan. This was combined with the UAS-derived

digital surface model and vector lines of surface outcrops to form a block model from which volumes could be calculated within the program. Basal surfaces were needed to form 3D solids for volume calculation. The basal surfaces were constructed by placing horizontal planes at various elevations depending on the volumes needed.

Ground penetrating radar

The control unit (GSSI 4000) contains the electronics which trigger the pulse of radar energy that the antenna sends into the ground. It also has a built-in computer and hard disk/solid state memory to store data for examination after fieldwork. This system allows data processing and interpretation without having to download radar files onto another computer.

The antenna 100 MHz receives the electrical pulse produced by the control unit that amplifies it and transmits it into the ground or other medium at a particular frequency. Antenna frequency is one major factor in depth penetration. The higher the frequency of the antenna, the shallower into the ground it will penetrate. A higher frequency antenna will also 'see' smaller targets. Antenna choice is one of the most important factors in survey design. The choice of 100 MHz antenna allows penetration up to 100 m into the ground.

Data is collected in parallel or perpendicular transects and then placed together in the appropriate locations for computer processing in a specialized software program. The computer then produces a horizontal surface at a particular depth in the record. This is referred to as a depth slice, which allows operators to interpret a plan view of the survey area. Detailed subsurface maps and depth to features are obtained by use of GSSI GPR processing software, which applies mathematical functions to the data in order to remove background interference, migrate hyperbolas, calculate accurate depth and more.

Two 100 MHz antennas, one a transmitter and the other a receiver, were used for this survey along with an SIR 4000 system computer from GSSI (Geophysical Survey Systems, Inc.). The antenna sleds were connected approx. 1 m apart with one pole on either side. A survey wheel was attached to the back sled (the receiver) to measure the distance travelled.

Boreholes

Three boreholes were made in the summer of 2022, and their location is shown in Figure 4. Samples were collected in every 3 m sections throughout all the boreholes. Samples were then analyzed in a microscope for consistency verification.



Figure 4 Location of boreholes four to six, drilled into Lambafell to verify the stratigraphy of the material forming the mountain. The orthomosaic and contour lines are sourced from Loftmyndir ehf. and Landmælingar Íslands, respectively.

Sample preparation

Samples from boreholes 4, 5, and 6 (BH4, BH5, and BH6; Figure 4) were sieved (1 mm and 0.5 mm-aperture sieves) and rinsed in an ultrasonic bath. They were then dried and glued onto glass slides using double-sided tape (Figure 5) before microscope analysis.

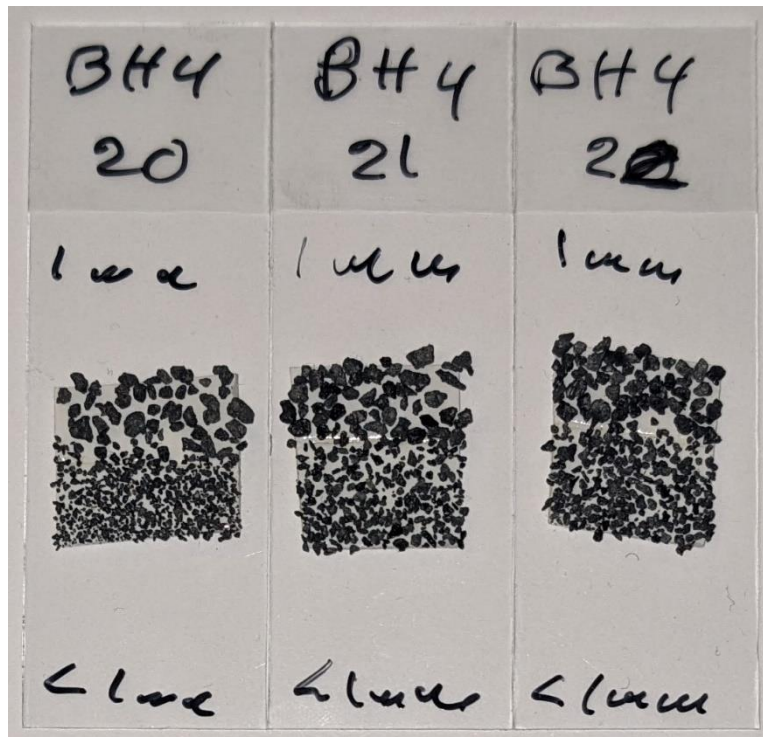


Figure 5 Glass slides prepared for microscopy. Double-sided tape was glued onto glass slide and the samples then poured onto to the tape.

Microscopy

The microscope used is a DVM6 digital microscope by Leica. It has a PlanAPO field of view (FOV) of 12.55 mm, a magnification range of 46x to 675x, and a max. resolution of 1073 lp/mm. The camera offers resolutions of 2MP (1600 x 1200), 5MP (2592 x 1944), and 10MP (3648 x 2736) (Leica Microsystems, n.d.).

3 General geology

The mountain Lambafell is located in the Prengsli region of southwest Iceland. The highest point of the mountain is 545 m above sea level (masl). The mountain itself rises some 250 m above the surrounding lava plains. The mountain is about 3.5 km long and 1.3 km wide. It is made up of subglacial tuff, pillow breccia, dikes, lava, tuff, and glacial sediments.

The strike of the mountain is oriented NE-SW in accordance with the general tectonic strike in the region. It is formed in a subglacial eruption during the Weichselian glaciation (Sæmundsson et al., 2016).

Lambafell is located between two main fissure systems, the Brennisteinsfjöll-Bláfjöll system to the north and the Hengill system to the south. During the Holocene, lava from the eruption of Leitin (5200 BP), Nesjahraun (2000 BP) and Eldborg, flowed up to the base of the mountain. During the Eldborg eruption the lava Svínahraunsbruni (or Kristnitökuhraun) was formed (~1000 AD; Jónsson, 1971).

Barja (2012) geologically mapped Lambafell and, accordingly, recognized four main stages in the buildup of the mountain. The subglacial tuff that is mostly exposed in the northern slopes and partially in the quarrying area of Björgun. Lava flows in the summit area of the mountain and subsequent flow foot breccia, which is exposed in all the quarrying areas, Eden, Björgun, and ÍAV. In the summit area, Barja further describes scoria from the main crater and glacial sediments. The mountain was substantially eroded by a glacier after its formation.

Lambafell is a subglacial volcanic formation and was formed in a single eruption and only one crater can be located within the mountain. Thus, it has similarity to other more modern volcanic formations in the region, the Eldborg craters. During its formation, a vault melted into the ice, generating space for the erupted material. The eruption lasted long enough to melt through the ice, thus forming lava flows and scoriaceous crater in the summit region. Barja (2012) suggested that the ice had been up to 250 m thick at the time of the eruption. However, the lava flows in the summit area suggest that it was not much thicker than 150 m, which is in accordance with H₂O solubility of magmas in the area (Figure 2).

Geological mapping shows that the eruption built out of the glacial lake in the vault and became effusive. Lava formed at this stage flowed into the ice bound lake east of the main volcanic massive. The geological division used in this report is based on the phase division in Figure 3. Further we do componentry analysis of samples from boreholes BH4, BH5 and BH6 (drill logs in Appendix) and run ground penetrating radar

along selected lines across the mountain, to better understand the internal stratigraphy of the mountain.

4 Composition of Lambafell

Microscopy

Samples from all levels of boreholes BH4, BH5 and BH6 were analyzed for freshness and componentry, all in all sixty-five samples. A microscope was used to examine the samples collected during the drilling. In general, there is not much pure glass in any of the three boreholes. Grains are mostly crystalline and/or altered throughout the boreholes. The thick alteration coat on many of the samples (e.g., Figures 40 and 120) is ground glass that comes from density currents that are common as the edifice builds up through the englacial lake during eruptions such as the one that formed Lambafell. The small grain size of the ground glass makes it easily altered.

Borehole 4 – BH4 (0-87 m)

The twenty-nine samples collected during drilling of borehole 4 (BH4) are described here. In this analysis we look at grains that are 1 mm and smaller and have been washed by clean water. The samples were mostly crystalline, about 85% overall, with minimal alteration throughout. Mineral content is unclear because of how crystalline most of the grains are, so proper percentages of minerals are difficult to determine in the microscope. Olivine (OL) and plagioclase (PLAG) are present as phenocrysts in many grains, both crystalline and glassy. Figures 6-61 show the samples in detail (the scale is 1 mm) and summarized results are shown in Table 1.

BH4-1 (0-3 m)

In sample BH4-1 there are mostly crystalline grains and some glass with dark yellow to orange alteration. Minerals (olivine and plagioclase) are present as phenocrysts. Figures 6 and 7 show 1 mm and <1 mm samples, respectively.



Figure 6 In the 1 mm sample there are mostly crystalline grains (~75%) but some altered glass is present (~25%). Alteration is dark yellow to orange, mostly in vesicles or cavities. Some PLAG and OL are present in most grains.



Figure 7 The <1 mm sample is the same as 1 mm. One large loose crystal, light yellow with a green tint, OL. Two red spots present.

BH4-2 (3-6 m)

Sample BH4-2 is the same as BH4-1 but glass grains are altered less. Phenocrysts are sparse. Figures 8 and 9 show 1 mm and <1 mm samples, respectively.

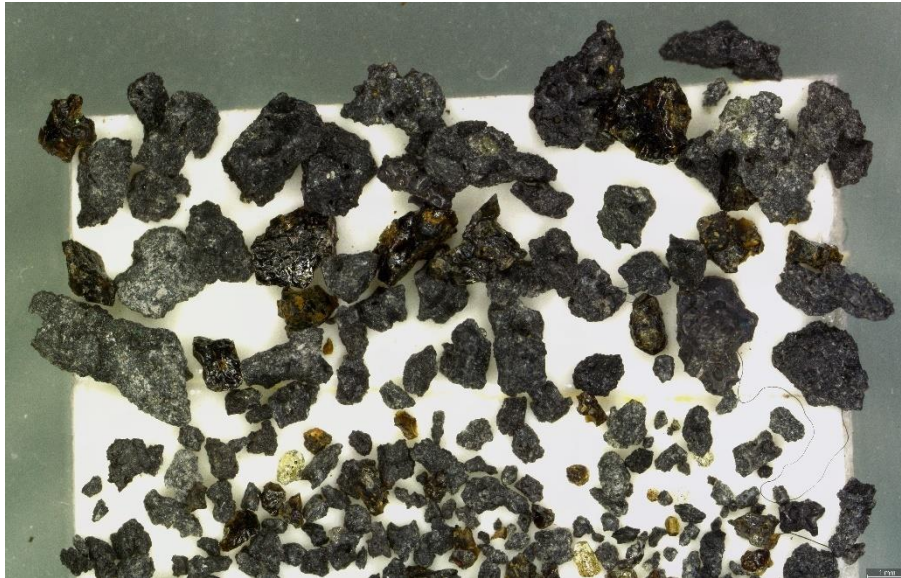


Figure 8 The 1 mm sample is similar to BH4-1 but less alteration in glass grains. The ratio of crystalline and glass is the same. Not as many obvious phenocrysts but some OL visible.



Figure 9 The <1 mm sample is the same as 1 mm. One grain has orange alteration. Some loose crystals, OL and PLAG.

BH4-3 (6-9 m)

In sample BH4-3 there are only crystalline grains and alteration is very minimal. The crystalline grains are both matte black with phenocrysts and gray with coarser groundmass but smaller phenocrysts. Figures 10 and 11 show 1 mm and <1 mm samples, respectively.

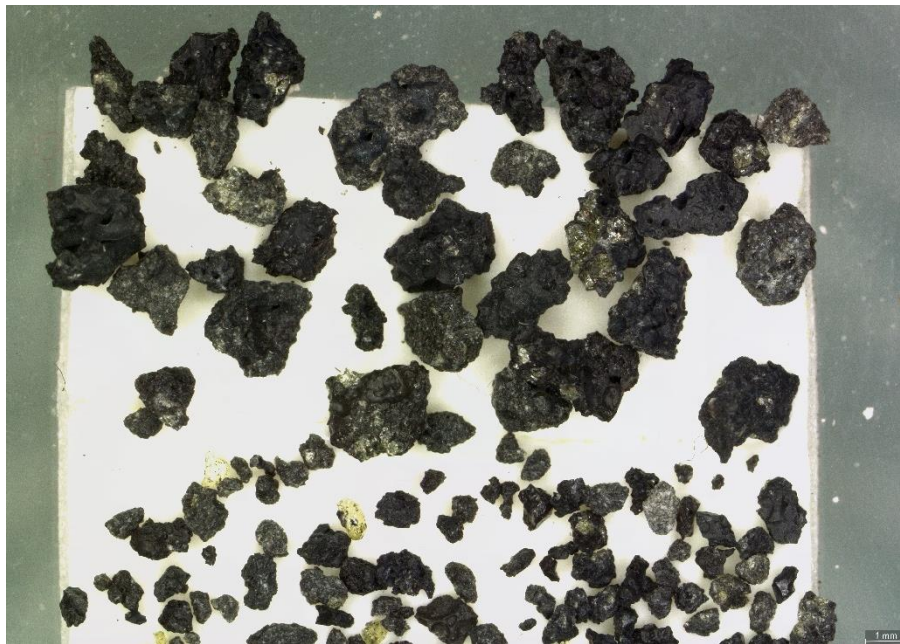


Figure 10 In the 1 mm sample there are only crystalline grains, both matte black with OL and PLAG phenocrysts (50%) and gray with coarser crystallinity but smaller phenocrysts (50%). Alteration is very minimal.



Figure 11 The <1 mm sample is the same as 1 mm. A single obvious grain of pure glass. Some loose OL and PLAG.

BH4-4 (9-12 m)

There is no glass in sample BH4-4. Most of the grains are the gray type with a coarse groundmass. OL is more common than PLAG. Figures 12 and 13 show 1 mm and <1 mm samples, respectively.

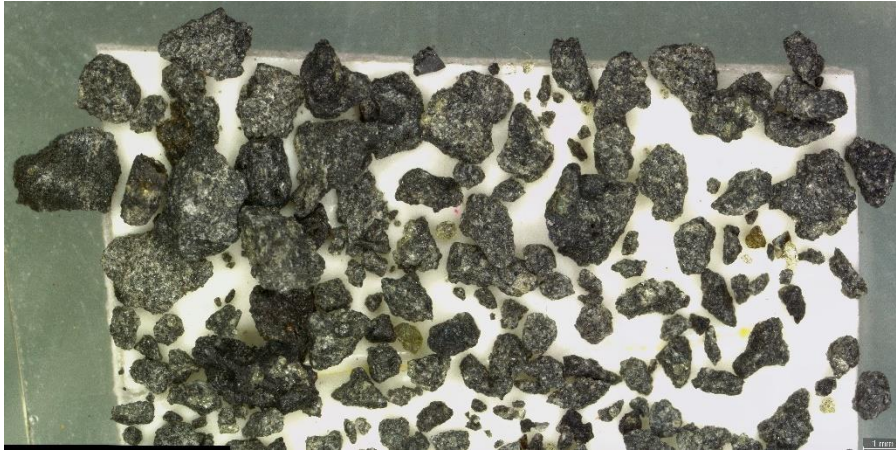


Figure 12 In the 1 mm sample there is no glass. The crystalline grains seem to have a very coarse groundmass except ± 4 grains that are like the matte black grains in prior samples. OL phenocrysts are common. PLAG is less distinguishable.

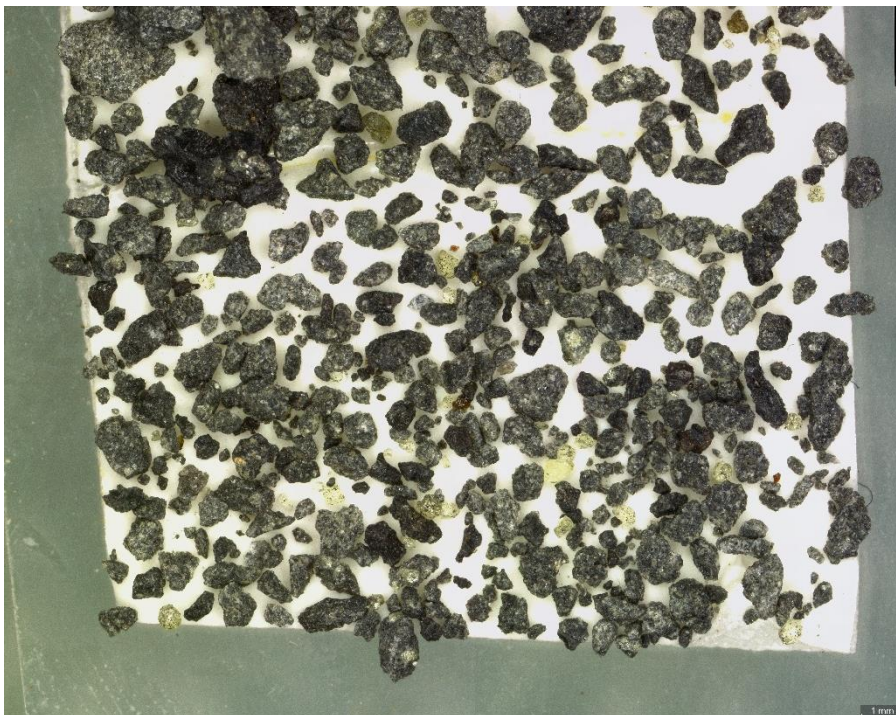


Figure 13 The <1 mm sample is the same as 1 mm. One spot of light orange alteration and two very small reddish pieces. Loose OL and PLAG (~1%).

BH4-5 (12-15 m)

Sample BH4-5 contains only crystalline grains that are darker than in sample BH4-4. PLAG and OL phenocrysts are common. Figures 14 and 15 show 1 mm and <1 mm samples, respectively.



Figure 14 In the 1 mm sample there are only crystalline grains but darker than in BH4-4, not matte as in BH4-3. PLAG and OL common.



Figure 15 The <1 mm sample is the same as 1 mm. 2-3 grains have patches of reddish surfaces. Only two loose crystals (OL and PLAG).

BH4-6 (15-18 m)

In sample BH4-6 there are only crystalline grains, both types, matte black and gray with a coarser groundmass. Phenocrysts are more visible in the gray grains. Figures 16 and 17 show 1 mm and <1 mm samples, respectively.

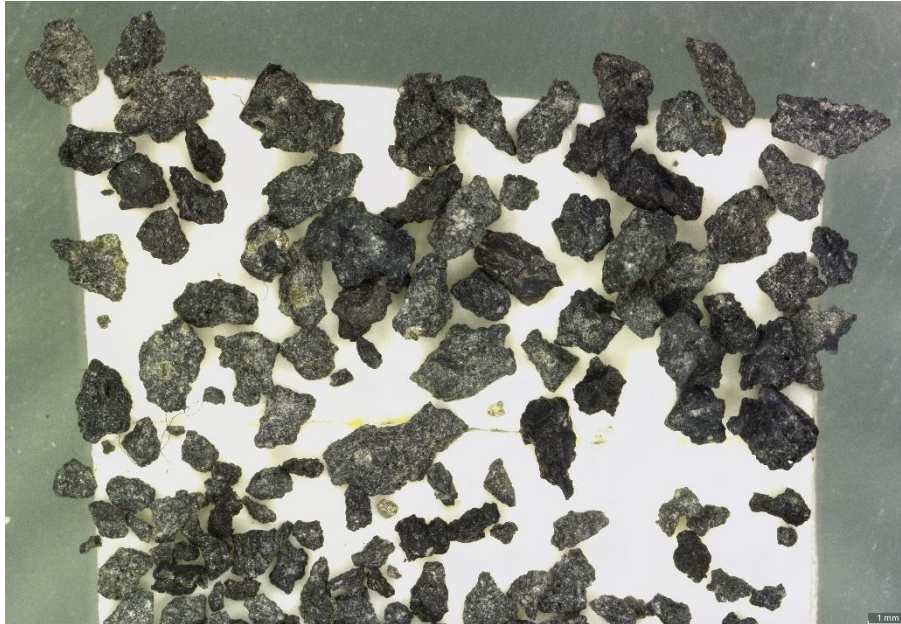


Figure 16 In the 1 mm sample there are mostly gray coarse crystalline grains (~65%), OL common in them and some PLAG phenocrysts. No obvious phenocrysts in the black crystalline grains (~35%).

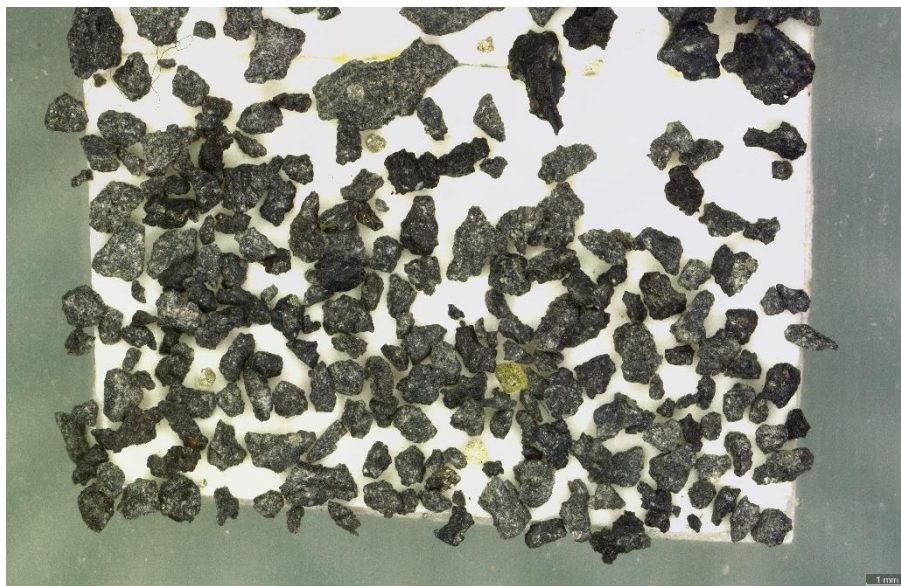


Figure 17 The <1 mm sample is the same as 1 mm. Two red dots. A few loose PLAG and OL (<1%).

BH4-7 (18-21 m)

Sample BH4-7 shows mostly crystalline grains, of which most are gray coarse. A small amount of slightly altered and crystalline glass grains is present. Phenocrysts are OL and PLAG. Figures 18 and 19 show 1 mm and <1 mm samples, respectively.



Figure 18 In the 1 mm sample there are some slightly altered and crystalline glass grains (10%), a few black crystalline grains (~25%) with phenocrysts (OL and PLAG), and the rest are gray coarse crystalline grains (65%) with phenocrysts (most obvious are OL).

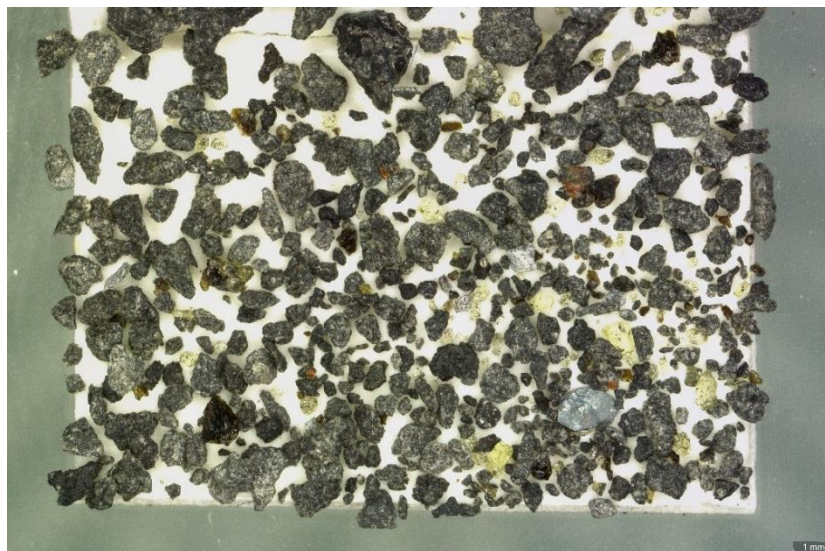


Figure 19 The <1 mm sample is the same as 1 mm. Many loose OL and PLAG (2-3%; mostly PLAG) and some red alteration present. One blueish gray grain with a shiny surface, likely foreign.

BH4-8 (21-24 m)

In sample BH4-8 there is slightly more glass and black crystalline grains, but gray coarse crystalline grains are most common. The glass is both less altered and less crystalline than in the sample prior. Figures 20 and 21 show 1 mm and <1 mm samples, respectively.

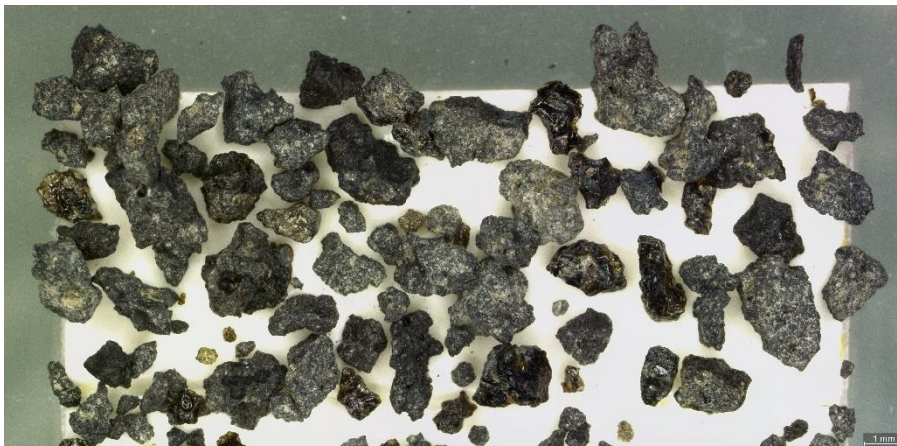


Figure 20 In the 1 mm sample there are higher ratios of glass (~20%) and black crystalline grains (~35%), the rest are gray coarse crystalline grains (~45%). Glass is clearer than in BH4-7. Obvious phenocrysts (OL and PLAG) are uncommon.



Figure 21 The <1 mm sample is the same as 1 mm. Vesicle rich, golden brown glass present. Some OL and PLAG (<1%).

BH4-9 (24-27 m)

In sample BH4-9 all grains are slightly more altered than before. There are mostly gray coarse crystalline grains but some black crystalline and a few glass grains are present. OL and PLAG are present in most grains but it is difficult to distinguish their outlines. Figures 22 and 23 show 1 mm and <1 mm samples, respectively.



Figure 22 In the 1 mm sample there are only three or four fairly altered glass grains (10%), one is less altered. A few black crystalline grains (~30%) but some are hard to distinguish from the gray coarse crystalline grains (~60%) so their proportions are unclear. OL and some PLAG phenocrysts. White/light colored alteration present in some grains.



Figure 23 The <1 mm sample is the same as 1 mm. Few (<1%) loose PLAG/OL. Some vesicle rich, golden-brown glass with some vesicles infilled.

BH4-10 (27-30 m)

Sample BH4-10 shows much less alteration than the sample prior. It contains mostly crystalline grains, of which most are matte black. There is some slightly altered glass present. Figures 24 and 25 show 1 mm and <1 mm samples, respectively.



Figure 24 In the 1 mm sample the grains are darker than in BH4-9. Proper glass grains with phenocrysts and slight alteration (~20%), black crystalline grains with phenocrysts and slight alteration (~60%), and dark crystalline grains with phenocrysts and coarser groundmass (20%).



Figure 25 The <1 mm sample is the same as 1 mm. Pieces of pure glass, highly vesicular and not. Some loose OL and PLAG. One light colored grain (opaque), unknown.

BH4-11 (30-33 m)

Sample BH4-11 is the same as sample BH4-10. Phenocrysts are OL and PLAG. Figures 26 and 27 show 1 mm and <1 mm samples, respectively.

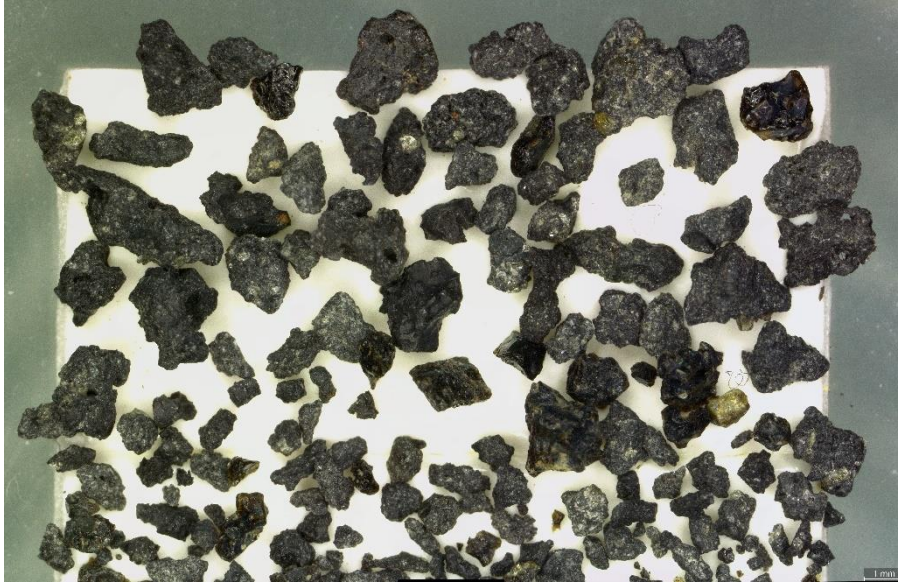


Figure 26 The 1 mm sample is the same as BH4-10.



Figure 27 The <1 mm sample is the same.

BH4-12 (33-36 m)

Sample BH4-12 is very similar to the two samples prior but contains more glass which is slightly to non-altered. Only a few obvious phenocrysts (OL and PLAG). Figures 28 and 28 show 1 mm and <1 mm samples, respectively.

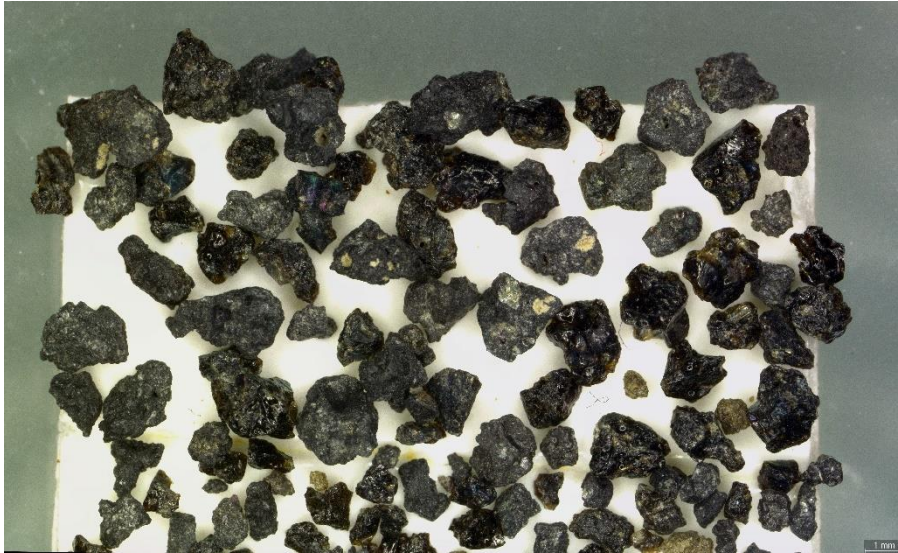


Figure 28 In the 1 mm sample there are the same types of grains as before but more glass (~45%). Not all glass grains have obvious phenocrysts.



Figure 29 The <1 mm sample is similar to 1 mm but some highly vesicular glass grains have alteration inside vesicles, light colored. Only two loose crystals.

BH4-13 (36-39 m)

Sample BH4-13 contains less glass than the sample prior, but otherwise the same as the last few samples. Phenocrysts are PLAG and OL. Figures 30 and 31 show 1 mm and <1 mm samples, respectively.



Figure 30 In the 1 mm sample there is less glass (~15%) again and one golden colored grain covered in easily altered ground glass, otherwise dark crystalline grains with some phenocrysts (OL and PLAG).



Figure 31 In the <1 mm sample there is more glass than in 1 mm (20-25%). Some grains have rust colored alteration. Few loose crystals.

BH4-14 (39-42 m)

Sample BH4-14 shows grains with light colored to yellow alteration, making it difficult to distinguish the different grain types. It contains mostly crystalline grains but some relatively crystallized glass. Phenocrysts are hard to distinguish in most grains but are OL and PLAG. Figures 32 and 33 show 1 mm and <1 mm samples, respectively.

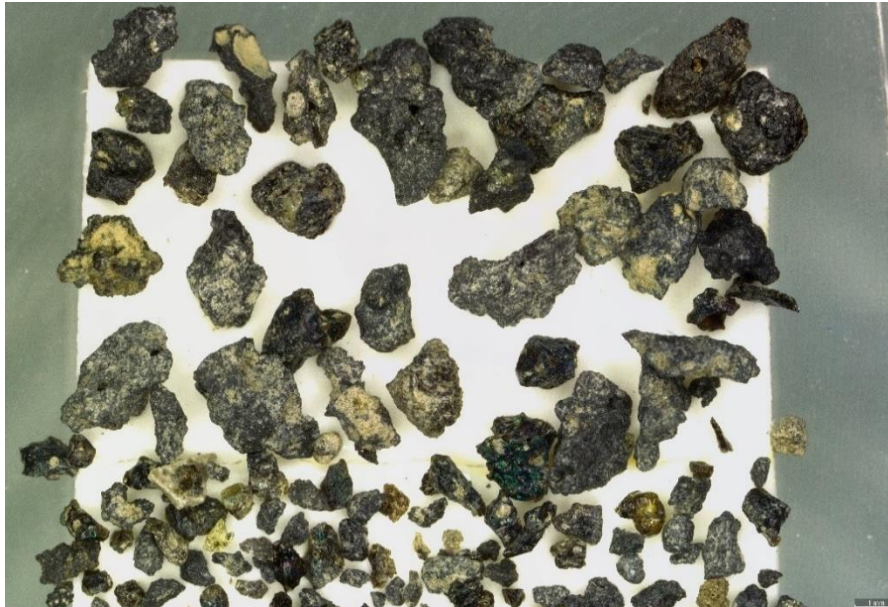


Figure 32 In the 1 mm sample many grains show light colored to yellow alteration which makes it difficult to distinguish between different grain types. There is some glass, probably around 30%, and most of them are relatively crystallized. One glass grain has a blueish green reflection. Some phenocrysts overall, mostly in the crystalline grains (most obvious is OL).



Figure 33 The <1 mm sample is very similar to 1 mm but some highly vesicular glass and completely altered grains, light yellow, are present. One light colored opaque grain like in BH4-10 <1 mm. No red alteration like in BH4-13 <1 mm.

BH4-15 (42-45 m)

Sample BH4-15 is very similar to the sample prior but is less altered. There are not many obvious phenocrysts but the ones visible are mostly PLAG and a few OL. Figures 34 and 35 show 1 mm and <1 mm samples, respectively.

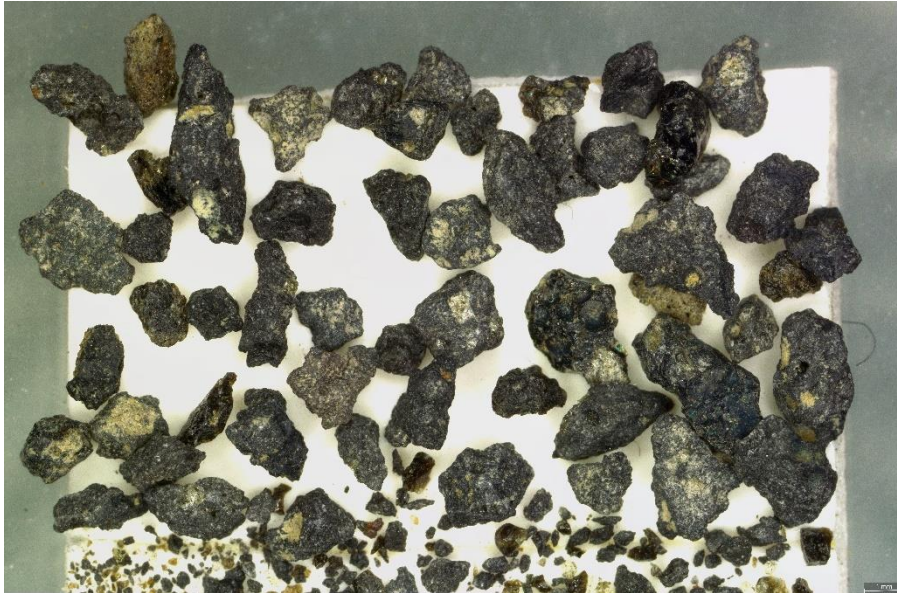


Figure 34 The 1 mm sample is the same as 14 but there is less alteration. Two completely altered grains are covered in ground glass. Very few phenocrysts.

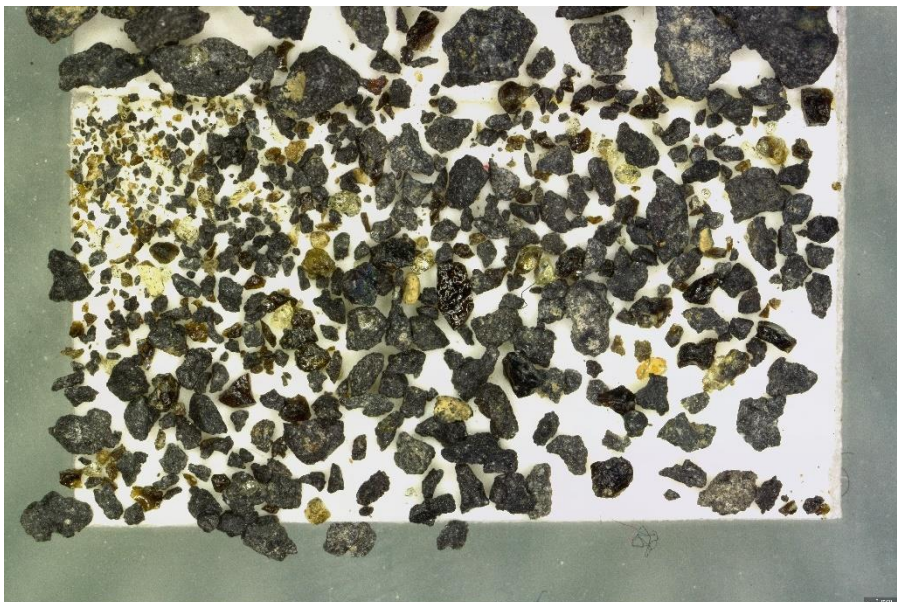


Figure 35 The <1 mm sample is the same as 1 mm. More loose crystals than in the BH4-14 <1 mm sample. One crystal (likely OL) has some orange on the surface. Even less alteration than in BH4-14.

BH4-16 (45-48 m)

In sample BH4-16 there are mostly crystalline grains but some slightly crystalline and a little altered glass grains are present. Obvious phenocrysts are sparse, but some PLAG is easily distinguishable. Figures 36 and 37 show 1 mm and <1 mm samples, respectively.



Figure 36 In the 1 mm sample there are more glass grains (~25%), a few without phenocrysts, others have some phenocrysts and slight alteration. Most grains are crystalline (~75%), some slightly altered. Phenocrysts are OL and PLAG.



Figure 37 The <1 mm sample is the same as 1 mm. At least five loose OL and PLAG.

BH4-17 (48-51 m)

The majority of grains in sample BH4-17 are crystalline and only a few are glass. Phenocrysts are mostly OL, but some PLAG is present. This was classified as lava in the field. Figures 38 and 39 show 1 mm and <1 mm samples, respectively.



Figure 38 In the 1 mm sample there are mostly crystalline grains (~90%), of those are slightly altered (~75%; some have red spots) and others not (~25%). A few glass grains (~10%), of which there are none altered. Obvious phenocrysts are mostly OL, some PLAG. In the drill log, this sample is classified as lava.

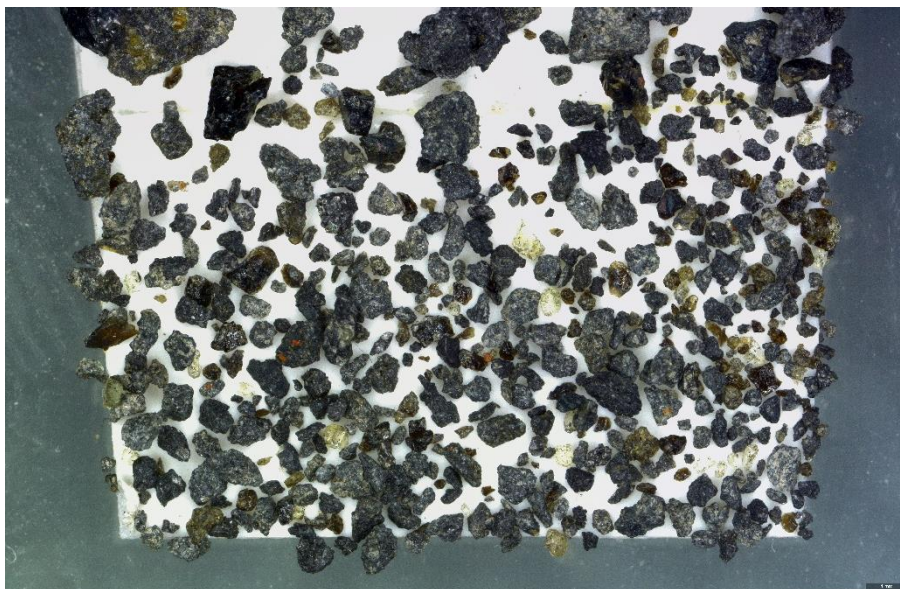


Figure 39 The <1 mm sample is the same as 1 mm. Many loose OL and PLAG (2-3%).

BH4-18 (51-54 m)

In sample BH4-18, most grains have a coat of altered ground glass. Almost all grains are crystalline. There are very few phenocrysts distinguishable. Figures 40 and 41 show 1 mm and <1 mm samples, respectively.

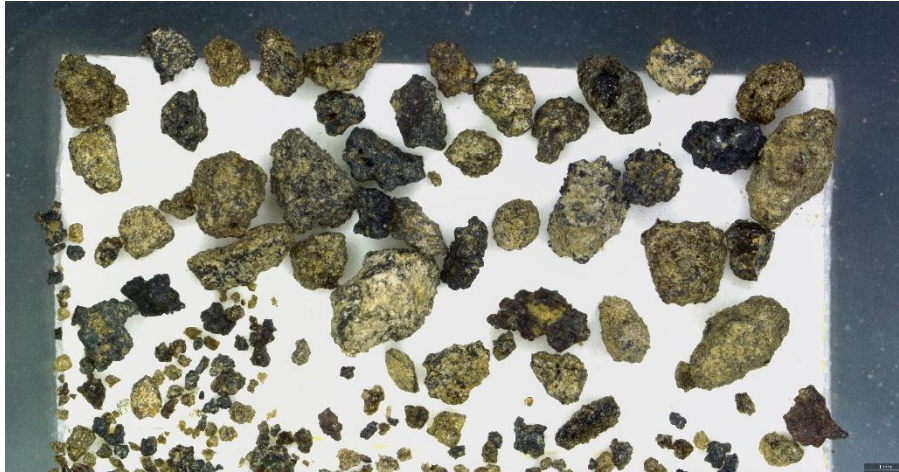


Figure 40 In the 1 mm sample there is much more alteration. Only two grains that could be pure glass but are slightly altered. Slightly vs. very altered crystalline grains are about 40/60%. Very few obvious phenocrysts. One red tinted grain.

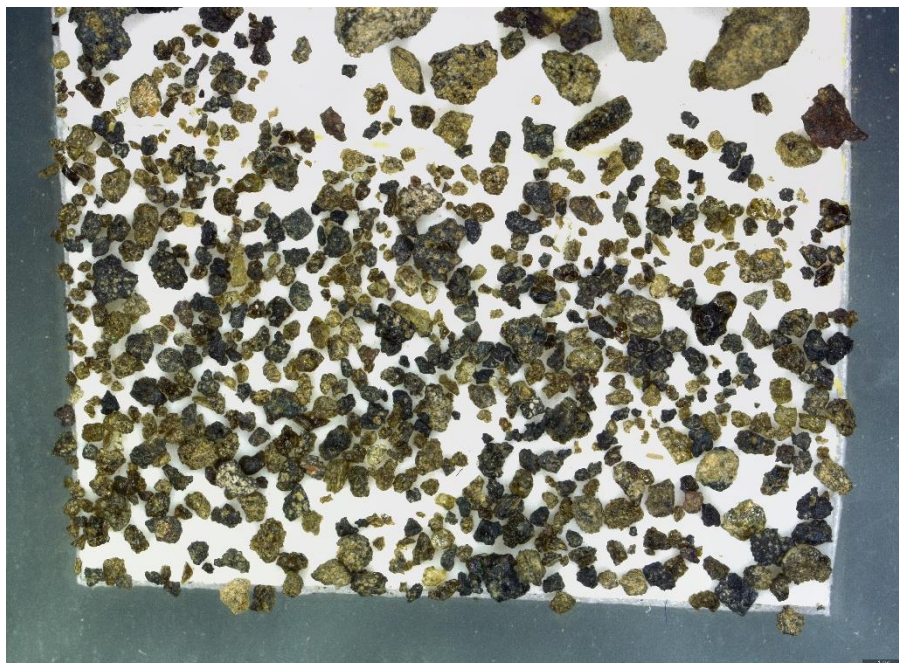


Figure 41 The <1 mm sample is very similar to 1 mm but more glass (2-3%), some vesicle rich (golden), and loose crystals (OL and PLAG; ~1%)

BH4-19 (54-57 m)

Sample BH4-19 has a much lower degree of alteration than the sample prior. It contains almost only crystalline grains. Obvious phenocrysts are very sparse. Figures 42 and 43 show 1 mm and <1 mm samples, respectively.

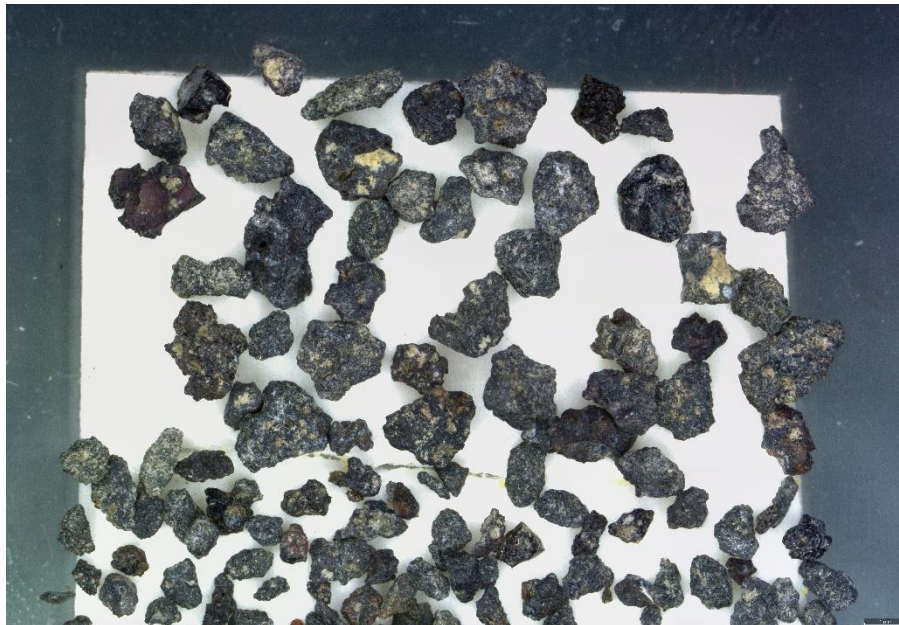


Figure 42 The 1 mm sample is more like samples BH4-16 and 17. Two or three glass grains are present, but they could be slightly crystalline, otherwise all other grains are crystalline, most slightly altered (~60-70%) and some not (~30-40%). Two grains have red tinted areas. No obvious phenocrysts. Light colored (very light yellow) alteration patches on some grains.



Figure 43 The <1 mm sample is the same as 1 mm but there are two completely red grains and two loose OL and PLAG.

BH4-20 (57-60 m)

Sample BH4-20 is very similar to the prior sample but there are no glass grains. Alteration is minimal and phenocrysts are more easily distinguished (OL and some PLAG). Figures 44 and 45 show 1 mm and <1 mm samples, respectively.

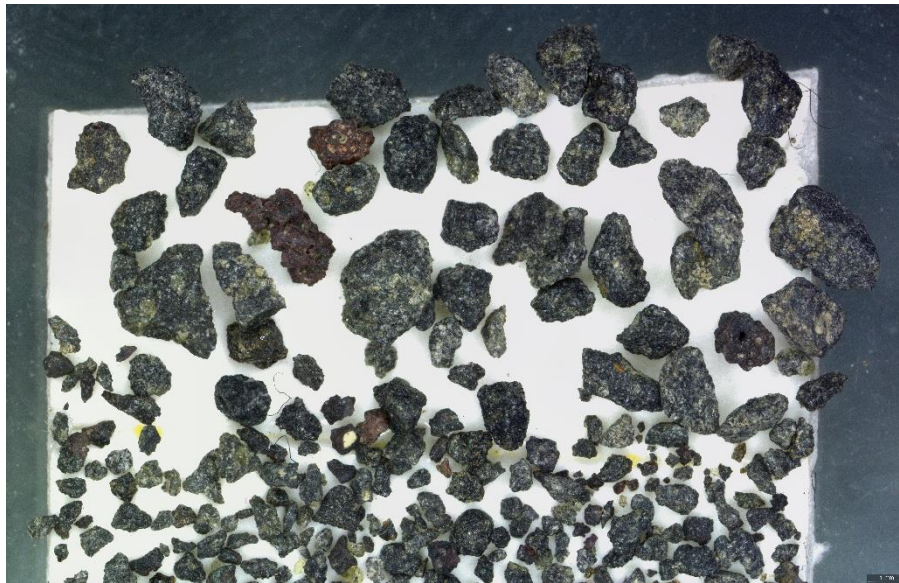


Figure 44 The 1 mm sample is very similar to BH4-19. No glass grains, barely any alteration, two red grains. Phenocrysts more obvious (OL and PLAG).

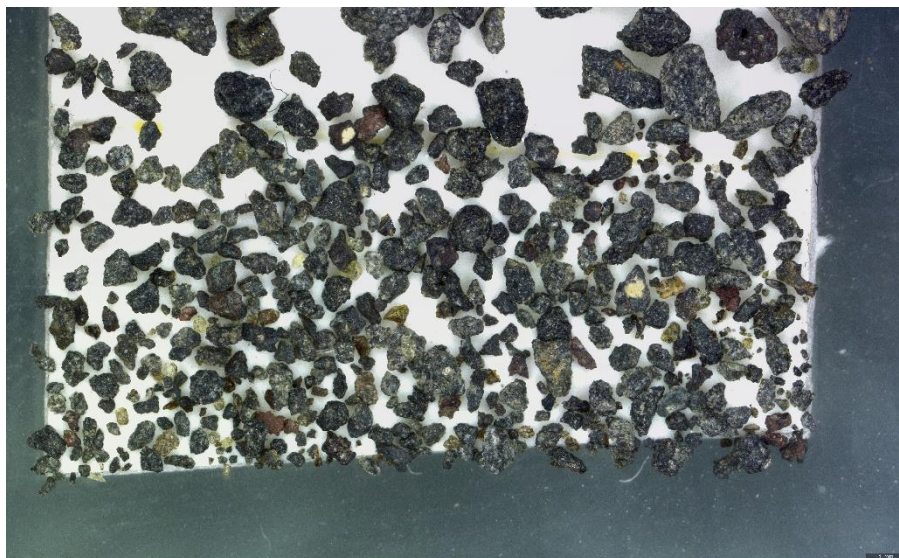


Figure 45 The <1 mm sample is the same as 1 mm. Two grains have very light yellow alteration patches like in BH4-19. More red grains than in 1 mm (~1%). One yellow grain. Loose crystals are OL (<1%) and PLAG (~1%). Phenocrysts are present (OL and PLAG).

BH4-21 (60-63 m)

There are mostly crystalline grains in sample BH4-21, the rest are rather crystalline glass grains. Phenocrysts are OL and PLAG and they are larger in the crystalline grains than in the glass. Figures 46 and 47 show 1 mm and <1 mm samples, respectively.

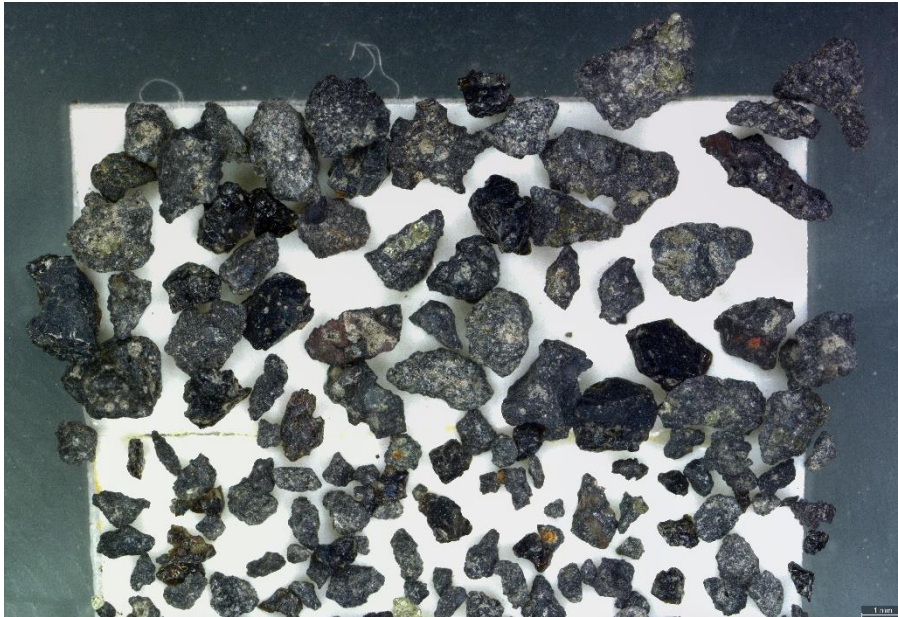


Figure 46 In the 1 mm sample there are mostly crystalline grains (~90%), both slightly altered and not. Only a few glass grains (~10%), some look rather crystalline and most have phenocrysts, mostly PLAG. Larger phenocrysts in crystalline grains, mostly OL. Two crystalline grains with red spots, two grains with red tint.



Figure 47 The <1 mm sample is similar to 1 mm but a little more glass. Only one loose PLAG.

BH4-22 (63-66 m)

Sample BH4-22 is the same as the prior sample but has no glass. Figures 48 and 49 show 1 mm and <1 mm samples, respectively.

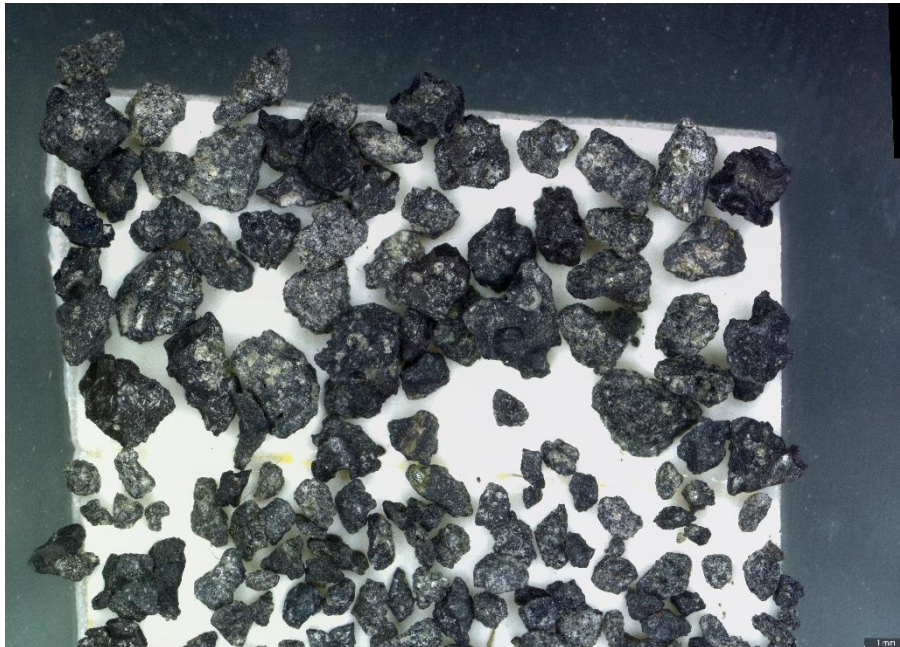


Figure 48 The 1 mm sample is the same as BH4-21 but no glass.

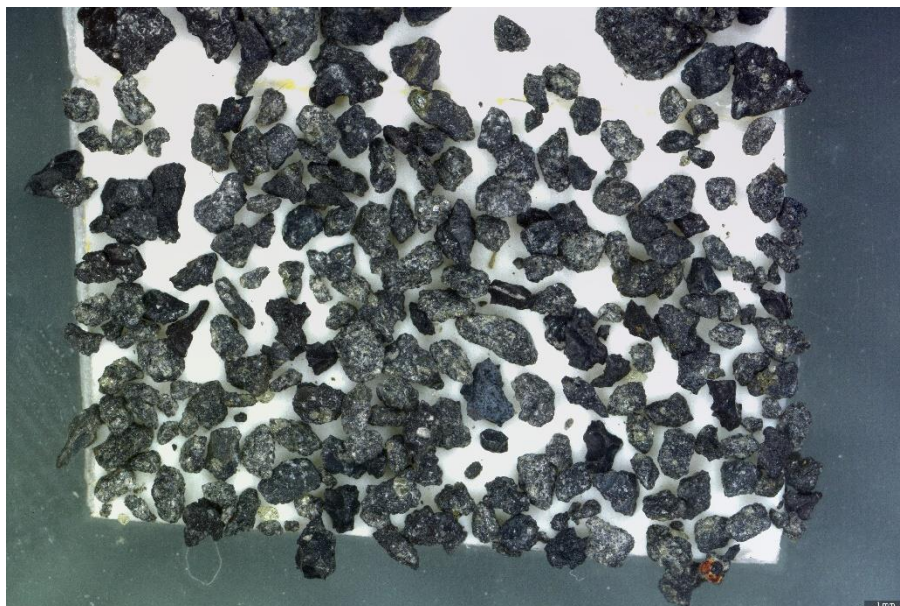


Figure 49 The <1 mm sample is the same as 1 mm. One blueish gray grain without obvious phenocrysts but with vesicles.

BH4-23 (66-69 m)

Sample BH4-23 mostly contains dark gray to black crystalline grains and some glass. Phenocrysts are sparse but are PLAG and OL. Figures 50 and 51 show 1 mm and <1 mm samples, respectively.



Figure 50 In the 1 mm sample there are mostly crystalline grains (~80%), some slightly altered, most not. A few more glass grains than before (~20%). One glass grain with very large phenocrysts (PLAG), others have some visible phenocrysts (OL and PLAG). A few crystalline grains have obvious phenocrysts (mostly OL), other grains have phenocrysts, but they are difficult to distinguish.



Figure 51 The <1 mm sample is the same as 1 mm. One unknown yellow grain, very likely foreign.

BH4-24 (69-72 m)

In sample BH4-24 there are mostly crystalline grains, dark gray to black and gray with a coarser groundmass. Some grains are slightly altered. The glass is slightly crystalline and altered. Phenocrysts are PLAG and OL. Figures 52 and 53 show 1 mm and <1 mm samples, respectively.

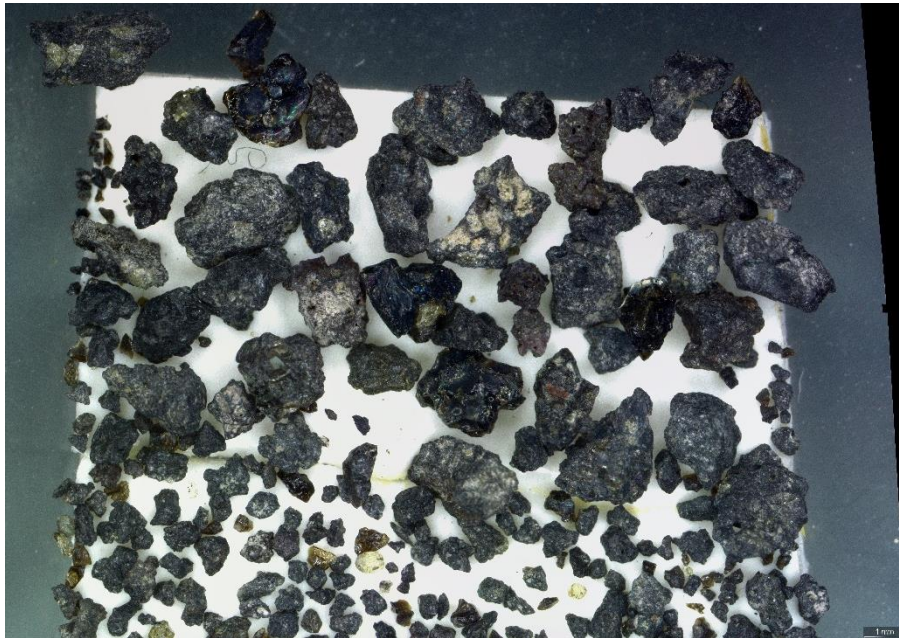


Figure 52 In the 1 mm sample there are mostly crystalline grains (~85%), some grains are slightly altered, most are not. Phenocrysts (OL and PLAG) are fairly large (± 0.5 mm), and the largest are OL. Glass grains (~15%) are not altered, phenocrysts are obvious in some of them, largest ~0.5 mm, OL.



Figure 53 The <1 mm sample is the same as 1 mm. Loose OL and PLAG (<1%).

BH4-25 (72-75 m)

In sample BH4-25 there are slightly more crystalline grains than glass. Grains are barely altered, but orange-red alteration does occur. Phenocrysts are mostly PLAG and some OL. Figures 54 and 55 show 1 mm and <1 mm samples, respectively.

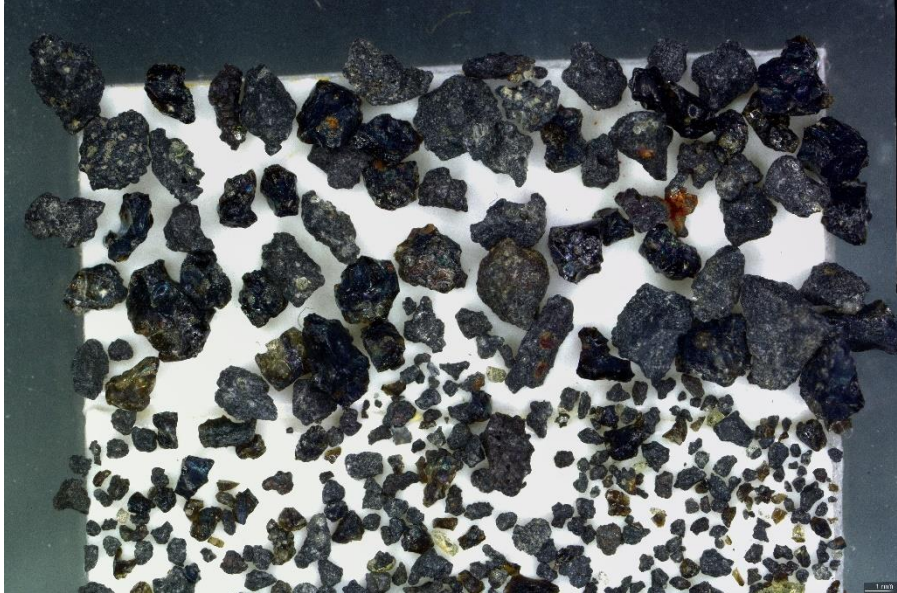


Figure 54 In the 1 mm sample there are mostly crystalline grains (55%) but more glass (45%) than in the las few samples. Barely any alteration, but a few glass grains are lackluster and could either be more crystalline or have a thin alteration coat. A few grains (both types) have orange-red alteration. Big (>0.3 mm) phenocrysts (PLAG and some OL) in both types of grains, but not in all grains.



Figure 55 The <1 mm sample is the same as 1 mm. A little higher ratio of crystalline grains. Loose OL and PLAG crystals (~1%) No orange-red alteration.

BH4-26 (75-78 m)

There are mostly crystalline grains in sample BH4-26 and fewer glass grains than in the sample prior, but in some grains the textures make it difficult to distinguish between the types of grains. Phenocrysts are sparse (PLAG and OL). Figures 56 and 57 show 1 mm and <1 mm samples, respectively.

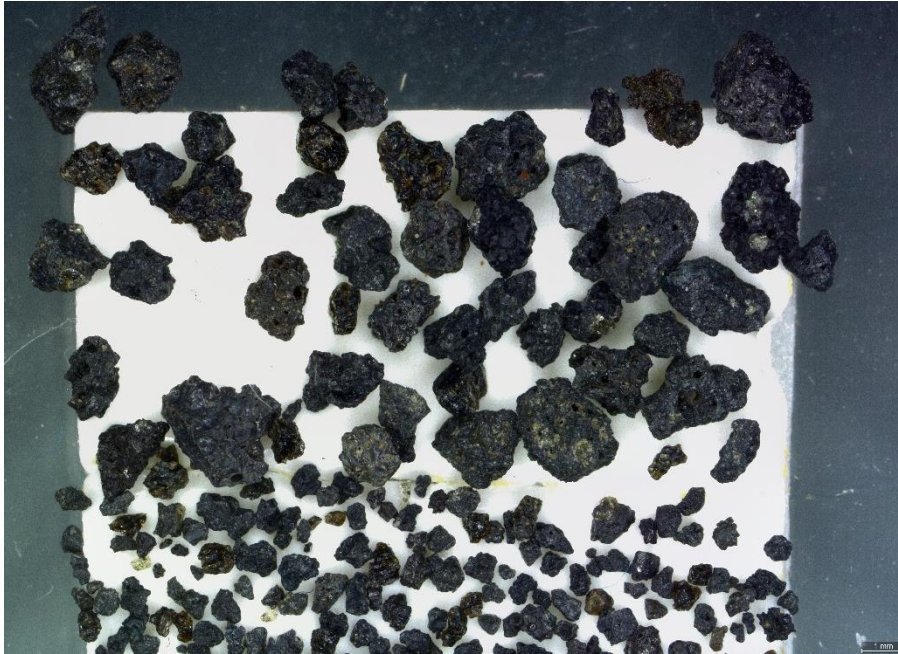


Figure 56 In the 1 mm sample there are mostly crystalline grains (80-85%), only four or five slightly altered grains. Only a few obvious phenocrysts (mostly PLAG). Fewer glass grains (15-20%) than in BH4-25 but hard to differentiate some of the grains because they share attributes and textures with both types.



Figure 57 The <1 mm sample is the same as 1 mm. Loose OL and PLAG (<1%).

BH4-27 (78-81 m)

Sample BH4-27 contains only crystalline grains save one glass grain. About half of the grains are slightly altered. Obvious phenocrysts are sparse. Figures 58 and 59 show 1 mm and <1 mm samples, respectively.

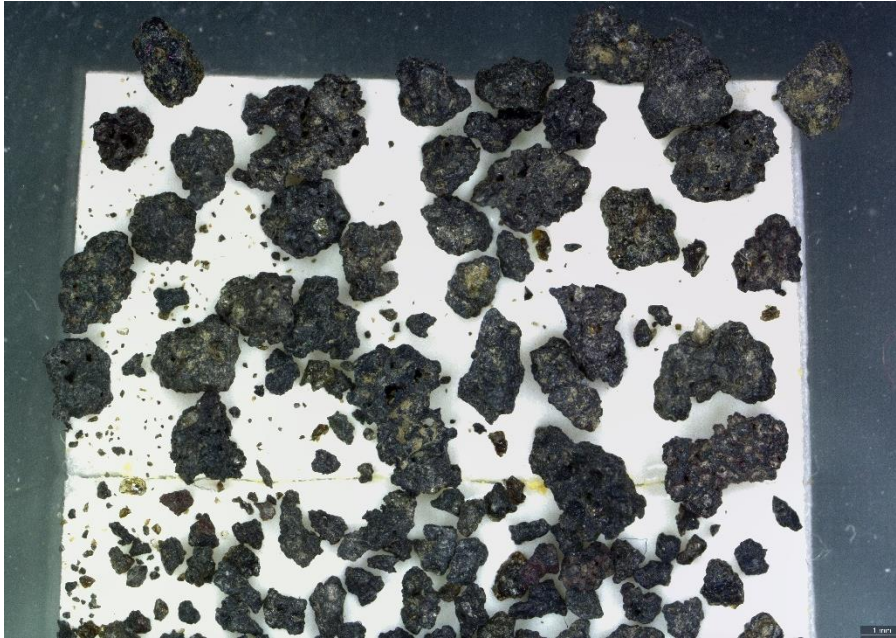


Figure 58 In the 1 mm sample there are mostly crystalline grains, about half slightly altered, the rest not. Only one glass grain, slightly altered. Only a few obvious phenocrysts overall, largest ~0.8 mm, likely altered PLAG.

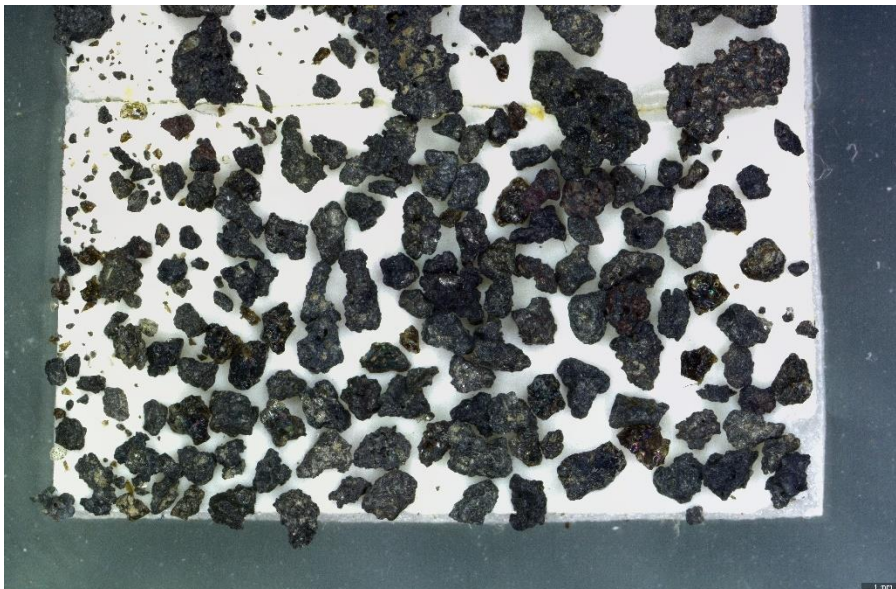


Figure 59 The <1 mm sample is the same as 1 mm but slightly more glass. Some obvious phenocrysts but only three loose crystals, likely all PLAG.

BH4-28 (81-84 m)

No sample: the drill got stuck.

BH4-29 (84-84 m)

In sample BH4-29, about one third of the grains are crystalline, the rest are slightly altered glass. Very few obvious phenocrysts are present. Figures 60 and 61 show 1 mm and <1 mm samples, respectively.

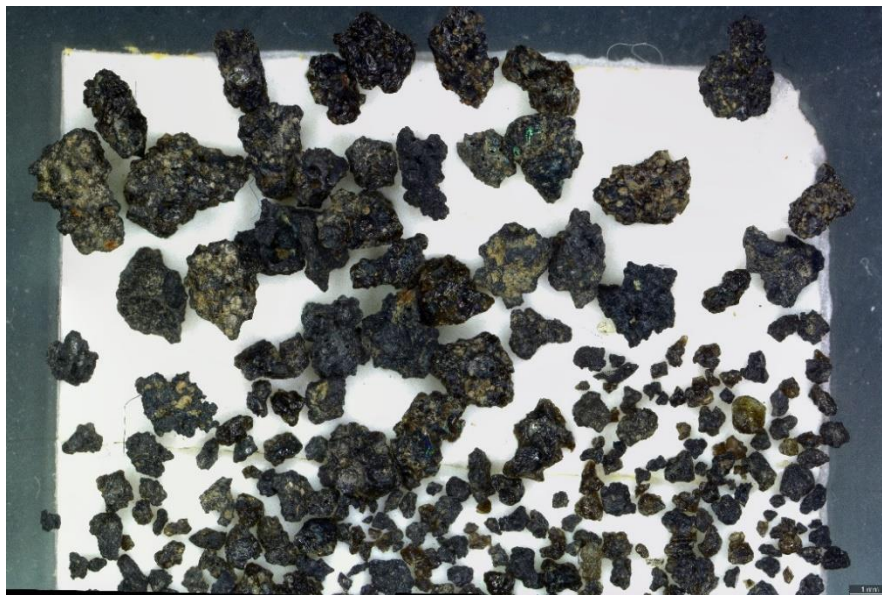


Figure 60 In the 1 mm sample there are mostly crystalline grains (~65%), about half altered, the rest not. About half of glass grains (~35% overall) are slightly altered. Very few obvious phenocrysts overall (PLAG).



Figure 61 The <1 mm sample is the same as 1 mm but less alteration. Some obvious phenocrysts, largest ~0.8 mm OL, the rest are mostly PLAG, some OL. Very few loose crystals (PLAG).

The results of the drilling of borehole BH4 are summarized in Table 1. The borehole is mostly crystalline throughout, with minimal alteration, and is therefore classified as a lava delta and is a part of Lambafell proper. There is one sample (BH4-18) that is heavily covered with altered ground glass and is thus taken to indicate a density current.

Table 1 This table expresses the main findings in BH4 of Lambafell. The colors represent glass content (blue) and crystalline content (orange), but density currents (yellow) are taken to be where the samples have a thick cover of altered ground glass.

Sample	Depth (m)	Glass vs. Crystalline	Interpretation	Alteration
BH4-1	0-3		Breccia	Some yellow
BH4-2	3-6		Breccia	Minimal yellow
BH4-3	6-9		Breccia	Very minimal
BH4-4	9-12		Breccia	Very minimal
BH4-5	12-15		Breccia	No alteration
BH4-6	15-18		Breccia	Minimal light gray
BH4-7	18-21		Breccia	Minimal light yellow
BH4-8	21-24		Breccia	Minimal light yellow
BH4-9	24-27		Breccia	Some light yellow
BH4-10	27-30		Breccia	Minimal light yellow
BH4-11	30-33		Breccia	Very minimal
BH4-12	33-36		Breccia	Minimal light yellow
BH4-13	36-39		Breccia	Minimal light yellow
BH4-14	39-42		Breccia	Some light yellow
BH4-15	42-45		Breccia	Some light yellow
BH4-16	45-48		Breccia	Some light yellow and yellow
BH4-17	48-51		Lava	Some light beige
BH4-18	51-54		Density current	Much light yellow
BH4-19	54-57		Breccia	Minimal light yellow
BH4-20	57-60		Breccia	Minimal light yellow, some purple/red grains
BH4-21	60-63		Breccia	Minimal light yellow, some purple/red grains
BH4-22	63-66		Breccia	Minimal light yellow
BH4-23	66-69		Breccia	Minimal yellow
BH4-24	69-72		Breccia	Minimal light yellow
BH4-25	72-75		Breccia	Very minimal light yellow, some red
BH4-26	75-78		Breccia	Very minimal light yellow
BH4-27	78-81		Breccia	Minimal light yellow
BH4-28	81-84	No sample		
BH4-29	84-87		Breccia	Minimal light yellow

Borehole 5 – BH5 (0-51 m)

The seventeen samples collected during drilling of borehole 5 (BH5) are described here. In this analysis we look at grains that are 1 mm and smaller and have been washed by clean water. The grains in the top ~15 m are mostly crystalline, but after that, glass is prevalent. The alteration is mostly caused by ground glass coating the grains, but secondary minerals also have a great effect on the appearance of the grains. These minerals are likely a type of calcite which is a common secondary mineral. Unfortunately, secondary minerals have been shown to have negative effects on strengths of concrete (Habert et al., 2008, and references therein). Primary minerals are OL and PLAG but they are not very common throughout the borehole. Figures 62-95 show the samples in detail and the drill log is shown in Table 2.

BH5-1 (0-3 m)

Sample BH5-1 contains only crystalline grains with a light gray altered coat of ground glass. Visible minerals are minimal but PLAG and OL are present. Figures 62 and 63 show 1 mm and <1 mm samples, respectively.

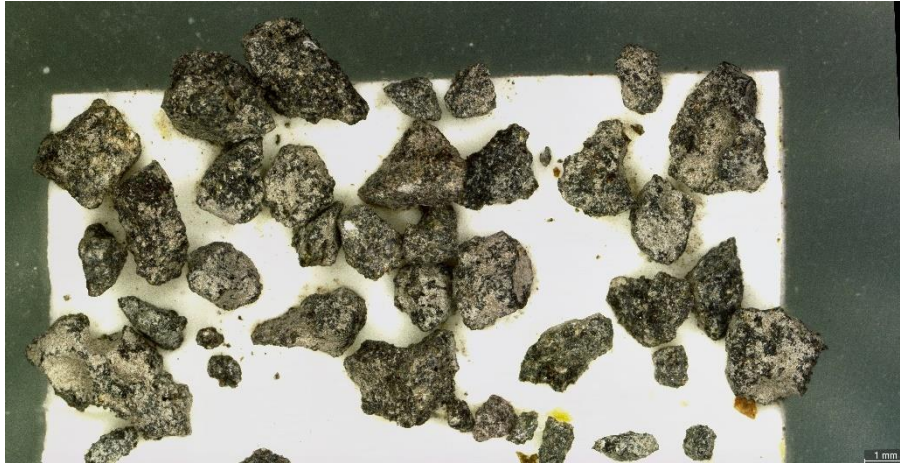


Figure 62 In the 1 mm sample there are mostly black or gray grains with light gray alteration. Only a few obvious crystals. No pure glass.

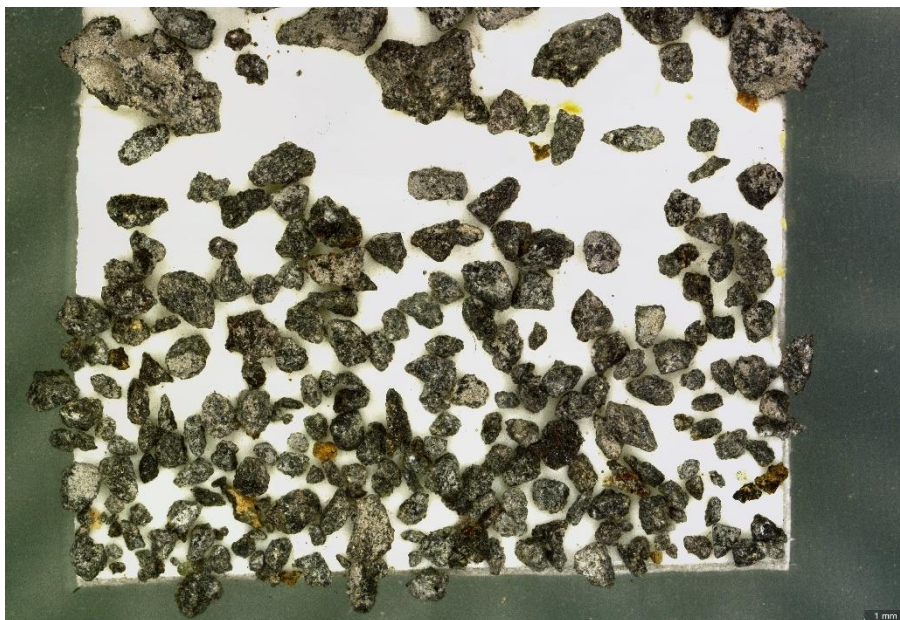


Figure 63 The <1 mm sample is the same as 1 mm but some black grains do not have the light gray alteration. Some grains have yellow alteration or completely altered yellow. Single PLAG and OL present. No pure glass.

BH5-2 (3-6 m)

Sample BH5-2 is very similar to the first sample, but the alteration is not as even. There are some orange and dark yellow grains present that seem to be clusters of altered ground glass or a combination of glass altered glass and ground glass. OL is common. Figures 64 and 65 show 1 mm and <1 mm samples, respectively.

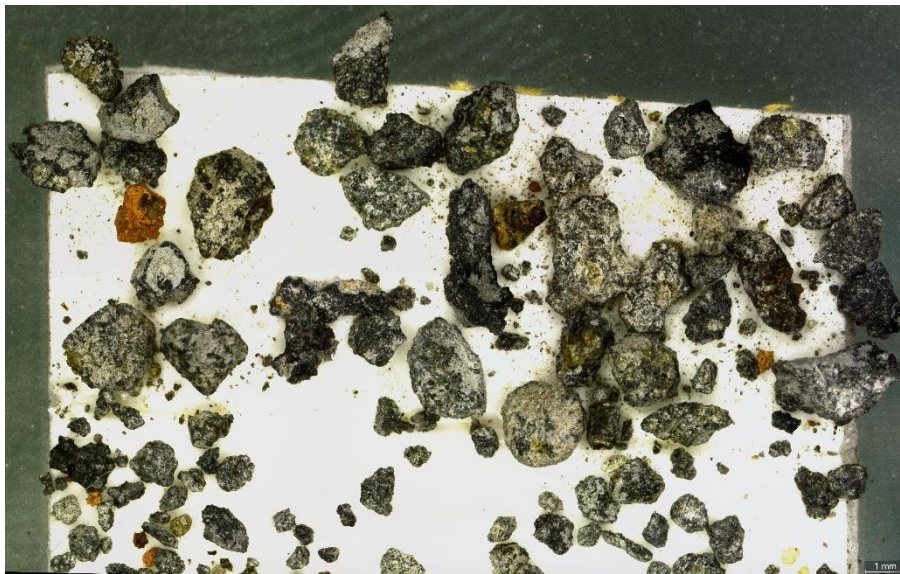


Figure 64 The 1 mm sample is very similar to BH5-1, but some grains are less or more altered (light gray). OL prevalent. A single orange altered grain. A single grain with dark yellow alteration.

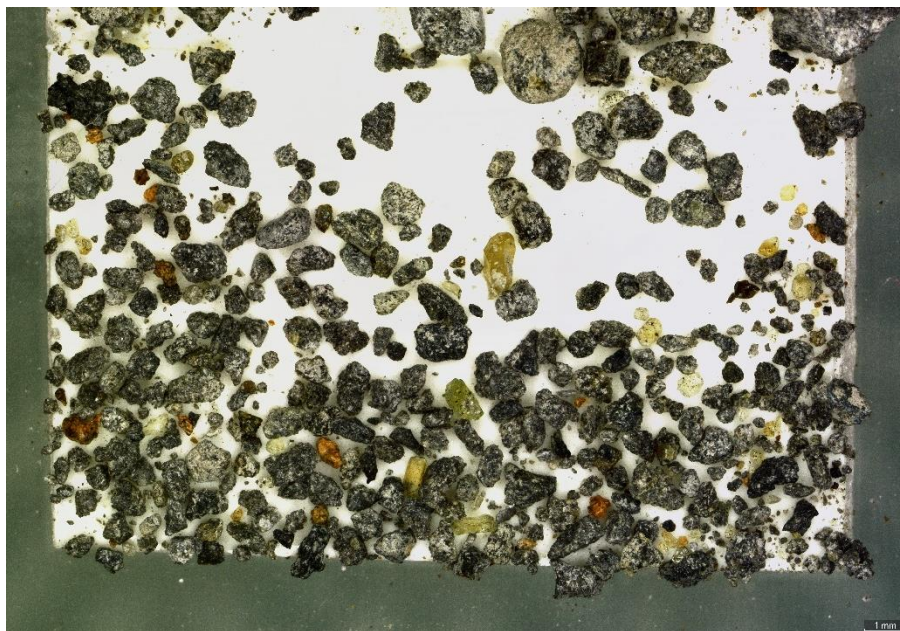


Figure 65 The <1 mm sample is the same as 1 mm. More orange altered grains. Loose crystals (~3%) are mostly OL.

BH5-3 (6-9 m)

Sample BH5-3 is very similar to the second sample in terms of degree of alteration, type of grains, and color. OL phenocrysts seem to be altered. Figures 66 and 67 show 1 mm and <1 mm samples, respectively.

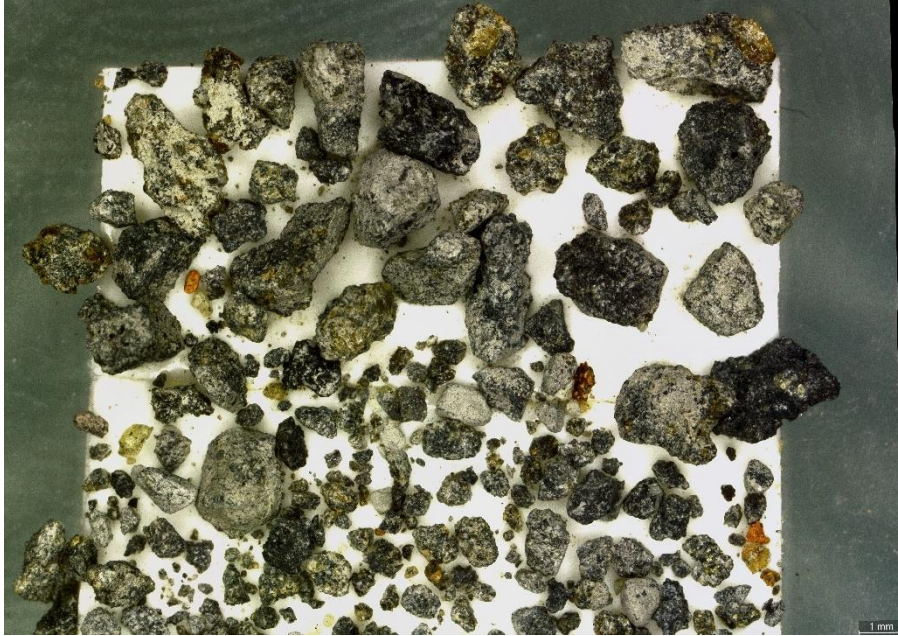


Figure 66 The 1 mm sample is very similar to BH5-2. Some OL phenocrysts are altered to a kind of orange-brown. One unaltered black crystalline grain.



Figure 67 The <1 mm sample is the same as 1 mm. Some loose OL are altered as in 1 mm.

BH5-4 (9-12 m)

At this depth, in sample BH5-4, the light gray to white alteration is still present on the grains. As in the prior samples, there are only crystalline grains in this one. Phenocrysts are minimal. Figures 68 and 69 show 1 mm and <1 mm samples, respectively.

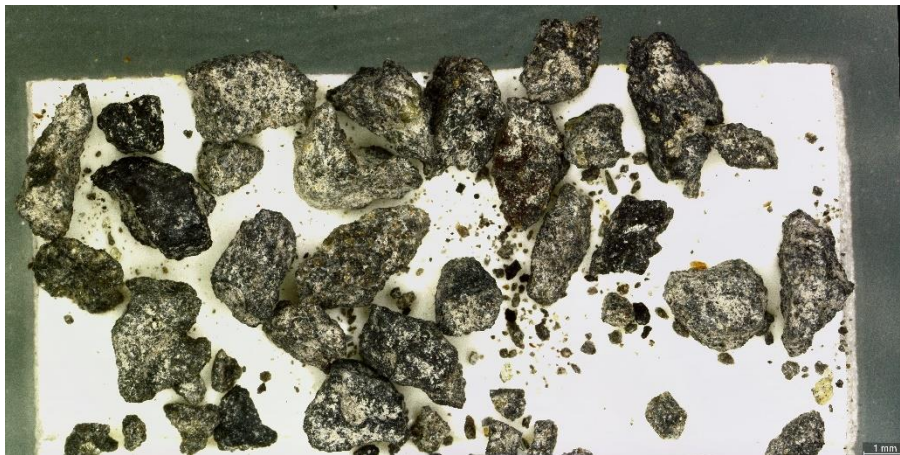


Figure 68 The 1 mm sample is very similar to last three samples. Black needles are present in some grains. Obvious phenocrysts are present (most obvious is OL). Some red crystals are present, likely altered OL.

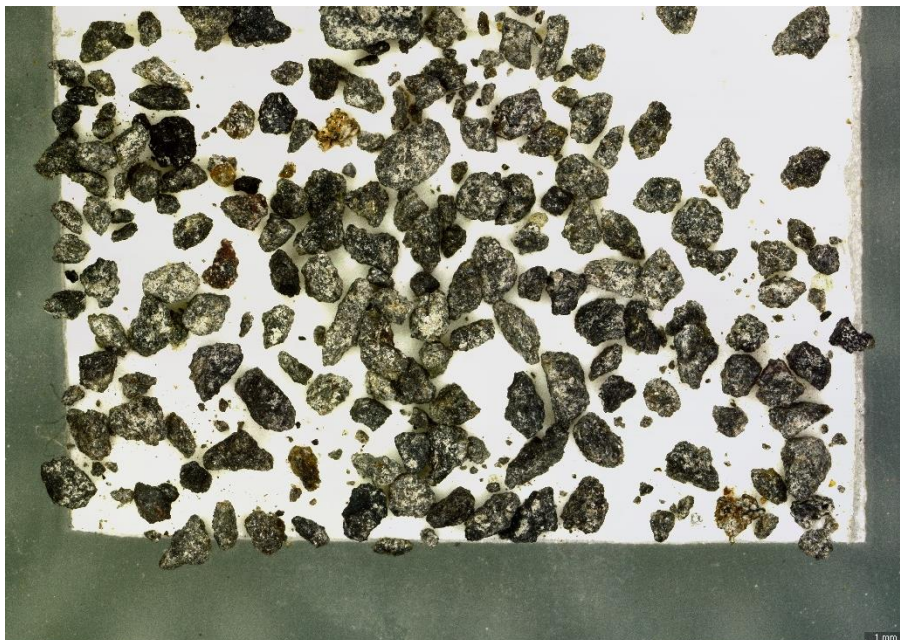


Figure 69 The <1 mm sample is the same as 1 mm. Two grains with orange alteration and speckles of white.

BH5-5 (12-15 m)

There is a great difference between sample BH5-5 and the others above. There is change in the types of grains and the light gray alteration is very minimal. About half or more could be glass and the rest crystalline grains. Visible minerals are minimal. Figures 70 and 71 show 1 mm and <1 mm samples, respectively.

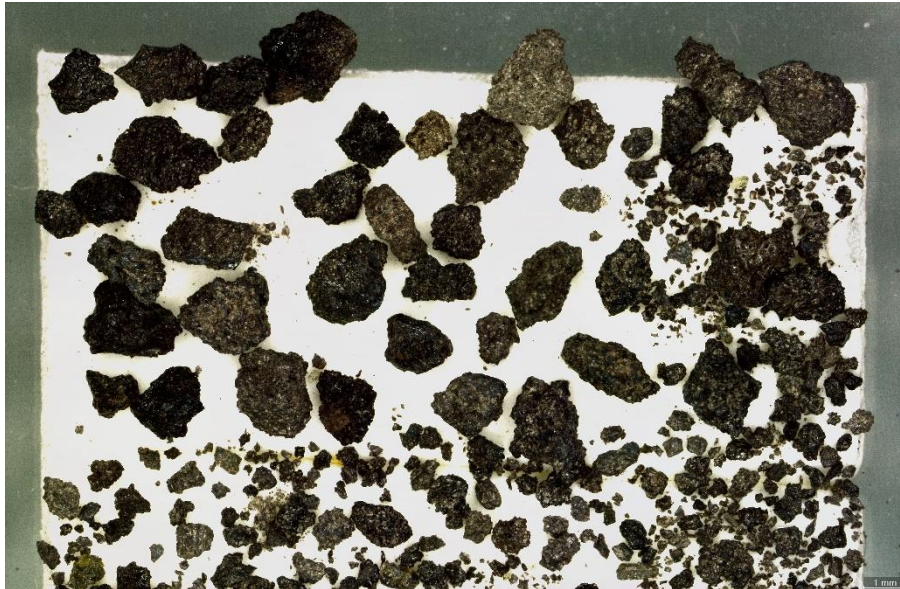


Figure 70 In the 1 mm sample there is much difference from BH5-4. Almost only black grains (some gray) of which most seem to be vesicular glass. No obvious minerals. Some grains are difficult to distinguish, they are either crystalline or glass grains.

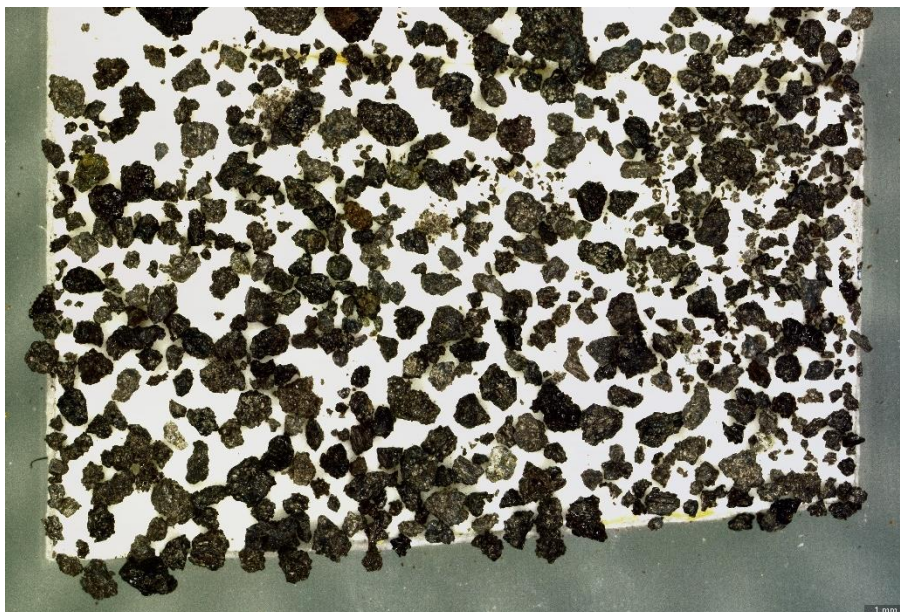


Figure 71 The <1 mm sample is the same as 1 mm. Few loose crystals (OL and PLAG). One brownish grain.

BH5-6 (15-18 m)

In sample BH5-6 the alteration appears again but is more yellow than before. The ratio between glass and crystalline grains seems to be the same as in sample BH5-5 but the alteration makes distinction between them difficult. Figures 72 and 73 show 1 mm and <1 mm samples, respectively.

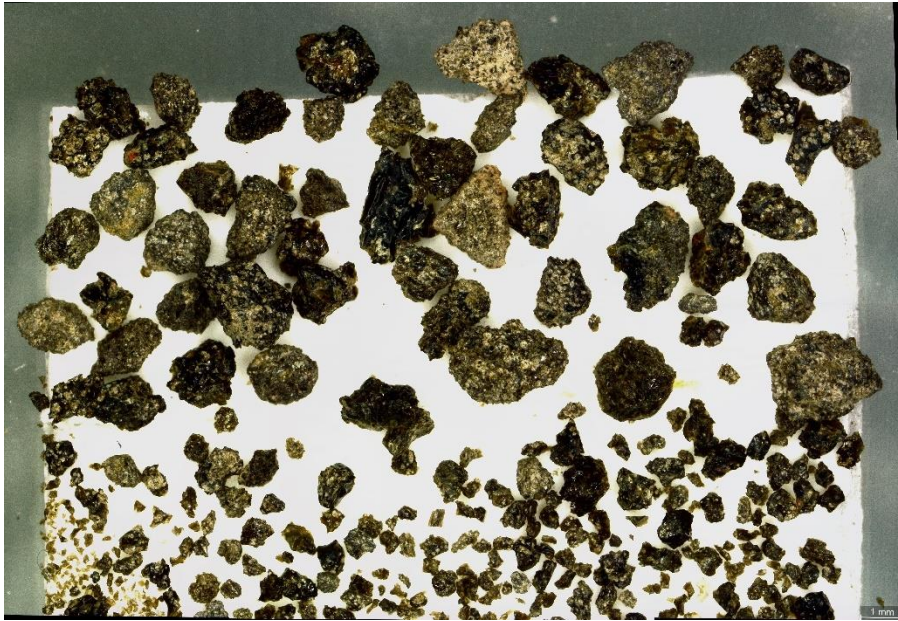


Figure 72 In the 1 mm sample the alteration appears again (light yellow). Some black grains seem to be vesicular glass. No obvious minerals but in one or two grains (OL). Difficult to distinguish between types of grains.

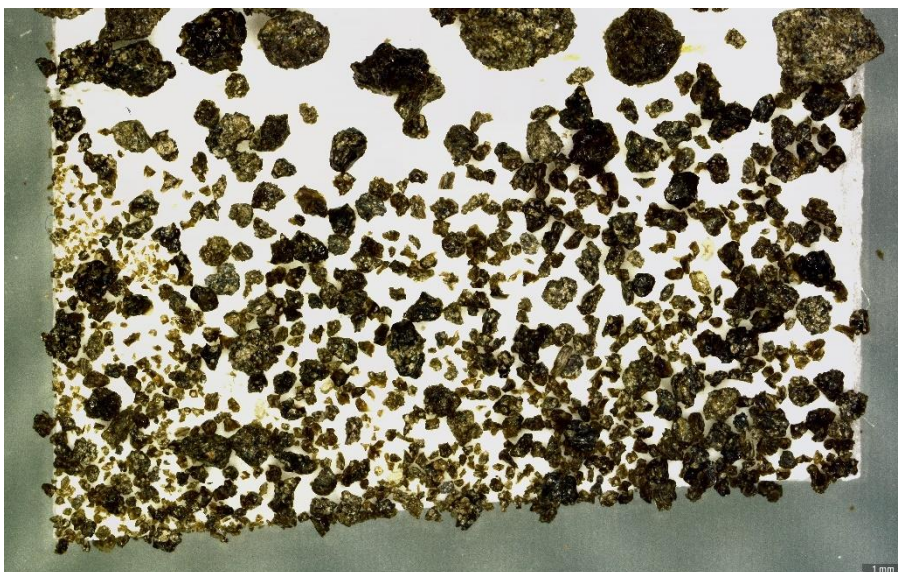


Figure 73 The <1 mm sample is the same as 1 mm but slightly less alteration. Some loose crystals, mostly PLAG.

BH5-7 (18-21 m)

In sample BH5-7 there are altered (yellow and dark orange) glass grains. Phenocrysts are very minimal but there are some white opaque secondary minerals present in a few of the grains. Figures 74 and 75 show 1 mm and <1 mm samples, respectively.

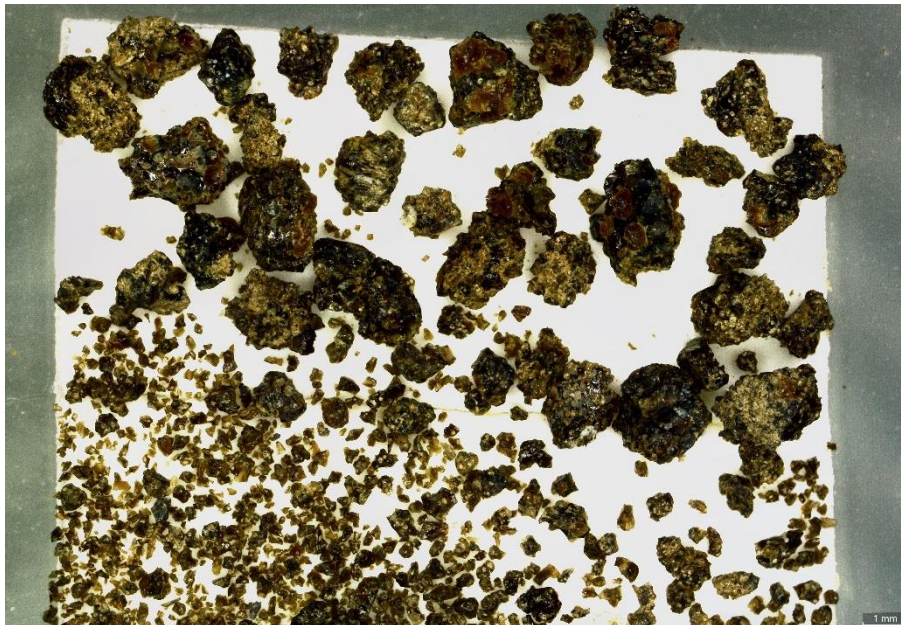


Figure 74 In the 1 mm sample there are altered (light yellow) grains, some with dark orange opaque spots (possibly altered OL). All black grains have some alteration. Most grains are likely glass, as seen by their vitreous surfaces where not altered.

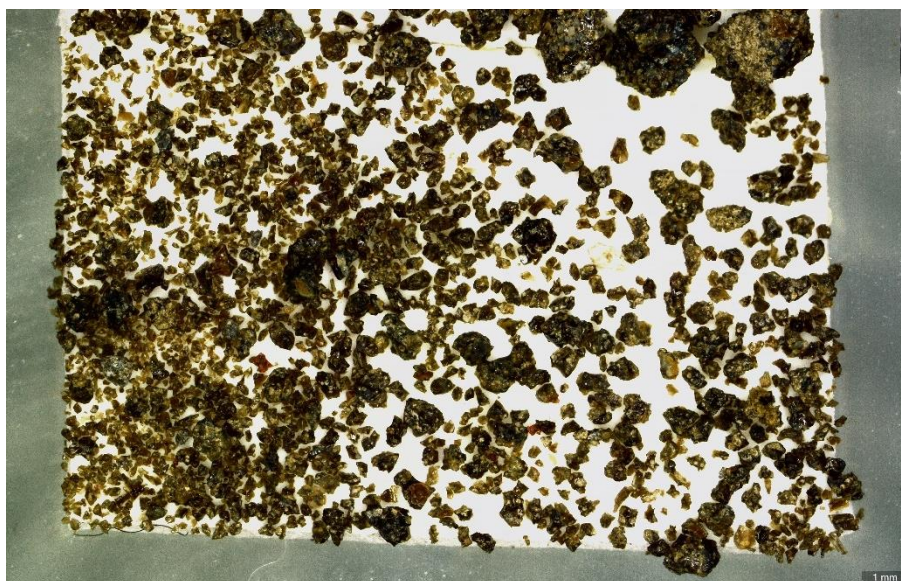


Figure 75 The <1 mm sample is similar to 1 mm but less alteration. Black grains have alteration, but fragments of pure glass are abundant. Two bright red fragments. Some loose crystals are present, mostly PLAG.

BH5-8 (21-24 m)

Sample BH5-8 is very similar to the sample above but is overall not as dark orange. All grains are likely glass, save one light yellow grain that seems to be a cluster of ground glass. Some PLAG is present along with a small amount of white opaque secondary minerals in some of the grains. Figures 76 and 77 show 1 mm and <1 mm samples, respectively.

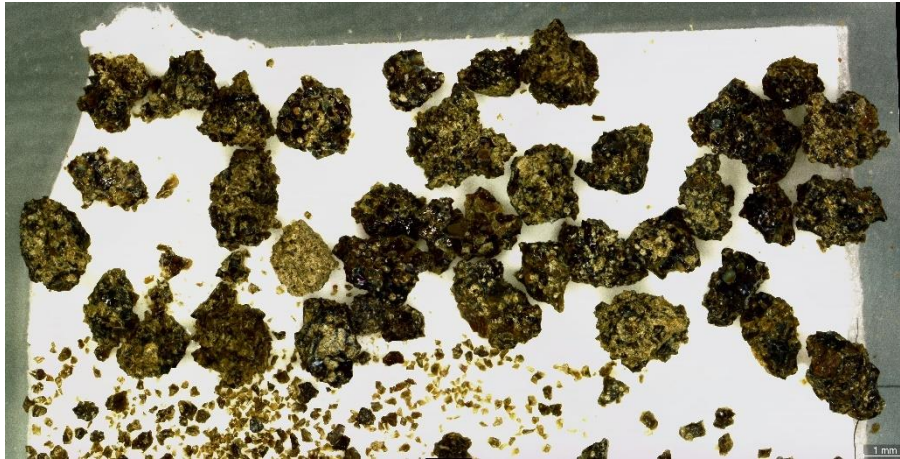


Figure 76 The 1 mm sample is very similar to BH5-7 but less dark orange spots. One grain completely altered (light yellow).

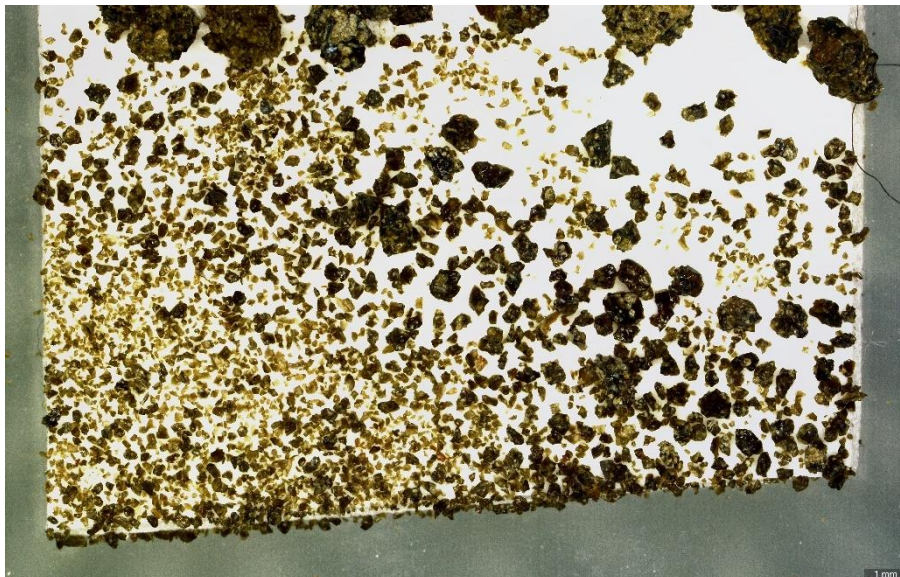


Figure 77 The <1 mm sample is the same as 1 mm but less alteration. Most fragments are <<1 mm so observations may not be very reliable. Small fragments seem to be pure glass.

BH5-9 (24-27 m)

Sample BH5-9 is similar to sample BH5-8 in terms of types of grains (glass) but white opaque secondary minerals are a part of almost all grains. Some grains still have some yellow alteration but that is minimal. Figures 78 and 79 show 1 mm and <1 mm samples, respectively.

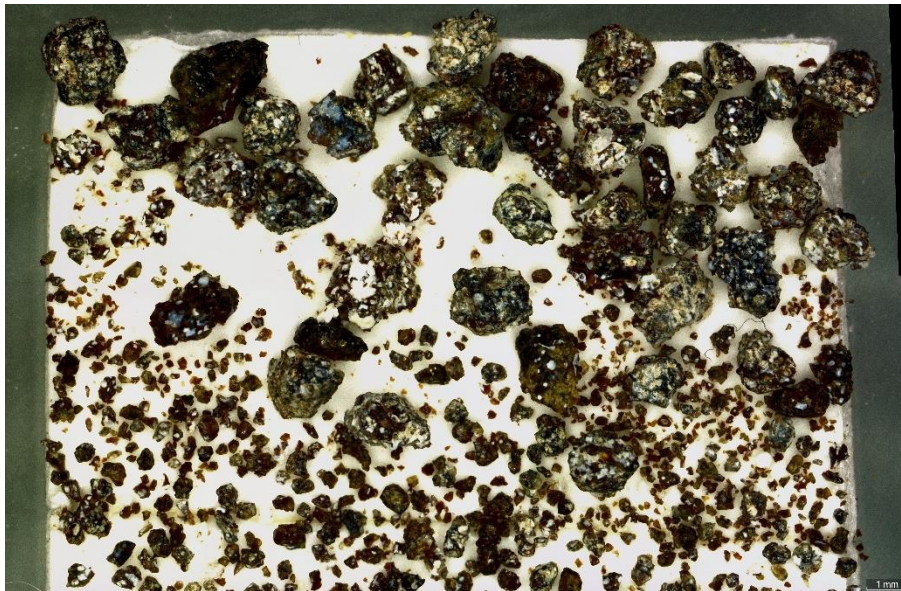


Figure 78 The 1 mm sample is similar to BH5-8 in most ways, but white opaque minerals are very common. Some reddish and light beige alteration present. PLAG crystals present, OL likely but not obvious.

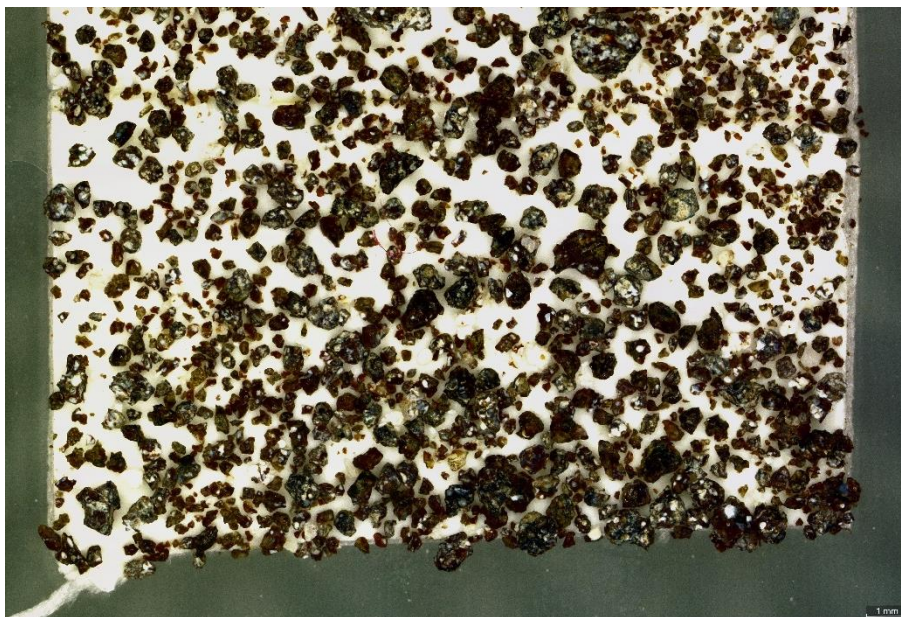


Figure 79 The <1 mm sample is the same as 1 mm. Loose crystals present (OL and PLAG) and white opaque minerals too. Some reddish and light beige alteration present.

BH5-10 (27-30 m)

In sample BH5-10 there is less alteration in the sample prior but the secondary minerals are still very common. All grains are glass altered in one way or another, save one mineral grain that could be PLAG. Figures 80 and 81 show 1 mm and <1 mm samples, respectively.

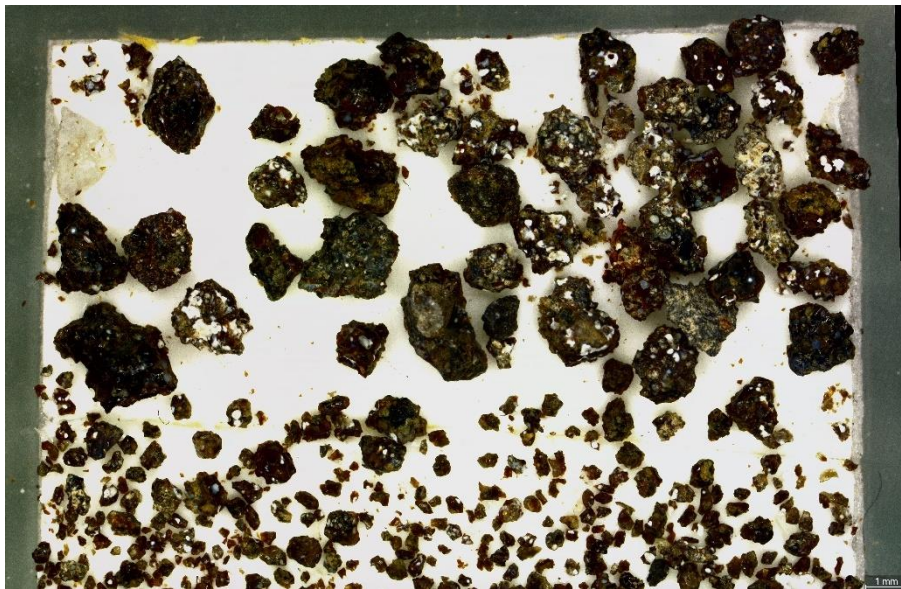


Figure 80 In the 1 mm sample there is less alteration than in BH5-9 but otherwise very similar. One loose PLAG crystal with white opaque spots within it. White opaque minerals are very common in grains (some seem light blue). Most grains (~70%) are likely glass judging from their vitreous surfaces.

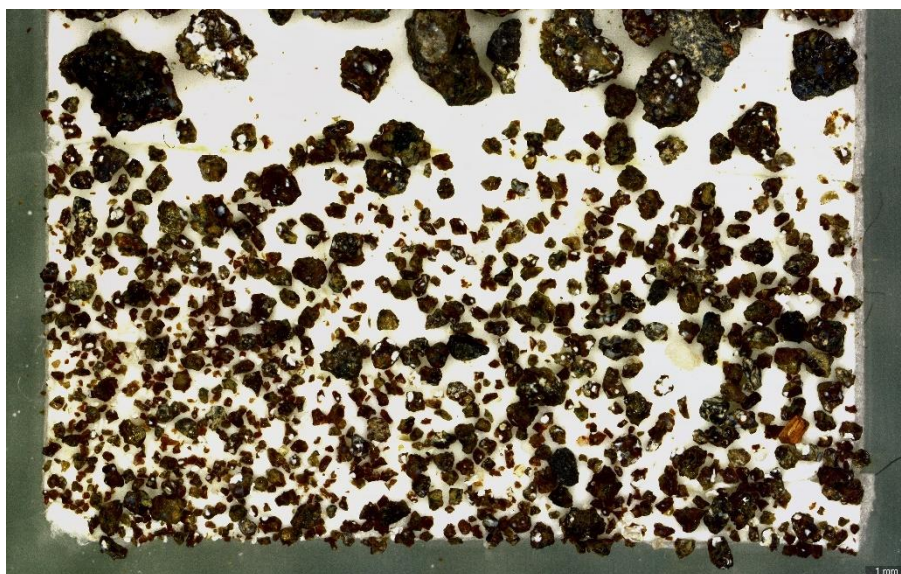


Figure 81 The <1 mm sample is the same as 1 mm but a little less alteration. White opaque minerals present. Loose PLAG and some OL. One orange grain.

BH5-11 (30-33 m)

Sample BH5-11 contains only glass and secondary minerals infilling vesicles in most grains. Yellow alteration is present in most grains, but many grains are also altered to a reddish-brown. The sample presents a few clusters of minerals, both secondary and primary. Figures 82 and 83 show 1 mm and <1 mm samples, respectively.

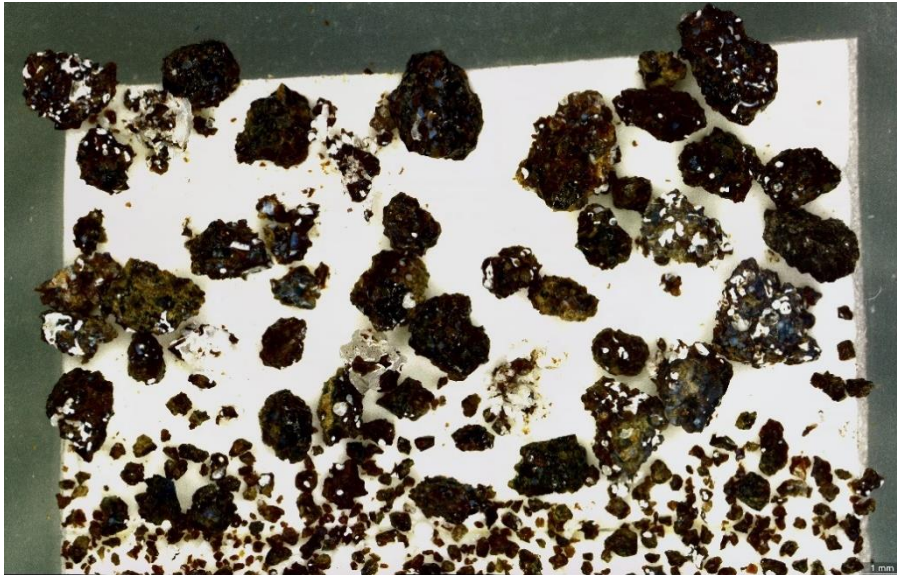


Figure 82 In the 1 mm sample there are black grains present but vesicles are filled in with blueish-milky to white opaque minerals which are found in almost all grains. Most grains have reddish brown to yellow alteration. Clusters of PLAG and white opaque minerals are present.

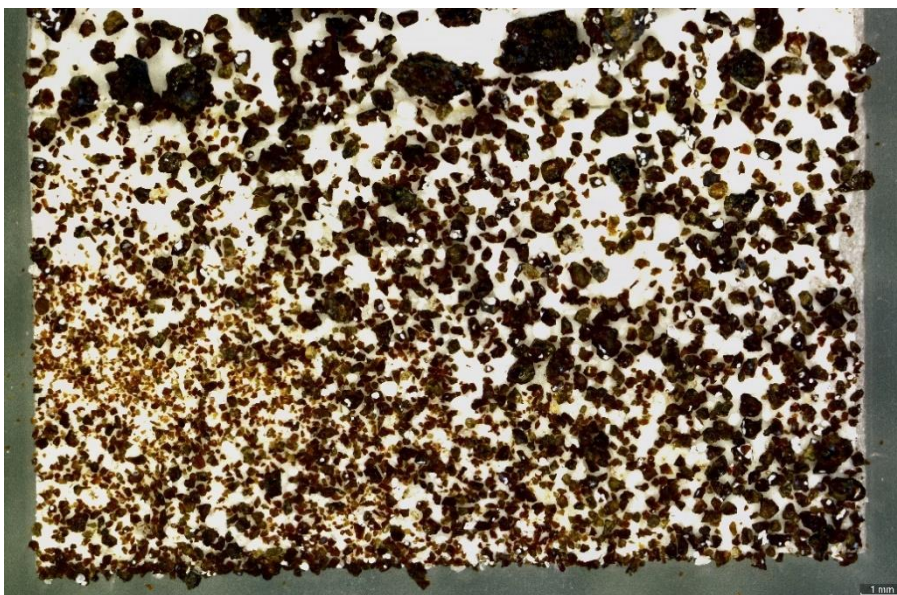


Figure 83 In the <1 mm samples there are many white opaque minerals present along with some clear PLAG and OL. Some reddish altered grains. Many glass fragments. The smallest grains seem red due to their small size.

BH5-12 (33-36 m)

Sample BH5-12 is the same as sample BH5-11. Figures 84 and 85 show 1 mm and <1 mm samples, respectively.

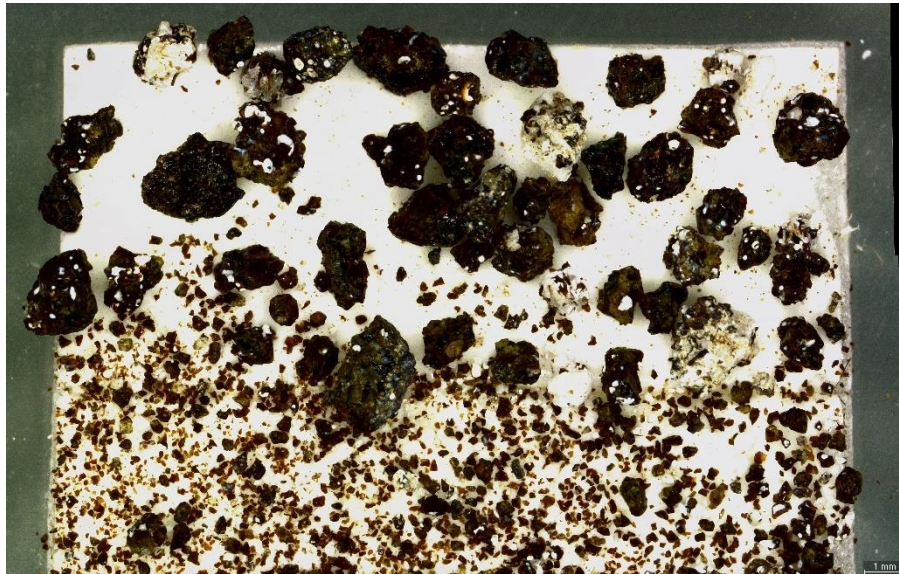


Figure 84 The 1 mm sample is the same as BH5-11.



Figure 85 The <1 mm sample is the same as BH5-11.

BH5-13 (36-39 m)

Most grains in sample BH5-13 have a coating of ground glass, altered to either greenish or yellow color. Other grains have a reddish-brown color like in the last two samples above. Most grains are likely glass. Clusters of secondary minerals are present. Primary minerals (OL and PLAG) are not easily distinguishable in any of the grains. Figures 86 and 87 show 1 mm and <1 mm samples, respectively.

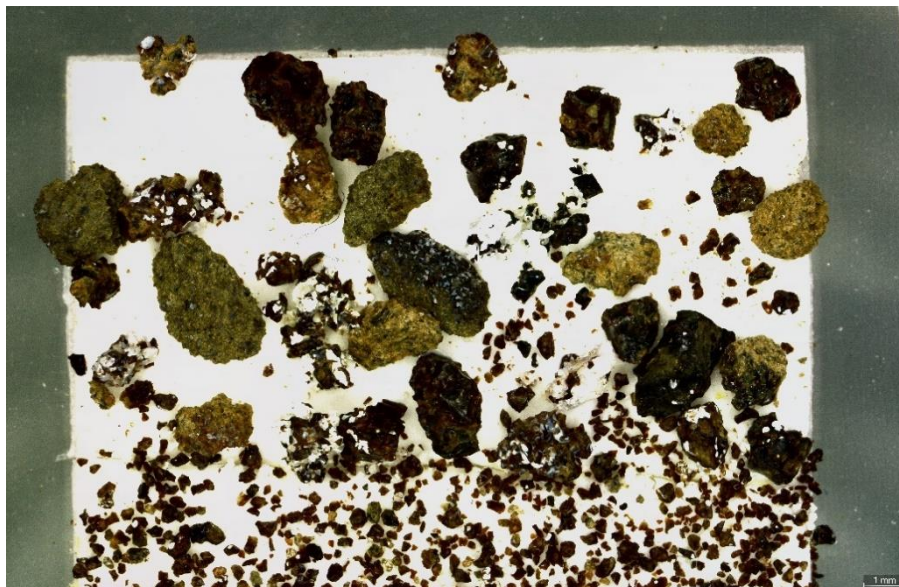


Figure 86 The 1 mm sample is without pure glass. Reddish (45%) to yellow (25%) to green (10%) altered grains. Clusters of white opaque minerals are present (20%), also in many reddish and yellow altered grains, but none in the green grains. They, however, have the blueish milky minerals and some have white semi-opaque minerals.

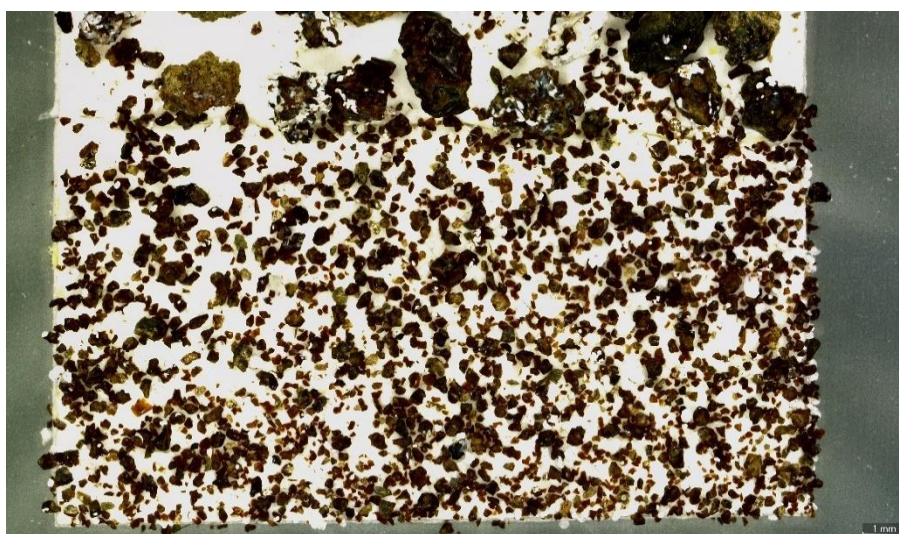


Figure 87 The <1 mm sample is not as altered as 1 mm. OL crystals are present, also PLAG but more of the white opaque and semi-opaque minerals. Most dark grains are reddish.

BH5-14 (39-42 m)

In sample BH5-14 there is only altered glass. Most grains contain a varying amount of secondary minerals (white opaque). Some yellow or light yellow alteration of ground glass is present on some of the grains, while most glass has been altered to a reddish-brown color. Figures 88 and 89 show 1 mm and <1 mm samples, respectively.

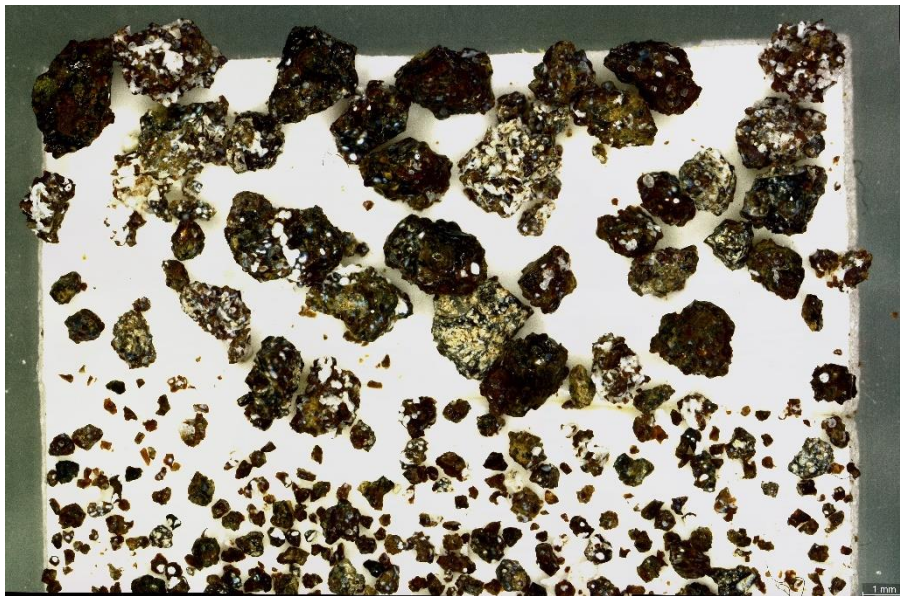


Figure 88 In the 1 mm sample there is no green alteration but some reddish (~45%), some yellow (~10%) and light yellow (~5%). Many grains (~40%) are speckled with white opaque minerals. Possibly some OL crystals present and some PLAG visible but mostly the white opaque minerals, some look blueish milky.

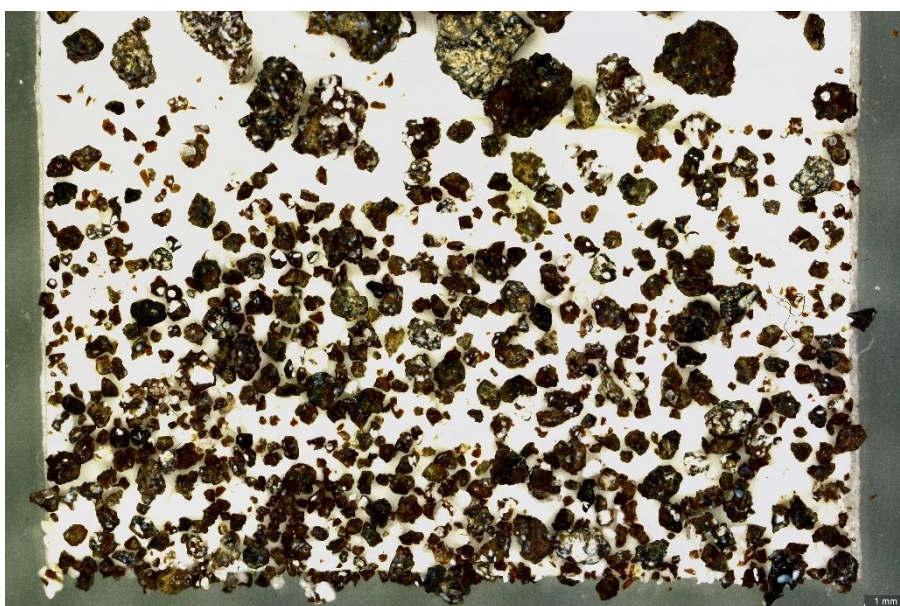


Figure 89 The <1 mm sample is the same as 1 mm.

BH5-15 (42-45 m)

In sample BH5-15 are only glass grains, save one cluster of minerals and a grain completely covered with altered ground glass. All grains are altered to some degree and contain secondary minerals. Figures 90 and 91 show 1 mm and <1 mm samples, respectively.

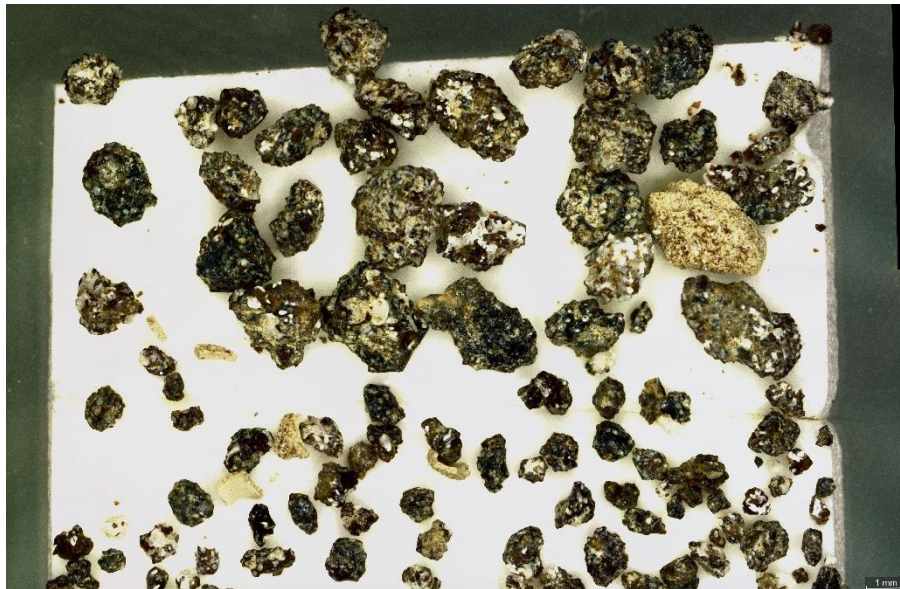


Figure 90 The 1 mm sample is more like sample BH5-9 than the last five samples. There is one completely altered light yellow grain, a cluster of ground glass. No obvious OL or PLAG but white opaque and semi-opaque abundant, some blueish milky.

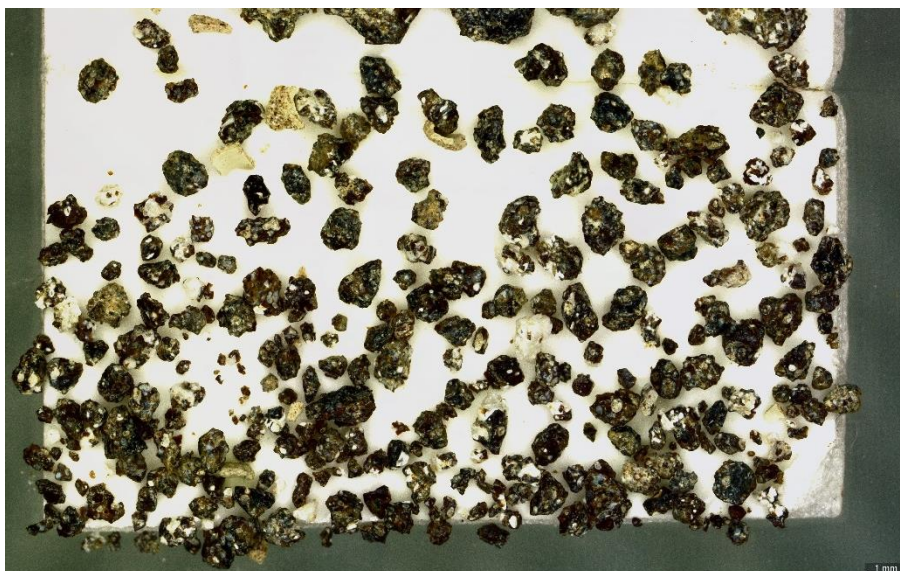


Figure 91 The <1 mm sample is the same as 1 mm. Some light yellow altered grains look like they may have encased another grain but broke apart, they have a smooth textured surface on one side but rough on the other. It looks like the altered grain in the 1 mm sample.

BH5-16 (45-48 m)

Sample BH5-16 is very similar to the sample above. Most grains seem to be glassy but the exact ratio cannot be determined. PLAG seems to be present in some grains but minerals are mostly secondary. Figures 92 and 93 show 1 mm and <1 mm samples, respectively.

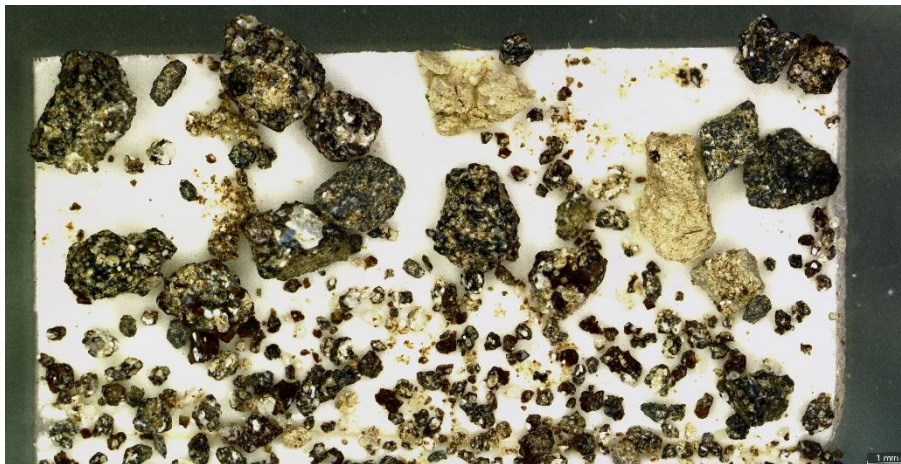


Figure 92 The 1 mm sample is similar to BH5-15. Two light yellow or beige grains. Some PLAG seems to be present.

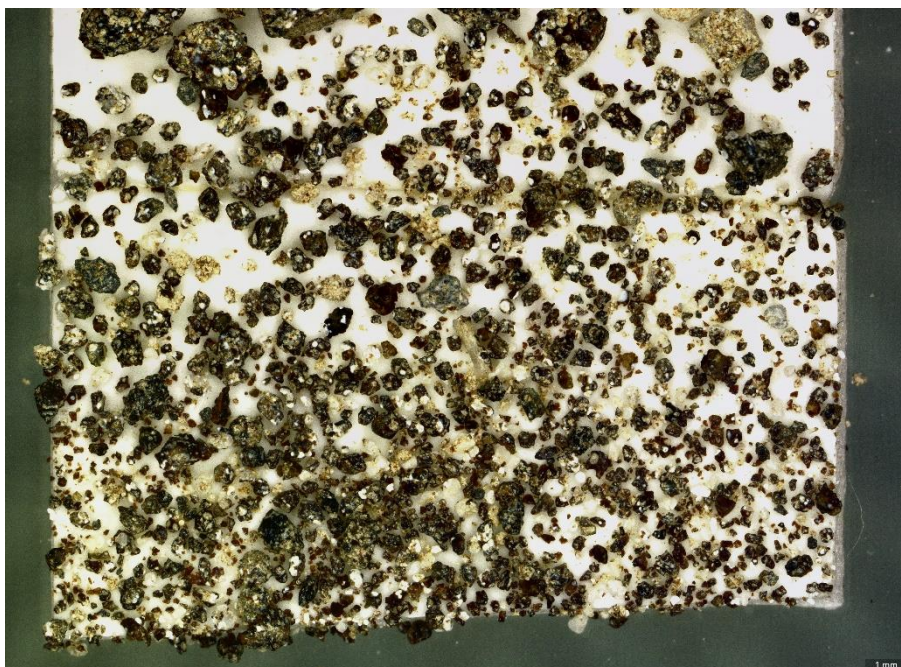


Figure 93 The <1 mm sample is very similar to BH5-15. Some light-blueish grains are present and a long semi opaque crystal. White opaque and semi-opaque minerals are abundant. Some PLAG and possibly OL present.

BH5-17 (48-51 m)

Sample BH5-17 contains mostly glass but some grains seem to be crystalline. Altered ground glass is present in some grains, as are secondary minerals. The crystalline grains seem to be much less altered than the glass. Figures 94 and 95 show 1 mm and <1 mm samples, respectively.

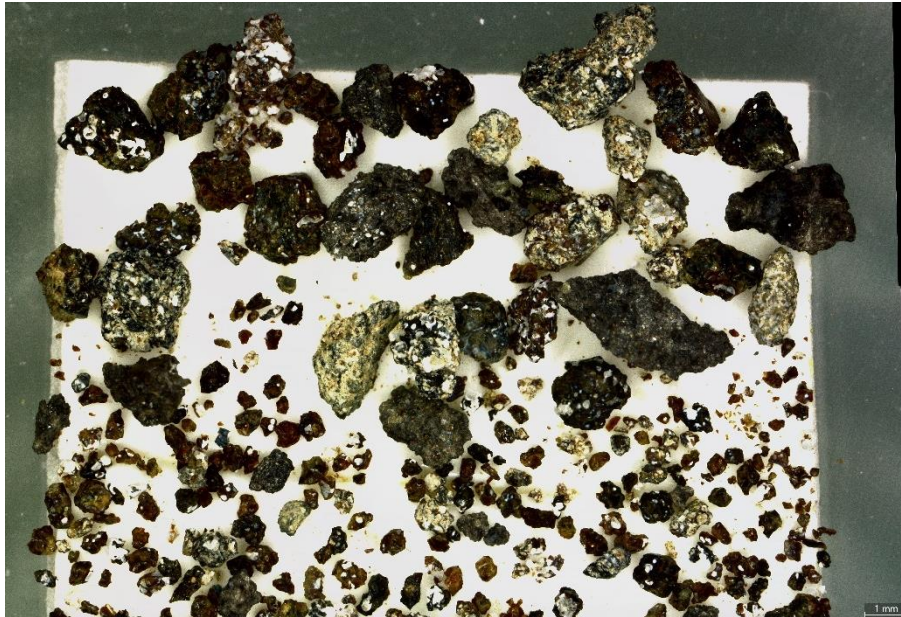


Figure 94 The 1 mm sample is similar to BH5-14 but some grains look very crystalline (~15%). Some grains have a red tint, some have light colored alteration, others are difficult to distinguish. Minerals look the same as before but one obvious OL is present.

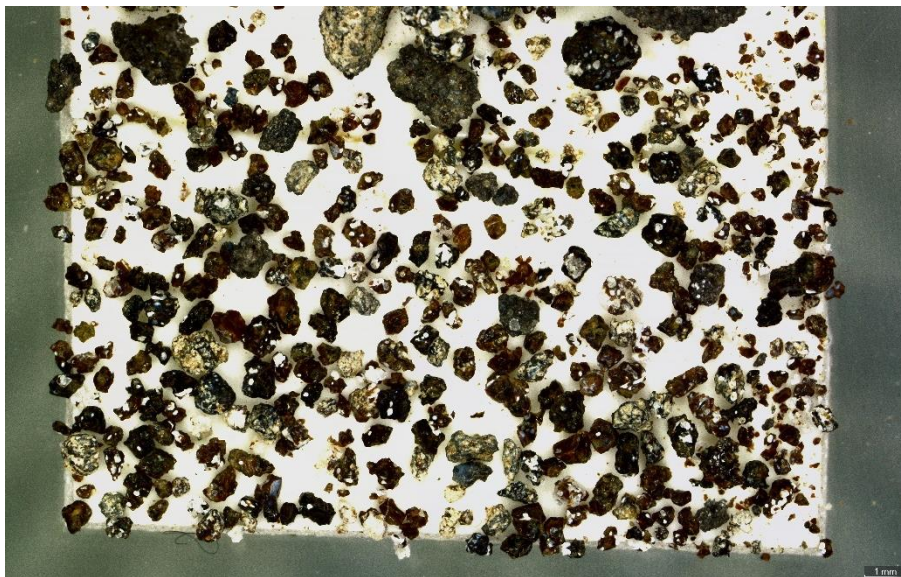



















Figure 95 The <1 mm sample is very similar to BH5-14 and same as 1 mm. Many grains have a red tint. There are some blue areas on some of the grains. Highly crystalline grains are present.

The results of the drilling of borehole BH5 are summarized in Table 2. The top 15 m or so are almost completely crystalline and are therefore classified as a lava delta but the rest of the samples are almost purely glass and are thus classified as hyaloclastite. Most samples include altered ground glass but no density currents occur in this borehole. The samples are all a part of Lambafell proper.

Table 2 This table expresses the main findings in BH5 of Lambafell. The colors represent glass content (blue) and crystalline content (orange).

Sample	Depth (m)	Glass vs. Crystalline	Interpretation	Alteration
BH5-1	0-3		Breccia	Light gray
BH5-2	3-6		Breccia	Light gray, some orange
BH5-3	6-9		Breccia	Light gray, some dark orange
BH5-4	9-12		Breccia	Light gray, some dark red
BH5-5	12-15		Breccia	Minimal light beige
BH5-6	15-18		Breccia	Some light yellow, some reddish in glass
BH5-7	18-21		Volcanic glass	Light yellow and some dark orange in glass
BH5-8	21-24		Volcanic glass	Light yellow, minimal dark orange in glass
BH5-9	24-27		Volcanic glass	Some light beige, some dark red in glass, secondary minerals
BH5-10	27-30		Volcanic glass	Minimal light yellow, some dark red glass, secondary minerals
BH5-11	30-33		Volcanic glass	Minimal yellow, some dark red glass, secondary minerals
BH5-12	33-36		Volcanic glass	Some dark red glass, secondary minerals
BH5-13	36-39		Volcanic glass	Yellow to green, some red glass, secondary minerals
BH5-14	39-42		Volcanic glass	Minimal light yellow, some dark red glass, secondary minerals
BH5-15	42-45		Volcanic glass	Light yellow, some dark red in glass, secondary minerals
BH5-16	45-48		Volcanic glass	Light yellow, some dark red in glass, secondary minerals
BH5-17	48-51		Volcanic glass	Some light yellow, some dark red in glass, secondary minerals

Borehole 6 - BH6 (0-60 m)

The twenty samples collected during drilling of borehole 6 (BH6) are described here. In this analysis we look at grains that are 1 mm and smaller and have been washed by clean water. The grains are almost only crystalline throughout the borehole and rather altered (ground glass). Some secondary minerals occur in some samples. Red grains are common throughout, some are altered red and some oxidized. One sample in particular, BH6-5, contains almost only very dark red grains and looks different from the rest of the samples. Primary minerals are plagioclase, olivine, and possibly pyroxene (PXN). Figures 96-135 show the samples in detail and the drill log is shown in Table 3.

BH6-1 (0-3 m)

In sample BH6-1 there are only crystalline grains, most coated with light gray to light yellow altered ground glass, sometimes yellow. Some grains have a small amount of red alteration. Minerals are PLAG and OL, some darker greens might be PXN. Figures 96 and 97 show 1 mm and <1 mm samples, respectively.



Figure 96 In the 1 mm sample there is light gray to light yellow alteration coat on many grains, sometimes yellow. Some red alteration is present in some grains. No pure glass. Mostly PLAG in crystalline grains, sometimes OL, some darker greens (PXN or OL).

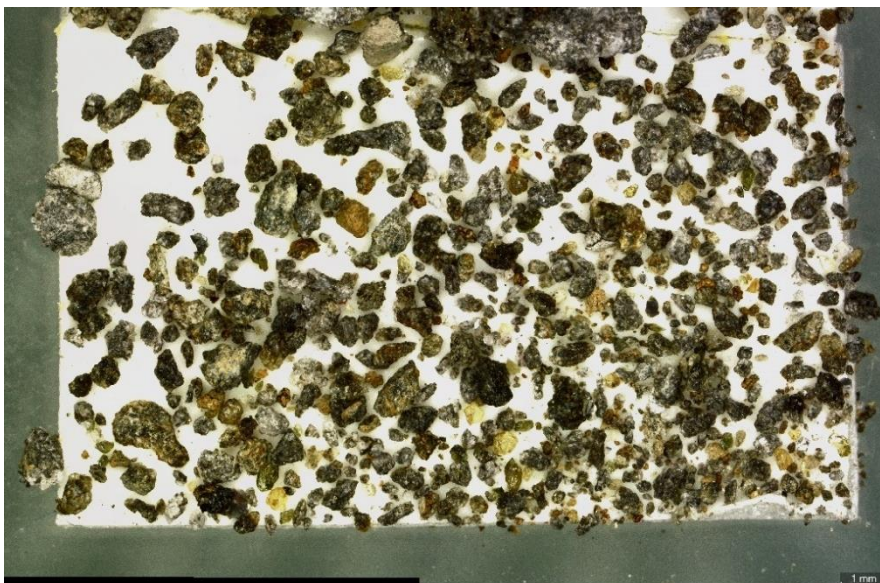


Figure 97 The <1 mm sample is the same as 1 mm, no pure glass. Loose crystals, white to yellow to green to dark green (PLAG, OL, PXN?), some brownish green, some may be gray or grayish blue.

BH6-2 (3-6 m)

In sample BH6-2 there are mainly crystalline grains with light yellow alteration on the surface and only a few glassy grains with many secondary minerals. A few grains have some red areas, possibly from oxidation, but some glass grains are altered to a dark orange or red. Distinguishable primary minerals are PLAG and OL. Figures 98 and 99 show 1 mm and <1 mm samples, respectively.



Figure 98 In the 1 mm sample there is light yellow alteration on most crystalline grains (~90%). Some PLAG is present in a few grains, no obvious OL. The glassy grains (~10%) have white opaque minerals within them and one crystal that is likely OL. Some grains are partly red.



Figure 99 In the <1 mm sample there is one loose OL. Mostly altered crystalline grains (light yellow) like in 1 mm. Opaque white minerals in glass. Orange red and deep and bright red minerals or patches in some grains.

BH6-3 (6-9 m)

Sample BH6-3 is more altered than the first two. All grains are covered, to a varying degree, with light yellow altered round sand. Rather many red grains are present, most likely from alteration than oxidation. There is some hint of glass in this sample but the alteration makes it difficult to determine. PLAG and OL are present. Figures 100 and 101 show 1 mm and <1 mm samples, respectively.

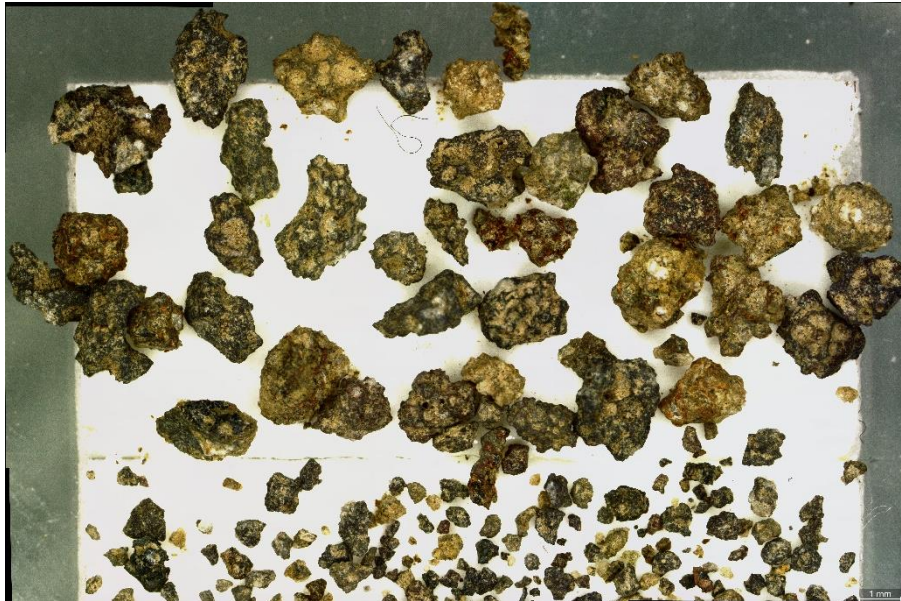


Figure 100 The 1 mm sample is more altered than the two previous samples. Some PLAG and OL, some orange-red and deep red minerals. Some hint of glass but grains are too altered to determine.



Figure 101 In the <1 mm sample there are some grains completely red with crystals and/or light yellow alteration. Minerals present are OL and PLAG. No clean glass.

BH6-4 (9-12 m)

Most grains in sample BH6-4 have a thick coat of altered ground glass. Red grains occur, seemingly both from alteration and oxidation. Figures 102 and 103 show 1 mm and <1 mm samples, respectively.

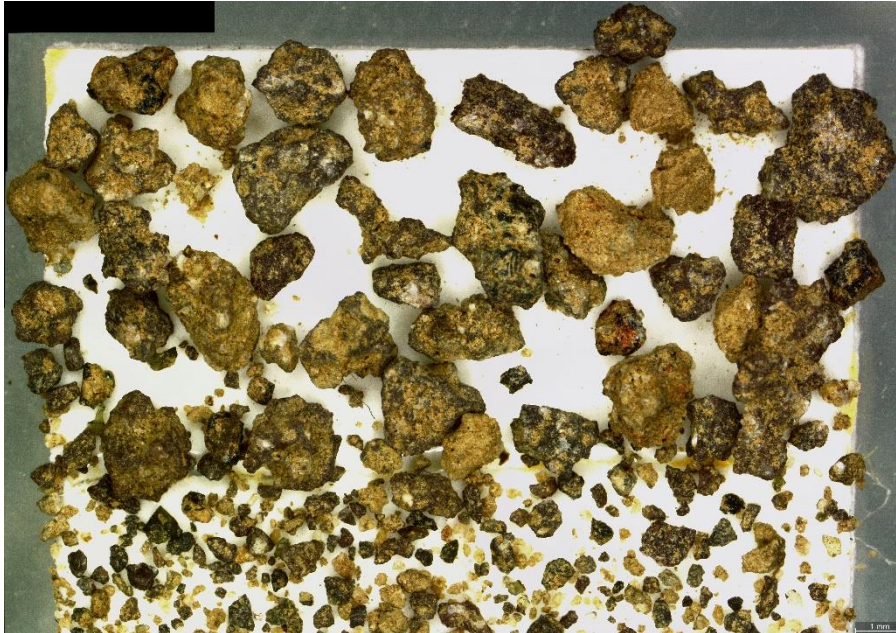


Figure 102 The 1 mm sample is similar to BH6-3 but no pure glass. Many grains are completely altered (yellow) or red colored, dark and bright.

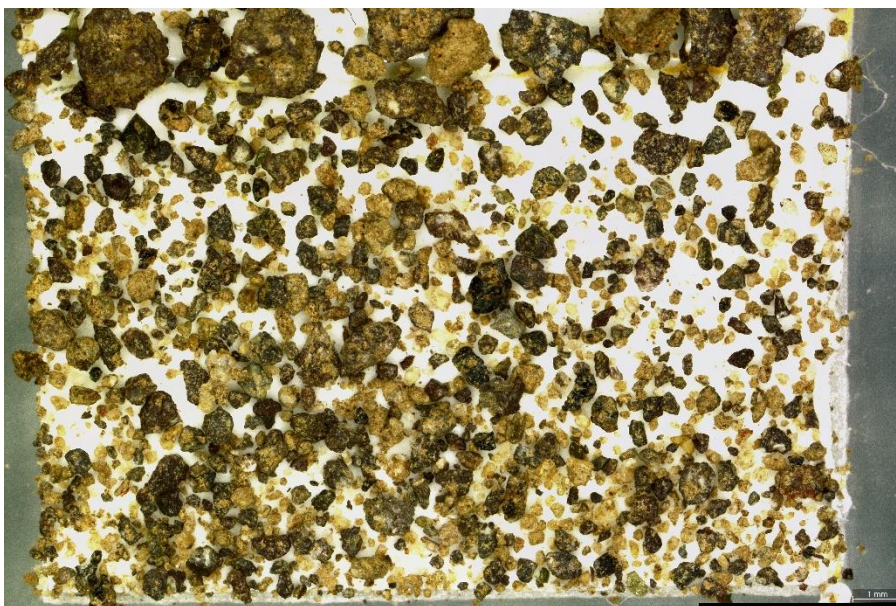


Figure 103 The <1 mm sample is the same as BH6-3, more loose crystals (white to light yellow to green; PLAG and OL). One opaque gray grain (PLAG?). One opaque blueish green grain. No pure glass.

BH6-5 (12-15 m)

Sample BH6-5 is very different from prior samples. Almost all grains have a very dark red color. This seems to be from alteration rather than oxidation because of how the grains look. The surface looks like it is made up of red sand (compared to sample BH6-18). Figures 104 and 105 show 1 mm and <1 mm samples, respectively.



Figure 104 In the 1 mm sample there is drastic difference between this and the prior samples. Everything seems dark red. PLAG and OL are common in grains. Some grains contain light yellow (altered) material. A dark green mineral in one grain (PXN?). No pure glass.



Figure 105 In the <1 mm sample there is variance in color – black, dark red, orange red, and almost pink. PLAG and OL common in grains and on their own. One dark green crystal on the bottom left, possibly PXN. No pure glass.

BH6-6 (15-18 m)

In sample BH6-6 there are only crystalline grains, either dark red, gray, or black. Some grains have a light yellow or green alteration coat. Some secondary minerals occur. Primary minerals are PLAG and OL. Figures 106 and 107 show 1 mm and <1 mm samples, respectively.



Figure 106 In the 1 mm sample there is no pure glass. Some dark red grains (~25%), some black with light patches (alteration and/or minerals, some opaque; ~50%). Some completely altered grains (light, some greenish; ~10%). The rest (~15%) are undefined.



Figure 107 In the <1 mm sample there is more color variance than in 1 mm. No pure glass. Grains are dark red, black with alteration and/or minerals, and completely altered (yellow, some greenish) in similar ratio as in 1 mm. Loose PLAG and OL.

BH6-7 (18-21 m)

Sample BH6-7 contains only crystalline grains that have very minimal light yellow alteration. Some red grains are present, dark red to dark orange. Some grains contain secondary minerals. PLAG is common but OL less so. There may be some PXN present. Figures 108 and 109 show 1 mm and <1 mm samples, respectively.



Figure 108 In the 1 mm sample there are more black or dark gray grains (70%), but no pure glass. PLAG and OL present in black grains. Some orange grains (~10%) with opaque minerals along with PLAG and OL. Some dark red grains (~10%) with minerals (at least PLAG). Crystalline grains with a coarse groundmass (~10%) are also present, with a slight green tint. One completely altered grain (brownish yellow). Others are undefined.



Figure 109 The <1 mm sample is the same as 1 mm. Some loose PLAG and OL (clear, light yellow, deep green (PXN?)).

BH6-8 (21-24 m)

In sample BH6-8 there are black crystalline grains and slightly altered coarse crystalline grains. There is hint of some glass but it is difficult to distinguish from the crystalline grains. Figures 110 and 111 show 1 mm and <1 mm samples, respectively.

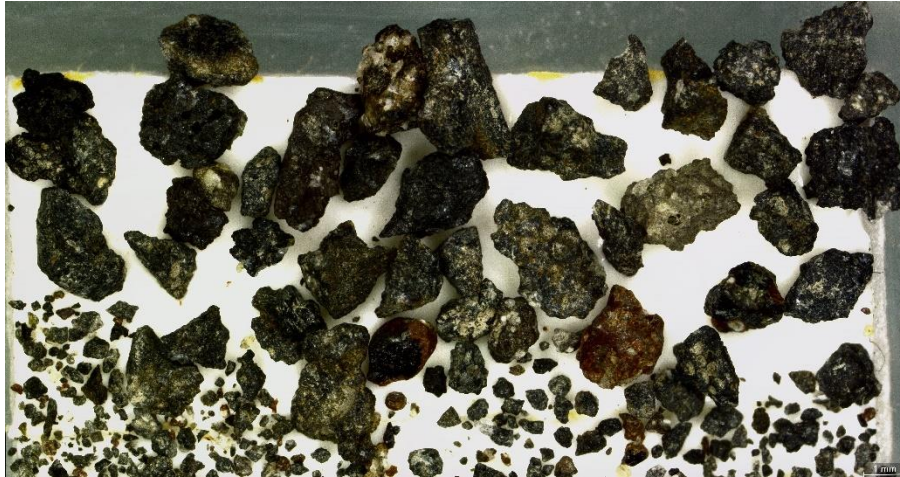


Figure 110 In the 1 mm sample there are black crystalline grains (~25%) with some phenocrysts and slightly altered coarse crystalline grains (~65%) with more prominent phenocrysts. Some hint of glass. One dark orange grain with some minerals, either primary or secondary. Two deep orange and black grains with 1-2 phenocrysts. One gray grain with minerals looks completely altered. PLAG is common, no obvious OL, some opaque secondary minerals are present overall.



Figure 111 The <1 mm sample is the same as 1 mm. Some loose crystals (clear, light yellow, dark green – PLAG, OL, PXN?).

BH6-9 (24-27 m)

In sample BH6-9 there are only crystalline grains, both coarse crystalline and black. Dark orange to red grains (alteration) are present. Some secondary minerals are present in a few grains. Distinguishable primary minerals are PLAG and possibly PXN. Figures 112 and 113 show 1 mm and <1 mm samples, respectively.

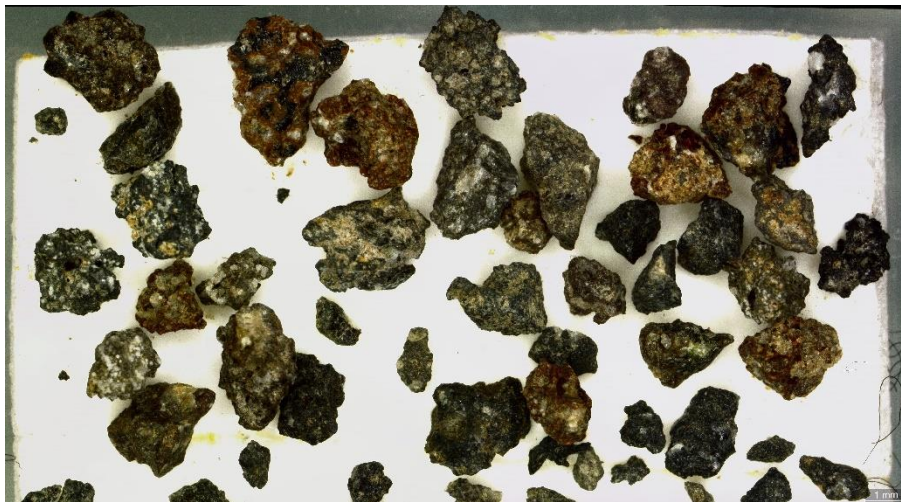


Figure 112 In the 1 mm sample there are coarse crystalline grains with an alteration coat and/or white opaque minerals and PLAG phenocrysts (40%). Black crystalline grains (~30%), some with PLAG phenocrysts, one with a dark green phenocryst (PXN?). Orange grains (~25%; some with black, some not) with PLAG phenocrysts and some other altered material. Only two dark red grains, altered and with PLAG phenocrysts (~5%).



Figure 113 The <1 mm sample is very similar to 1 mm but some grains have yellow alteration, one with orange-yellow alteration.

BH6-10 (27-30 m)

Sample BH6-10 contains some glass but mostly crystalline grains. Red grains and secondary minerals occur. Figures 114 and 115 show 1 mm and <1 mm samples, respectively.

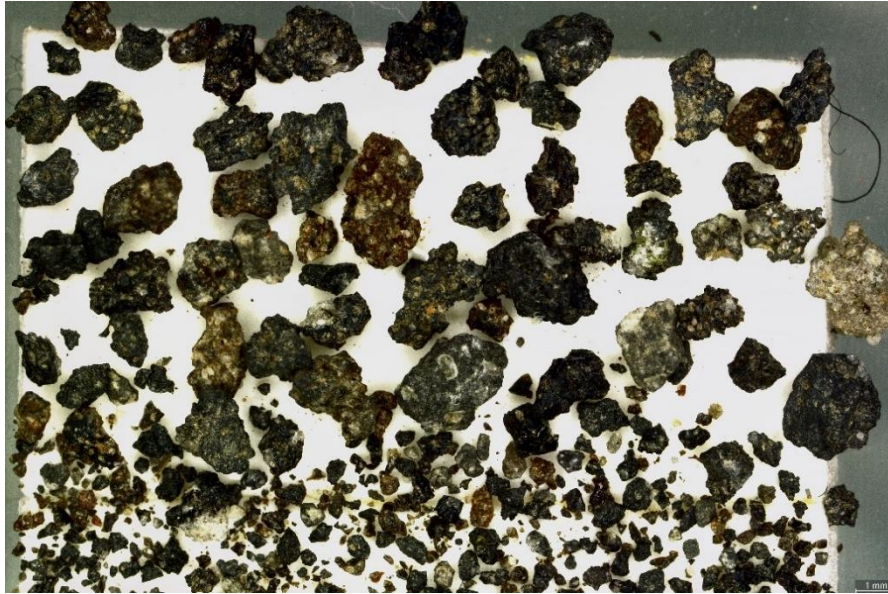


Figure 114 In the 1 mm sample there is some glass present (~10%), some of it is slightly altered and some grains seem relatively crystalline. There are mostly black crystalline grains (~55%), some slightly altered and most have PLAG phenocrysts, one with two large vibrant green phenocrysts (OL or PXN). There are also crystalline grains with a coarse groundmass (20%), some slightly altered, some with obvious PLAG phenocrysts, some with white opaque minerals. A few red grains are present (15%), all with secondary minerals.



Figure 115 The <1 mm sample is the same as 1 mm. Some loose crystals, clear white (PLAG) and vibrant green (OL or PXN).

BH6-11 (30-33 m)

Sample BH6-11 contains only fairly altered crystalline grains. Minerals are mostly PLAG and secondary. Some red or dark orange in some grains. Figures 116 and 117 show 1 mm and <1 mm samples, respectively.



Figure 116 In the 1 mm sample there are black crystalline grains (~85%), with alteration of varying degree, and coarse crystalline grains (~15%). Some of the black grains have vitreous surfaces and could be glassy but most are likely rather crystalline. PLAG is the most clearly visible primary mineral but not very common overall. There are hints of green in some of the grains, but it is difficult to determine if that is OL. Secondary minerals are present.



Figure 117 The <1 mm sample is the same as 1 mm. A few red grains. Three loose light yellow to yellow crystals (PLAG and/or OL). Some glass grains seemingly without phenocrysts are present.

BH6-12 (33-36 m)

Most grains in sample BH6-12 are coated with light gray altered ground glass. There are a few glass grains. PLAG and OL are present along with secondary minerals. Figures 118 and 119 show 1 mm and <1 mm samples, respectively.

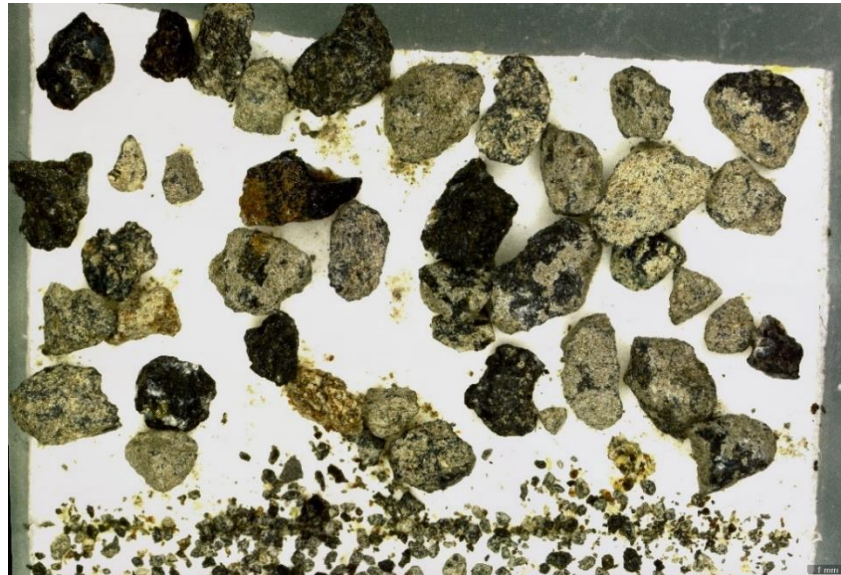


Figure 118 Most grains in the 1 mm sample have a thick light colored alteration coat (~75%) and thus it is difficult to determine the type of grain. Some grains are vitreous, one more so than others (black with orange alteration), but most are relatively crystalline. Obvious phenocrysts (PLAG and OL) are not common in unaltered grains. Some white opaque secondary minerals are present.



Figure 119 In the <1 mm sample the alteration coating is thinner than in 1 mm. Many black grains are vitreous. There are a few loose PLAG and OL (clear to light yellow to green). Some orange/red grains are present.

BH6-13 (36-39 m)

Almost all grains in sample BH6-13 are covered with light yellow altered ground glass. A few glass grains are present along with some red altered grains with secondary minerals. Most grains seem to be crystalline. There are very few phenocrysts visible but PLAG is present. Figures 120 and 121 show 1 mm and <1 mm samples, respectively.



Figure 120 In the 1 mm sample there is altered coating (light yellow) on almost all grains, making distinction between them difficult. There are a few fully crystalline grains. There seem to be a few glass grains of varying crystallinity. Some red grains are present. Two crystalline grains have PLAG phenocrysts. Not many obvious phenocrysts are present overall, but the red grains contain white opaque minerals.



Figure 121 The <1 mm sample is the same as 1 mm. Some grains have no altered coating. Loose crystals are very sparse.

BH6-14 (39-42 m)

There is still some light yellow altered ground glass in sample BH6-14 but much less than in the previous sample. There is a hint of glass in the sample. Red altered grains are common, as are secondary minerals. Some PLAG is present. Figures 122 and 123 show 1 mm and <1 mm samples, respectively.

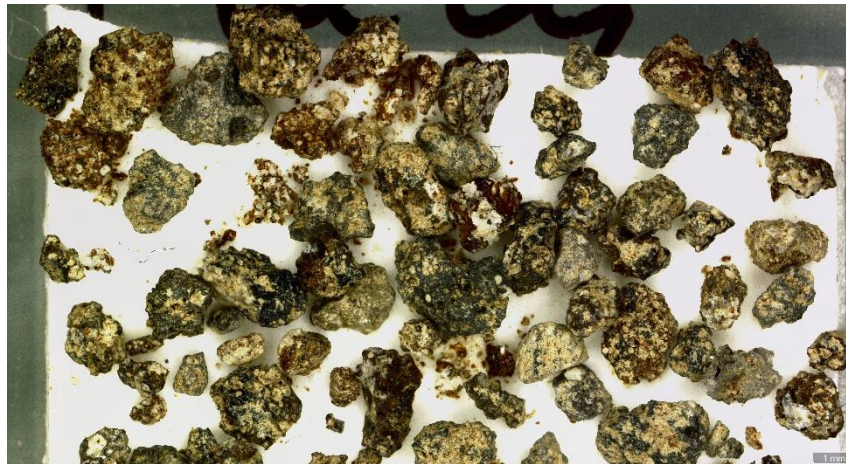


Figure 122 In the 1 mm sample there is still some altered coating on some grains, making distinction difficult, but to a lesser extent than in BH6-13. Crystalline grains seem to be the most common type, then black vitreous grains, and fewest are the red grains. Very few phenocrysts overall, but white opaque minerals are very common in the red grains.

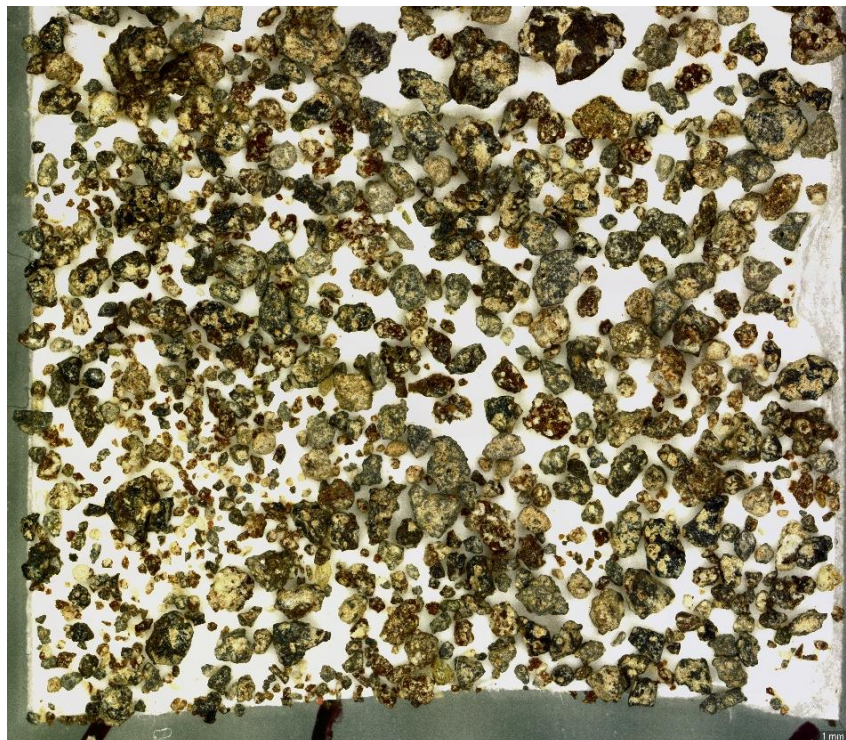


Figure 123 The <1 mm sample is the same as 1 mm. Loose crystals are more common than in BH6-13 (clear, light yellow, green).

BH6-15 (42-45 m)

In sample BH6-15 are mostly crystalline grains but a few glass grains are present but they are rather crystalline. Red grains are present along with a grain coated with altered ground glass. No obvious primary minerals but secondary minerals are present. Figures 124 and 125 show 1 mm and <1 mm samples, respectively.



Figure 124 In the 1 mm sample there are mostly crystalline grains (~75%) along with a few glassy grains (~20%), two red grains and one with an altered coating. No phenocrysts to speak of but there is a hint of OL in some grains. The red grains and one crystalline grain contain white opaque minerals.



Figure 125 The <1 mm sample is the same as 1 mm. Only two to three loose crystals, PLAG and OL.

BH6-16 (45-48 m)

Sample BH6-16 mostly contains crystalline grains but vitreous grains, black and dark red, are present as well. Most grains are somewhat altered which makes distinction between grains difficult. There are no secondary minerals present and only a few OL. Figures 126 and 127 show 1 mm and <1 mm samples, respectively.



Figure 126 In the 1 mm sample there are mostly crystalline grains (~55%; some reddish), some black vitreous grains (~25%), and some dark red vitreous grains (~20%). All types have both altered and non-altered grains, but most grains are altered which could obscure the distinction between grain types. One obvious OL phenocryst, no white opaque minerals.



Figure 127 The <1 mm sample is the same as 1 mm. Some grains have dark orange areas. A few loose OL.

BH6-17 (48-51 m)

Sample BH6-17 contains more crystalline grains than the prior sample but contains a few red oxidized grains. Some vitreous grains are dark red and secondary minerals are very sparse. Very few OL and PLAG are present. Figures 128 and 129 show 1 mm and <1 mm samples, respectively.

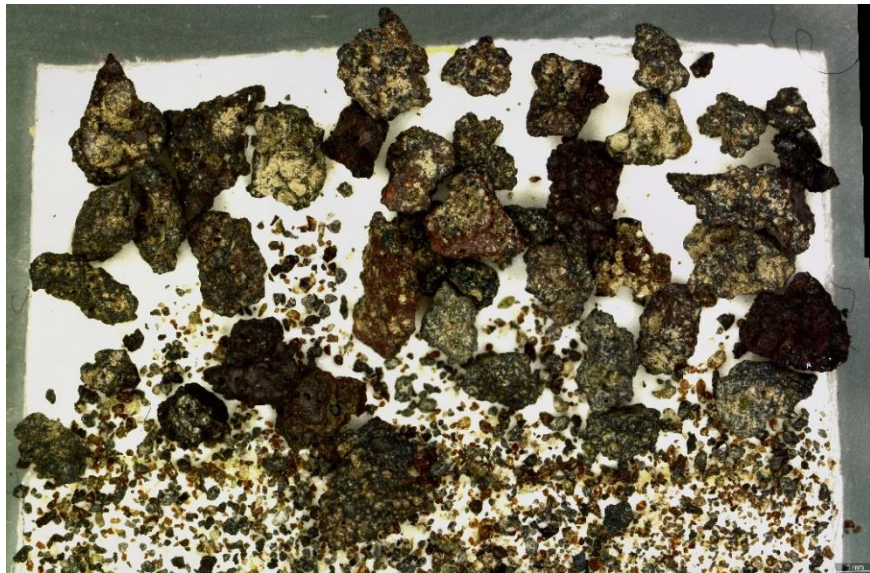


Figure 128 In the 1 mm sample there are mostly crystalline grains (~85%) of which about half are reddish. Other are black vitreous (some slightly crystalline; ~10%) and dark red vitreous grains (~5%). Very few obvious phenocrysts, two PLAG and possibly one OL. Some white opaque minerals are found in one red vitreous grain.



Figure 129 The <1 mm sample might be the same as 1 mm but most grains are <<1 mm so it is difficult to determine. PLAG and OL present.

BH6-18 (51-54 m)

Sample BH6-18 contains only crystalline grains of which about half are oxidized red. The light yellow altered ground glass is minimal in all grains. No phenocrysts are detectable and secondary minerals do not seem to be present. Figures 130 and 131 show 1 mm and <1 mm samples, respectively.

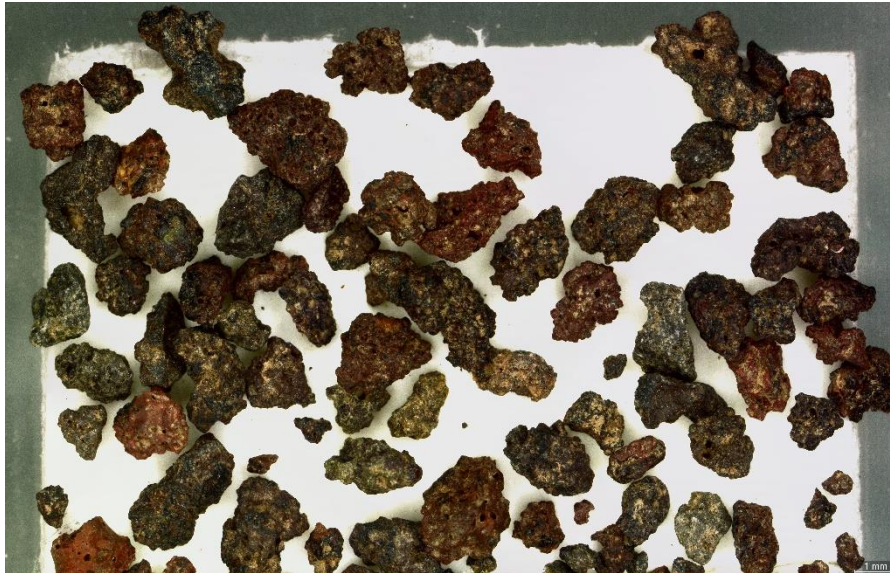


Figure 130 In the 1 mm sample there is almost no light colored alteration. Mostly orange red to deep red crystalline grains, only about five dark crystalline grains, no glass. Not many obvious phenocrysts.

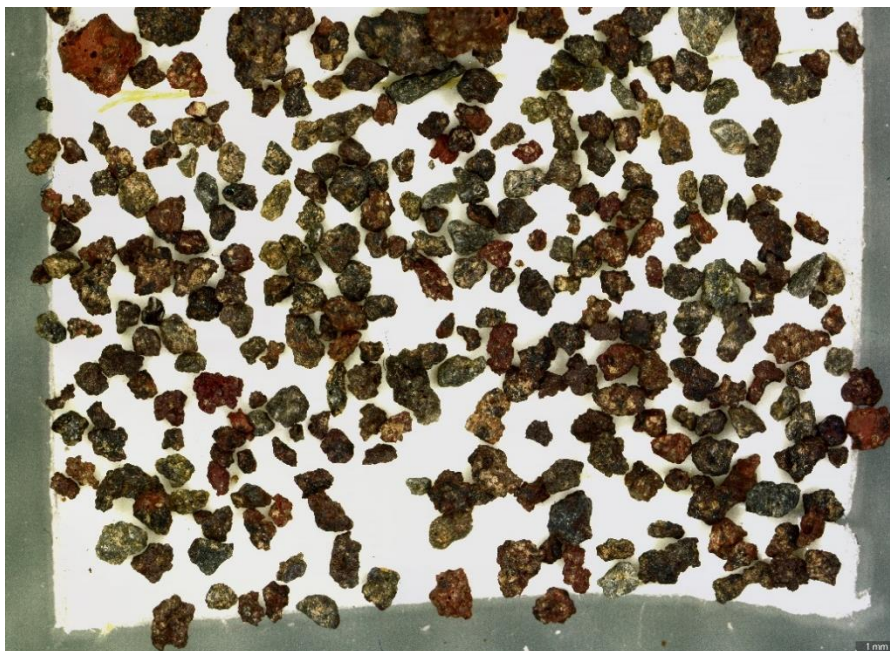


Figure 131 The <1 mm sample is the same as 1 mm. No glass.

BH6-19 (54-57 m)

Sample BH6-19 only contains crystalline grains but some of them have slightly vitreous surfaces. Light yellow altered ground glass is present in most grains. There are no obvious primary minerals in the sample but a few spots on secondary minerals are present. Figures 132 and 133 show 1 mm and <1 mm samples, respectively.



Figure 132 The 1 mm sample contains only crystalline grains and only a few of them are dark gray, almost all of them seem to be orange red, deep red, or have some red in them. Only a handful of black grains have vitreous surfaces but none of them are pure glass. No obvious minerals.



Figure 133 The <1 mm sample is the same as 1 mm. No blueish green speckles, no loose crystals.

BH6-20 (57-60 m)

In sample BH6-20 there are only crystalline grains of various colors, red to black. No primary minerals are visible but there is a hint of a few secondary minerals. Figures 134 and 135 show 1 mm and <1 mm samples, respectively.

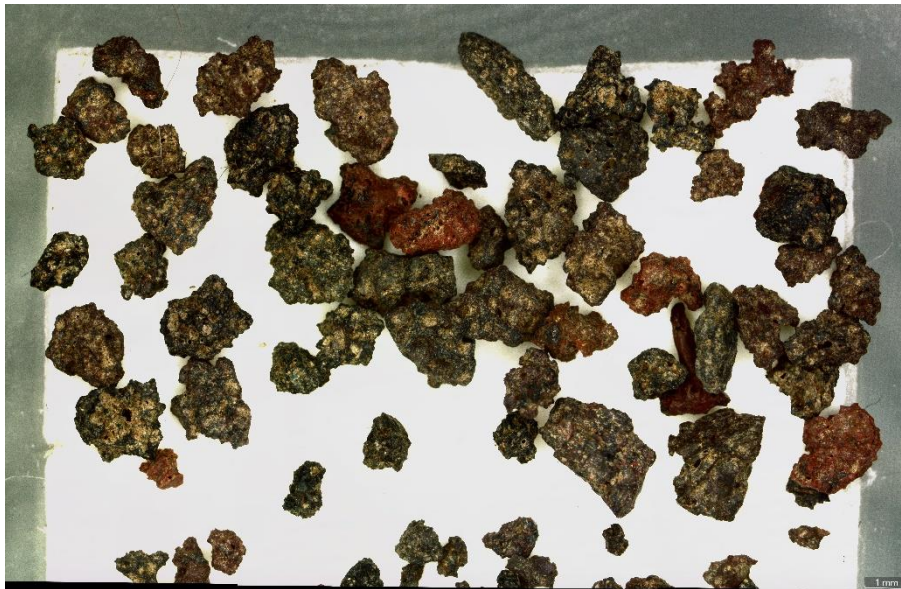


Figure 134 In the 1 mm sample there is no glass. The crystalline grains are red, deep red, black, and dark gray, in about even proportions. One red grain with smooth surfaces, non-vitreous. No obvious crystals.

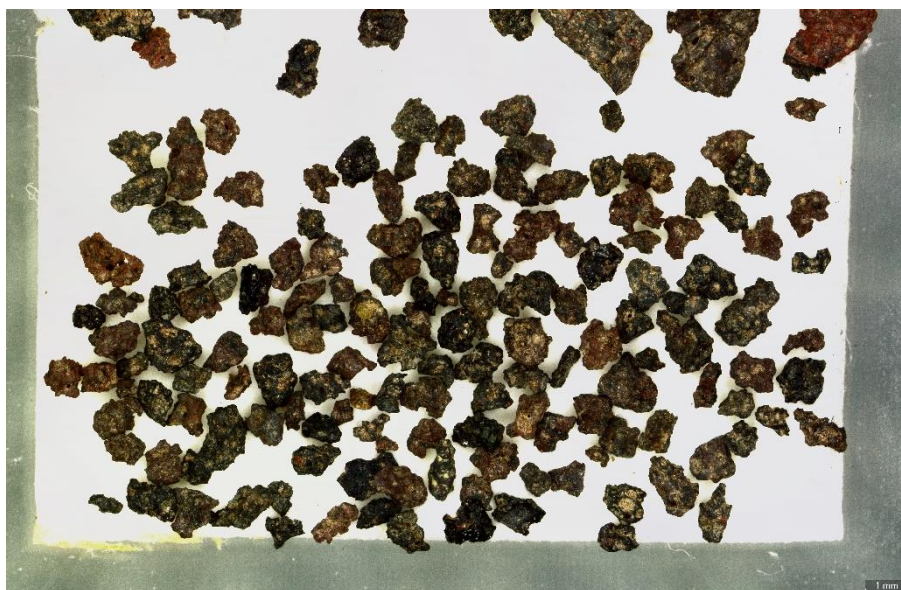


Figure 135 The <1 mm sample is the same as 1 mm but the red colors are more muted.

The results of the drilling of borehole BH6 are summarized in Table 3. This borehole is the most crystalline out of the three and the most altered in reference to glass and secondary minerals. Altered ground glass is common in most samples and density currents are considered to occur twice in the borehole. Likewise, red grains are common and have been altered to a red color or oxidized. In sample BH6-18, most grains are oxidized red and could thus be taken to represent the top of an older formation to Lambafell proper. More likely, all samples in BH6 are a part of phase IV, when lava started flowing subaerially during the eruption that formed the mountain, as subaerial lava is visible on the surface by BH6 at and above about 420 masl (Figure 145).

Table 3 This table expresses the main findings in BH6 of Lambafell. The colors represent glass content (blue) and crystalline content (orange), but density currents (yellow) are taken to be where the samples have a thick cover of altered ground glass. The dark red line represents the bottom of Lambafell proper.

Sample	Depth (m)	Glass vs. Crystalline	Interpretation	Alteration
BH6-1	0-3		Lava	Light gray to yellow, red in some grains
BH6-2	3-6		Breccia	Light yellow, some red in some grains (oxidized?)
BH6-3	6-9		Density current	Yellow, red grains
BH6-4	9-12		Density current	Yellow, dark red grains
BH6-5	12-15		Breccia	Minimal light beige, almost only very dark red grains
BH6-6	15-18		Breccia	Light yellow, dark red grains
BH6-7	18-21		Breccia	Minimal, some dark red grains
BH6-8	21-24		Breccia	Minimal, some red grains
BH6-9	24-27		Breccia	Light beige, red grains, some secondary minerals
BH6-10	27-30		Breccia	Minimal, some red grains, some secondary minerals
BH6-11	30-33		Breccia	Light yellow
BH6-12	33-36		Density current	Light gray to light yellow, some yellow on a glass grain
BH6-13	36-39		Density current	Light yellow, some red grains, secondary minerals
BH6-14	39-42		Density current	Light yellow, red grains, secondary minerals
BH6-15	42-45		Breccia	Minimal light yellow, one red grain, secondary minerals
BH6-16	45-48		Breccia	Light yellow, some dark red grains
BH6-17	48-51		Breccia	Light yellow, a few red (oxidized) and dark red grains
BH6-18	51-54		Breccia	Minimal, many red grains (oxidized)
BH6-19	54-57		Breccia	Minimal light yellow, many red grains (oxidized)
BH6-20	57-60		Breccia	Minimal light yellow, many red grains (oxidized)

5 Geological interpretations of Lambafell

This geological assessment of Lambafell started during the summer of 2022 with lidar droning and drilling of the three boreholes. The aim was to quantify different geological units that make up the mountain. In comparison to ideal subglacial eruptive formations (Figure 3) we have identified five of the main phases that characterize subglacial volcanic mountains. Only one of the units, the pillow lava formed at the base in subglacial eruptions, is not seen at surface or in geological sections. This suggests that either it is absent or that it is buried at considerable depth underneath the mountain.

The general structure of the massive is that pillow basalts and pillow breccias cover the southeast, east, and north slopes of the mountain. These units show dipping from the summit to the foot of Lambafell. That suggests that they erupted from the summit crater and flowed down the slopes of the mountain. These units further show lower angle of dipping with altitude, in accordance with formation of a lava delta in an intraglacial lake (Figure 136). The northwest side of Lambafell, on the other hand, only has sporadic pillow lava streams coming from the summit area (Figure 141). However, in the summit region there are relatively flat lava flows that flowed towards the southeast, feeding the pillow-breccia delta observed in the Eden quarry and in the southeast slopes of Lambafell (Figures 139 and 140).

In the summit area of Lambafell we observed that as the dipping of the lava delta decreases, the lava flows become more massive with occasional airfall tuff layers in between until the lava flows dominate the succession. The remains of surface lava flows are observed as broken up boulders of lava on the surface mixed partially into light-brownish glassy glacial deposits. This observation suggests that after the eruption and formation of Lambafell, the mountain was covered by glaciers.

Only one crater could be identified in the summit region (Figures 142 and 148). In the northeast quarry area occupied by Björgun and ÍAV, there is excellent exposure into the interior of the mountain (Figures 136-138). In the Björgun quarry, extremely steep dipping pillow lavas are observed to sink into wet fine-grained sediments made up of volcanic glass from Lambafell (Figure 137). In the eastern part of the quarry, occupied by ÍAV, the lava delta formation is dominating. In the center of this quarrying area there is an excellent cross-section through the mountain's core. Here we observe the lava delta formations covering the subglacial eruptive material (Figure 136). There is a silty horizon separating the main subglacial formation from the lava delta formation. This silty horizon coincides with the fine-grained sediments that the steeply dipping pillow breccia sinks into (Figure 136). The silty material and the fine-grained sediments are sedimented in a lake. Thus, indicating minimum depth of the glacial lake that Lambafell

erupted into and the onset of the effusive activity in the summit region. The outer extent of the lava delta, however, indicates the lake's extent from the crater area (Figure 148). From these data we can deduce that the lake, into which Lambafell was deposited, extended to the east in accordance with the general slope of the land in the area.

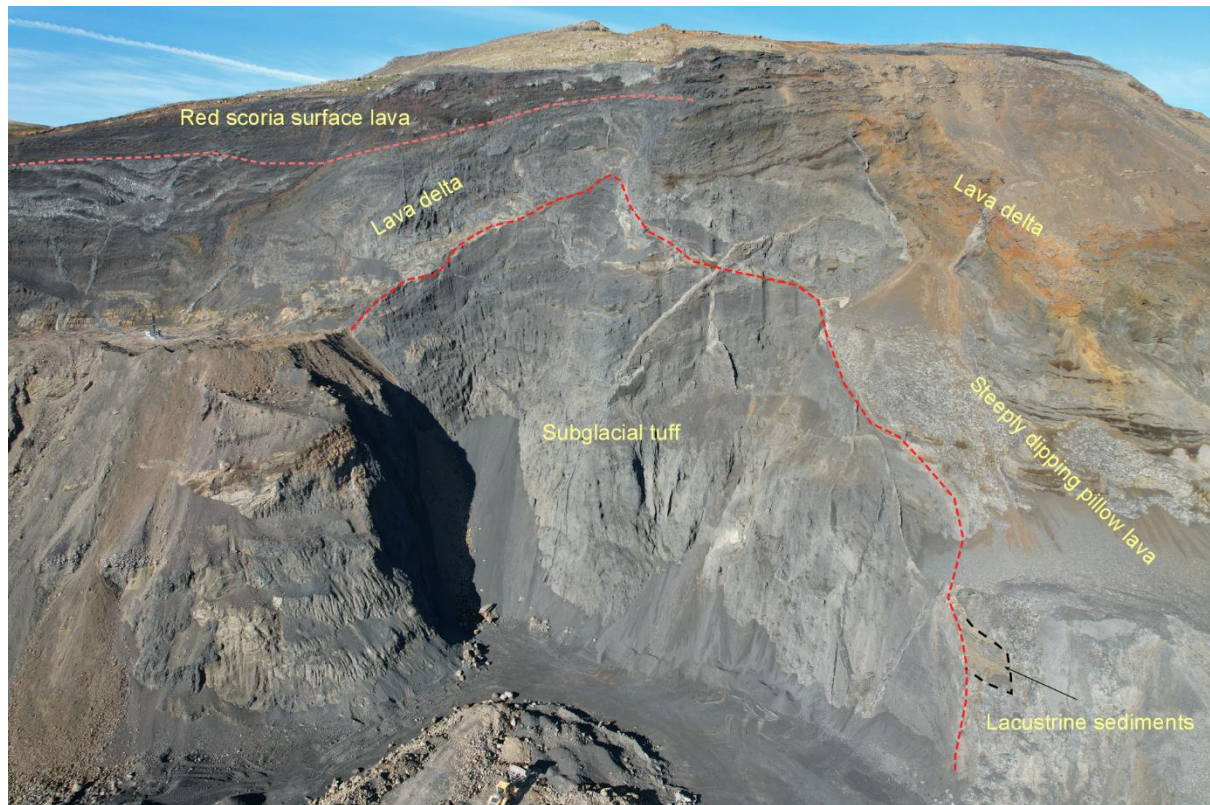


Figure 136 A view toward the SW, the main quarrying area of Lambafell. The core of the mountain is made of subglacial tuff (red dashed line). The core is covered by lava delta, which dipping becomes progressively less steep as it approaches the top of the mountain. At the base, lacustrine sediments are observed. Pillow lava has penetrated the sediments. Numerous dikes are observed cutting through the massive. Atop the lava delta, lavas with red scoria are dominating (pink dashed line), suggesting that the eruptive edifice has grown out of the glacial lake. Note that figure 138 has a view more to the west. This photo was taken on August 25, 2023, at the boundary of Björgun and ÍAV quarries and does not represent the present appearance of the quarries.



Figure 137 Steeply dipping pillow breccia that is sinking into wet sediments at the base of Björgun quarry area. These photos were taken August 26, 2023, so this may not represent the present appearance of the quarry.

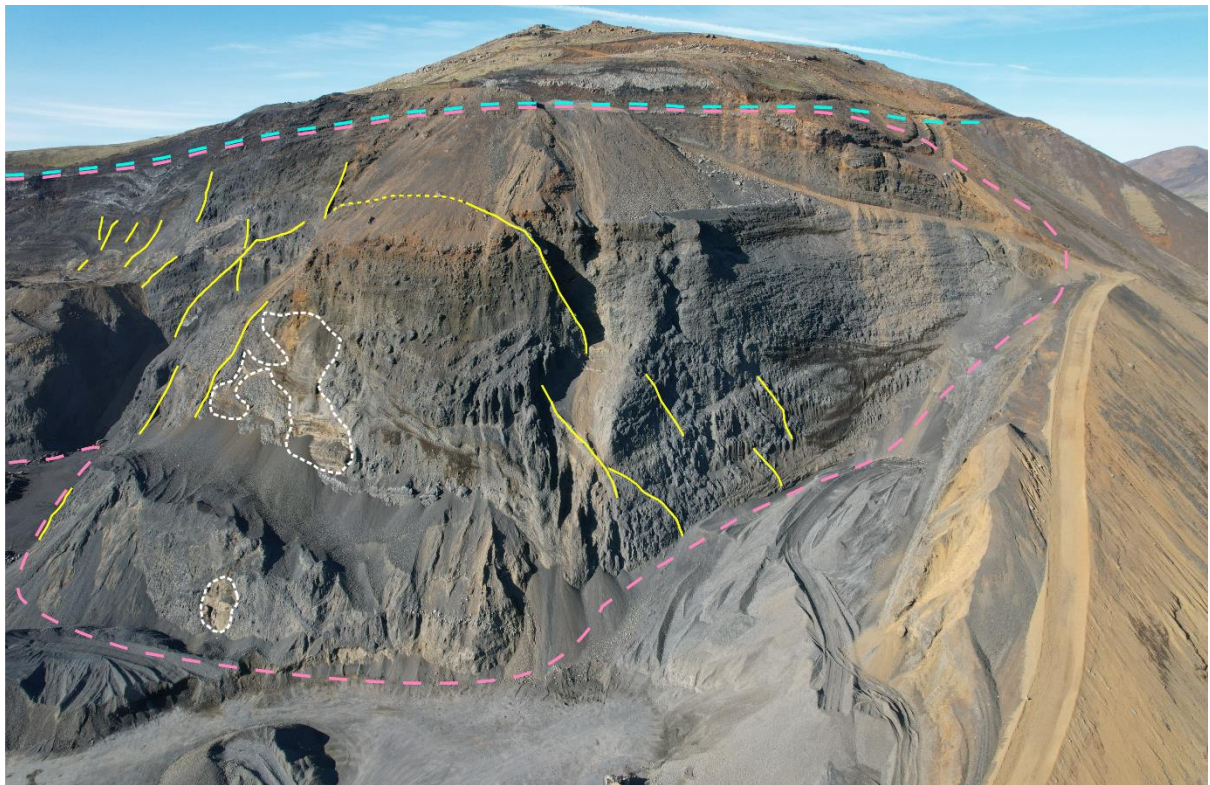


Figure 138 A drone image of the Björgun quarry in Lambafell. The cyan dashed line at to top depicts where subaerial lavas are visible at the surface. The pink dashed lines depict the flow foot breccia of Lambafell. Some individual pillows are present here. The white dashed lines inside this section depict areas of layered volcanic glass. The yellow lines mark dikes (intrusions) visible at the quarry face. In the top right corner of the photo the volcanic glass of the west side is visible. This photo was taken on August 25, 2023, so this does not represent the present appearance of the quarry.

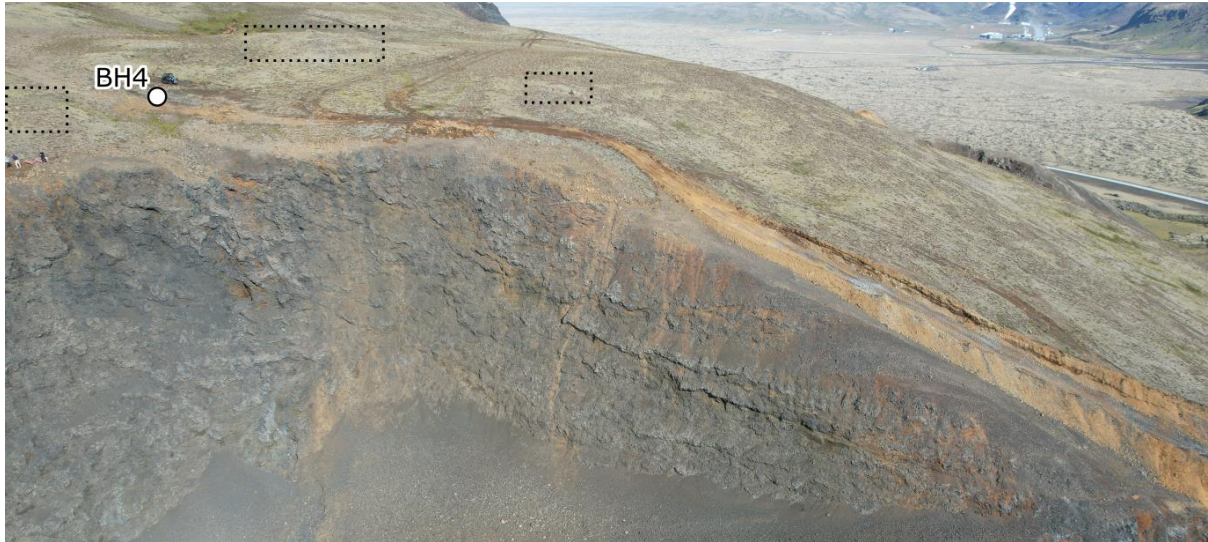


Figure 139 A drone image of the Eden quarry with a view towards the NNE. Visible in the quarry walls is the dipping lava delta that flowed from the summit of Lambafell. Marked with a white dot is the BH4 borehole (Figure 141). The dotted line rectangles represent areas where lava is visible on the surface.



Figure 140 A drone image of the Eden quarry with a view of the quarry's face. The white dashed line represents a horizon where glassy turbidity currents are interbedded with the pillow lava breccia. Representing the time the eruption is growing out of the lake and alternating between explosive and effusive activity. This photo was taken on May 4, 2022, and does not represent the present appearance of the quarry.



Figure 141 A drone image of the west side of Lambafell. The colors correspond to Figure 138. Here, the flow foot breccia is very minimal. The arrows depict the estimated direction of flow at the units' formation. The light brown to reddish brown areas on the surface is areas of palagonitization, the volcanic glass is otherwise black. The white dashed line demarcates the Svínahraunsbruni lava of 1000 AD that surrounds the majority of Lambafell.

Cross sections through Lambafell

Three boreholes were made on the eastern slopes of Lambafell, boreholes BH4, BH5, and BH6 (Figure 142). They range in depth and are 87 m, 51 m, and 60 m, respectively (Tables 1-3). Only BH5 penetrated the pillow breccia that makes up the lava delta and into the main subglacial tuff (hyaloclastite) at the depth of about 12-15 m.

Simplified schematics of five profiles (Figure 142), one through each of the boreholes and one through each of the two quarries, Björgun and Eden, can be seen in Figures 143 to 147. Geological observation in the Björgun and ÍAV quarry area indicates that the subglacial tuff, representing the subglacial phase of the eruption, is very steep sided and should be relatively symmetrical in form during that phase. Further supported by the outcrops in the quarry area (Figures 136-141). Thus, in defining where the contact between the subglacial phase and the pillow breccia is, we use the topographic profile on the west side of Lambafell to define the plausible outlines of the contact under the pillow breccia in the east. The projection is in good agreement with the results from the boreholes and shown in the cross sections in Figures 143-147.

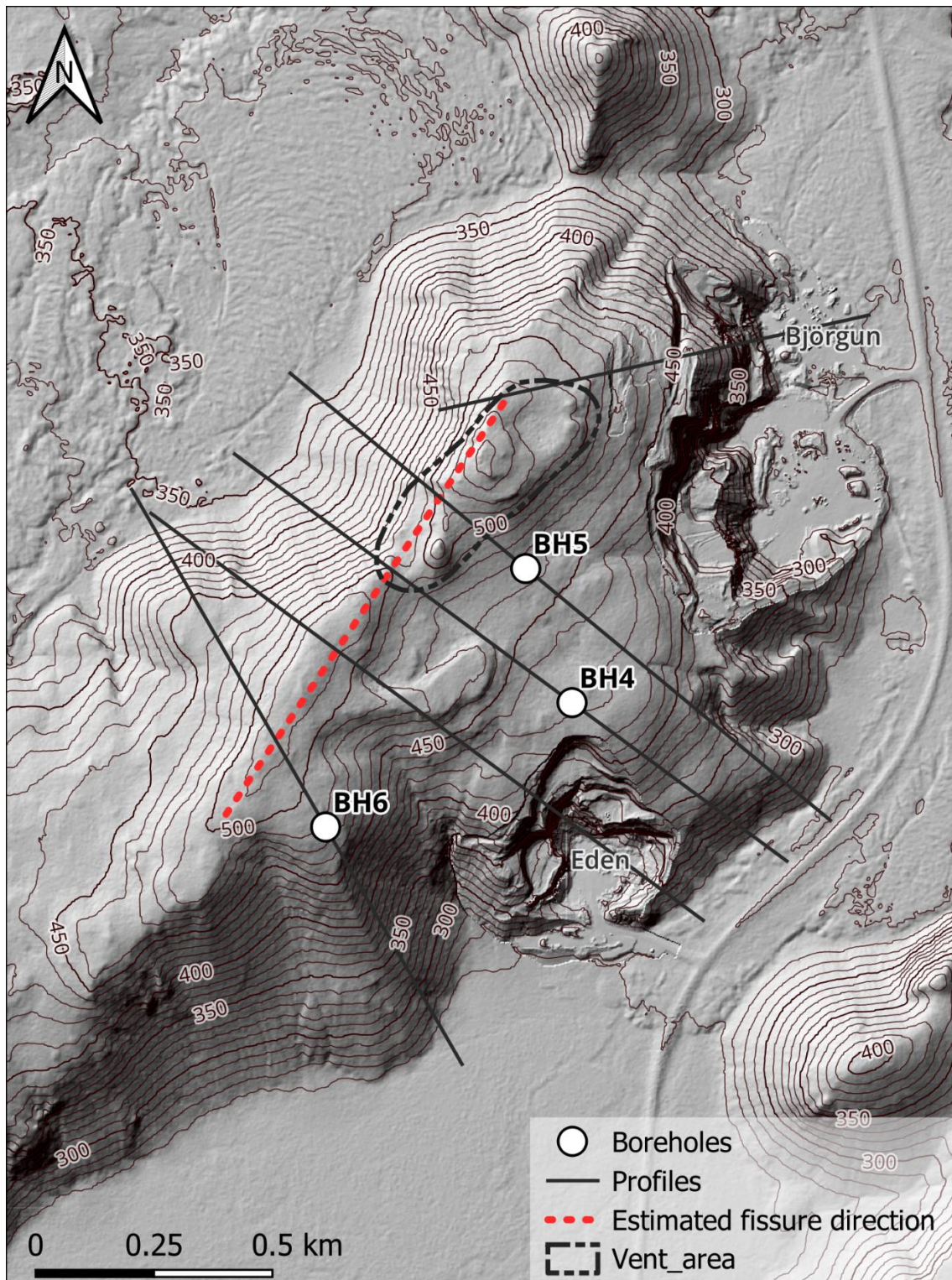


Figure 142 A map showing the three boreholes and their corresponding profiles (black lines). Included are profiles through the Björgun and Eden quarries. The DEM is sourced from Landmælingar Íslands and supplemented by our lidar data of the quarries (from summer 2022).

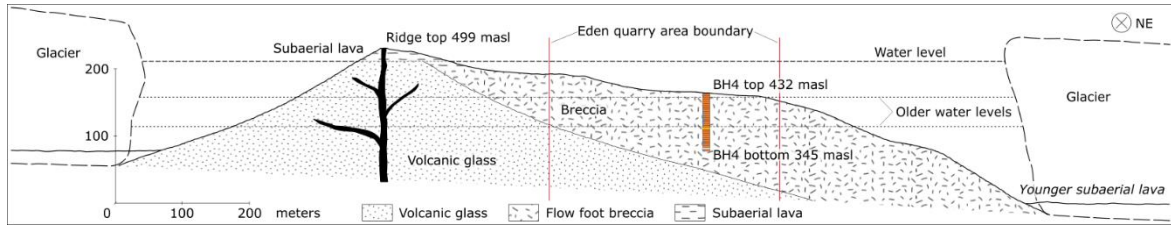


Figure 143 A schematic showing the theoretical internal structure of Lambafell through borehole BH4 (87 m deep), where the samples are almost only crystalline. The borehole samples show no evidence of crossing the hyaloclastite-breccia boundary and that is depicted in the schematic. The topographic profile and borehole are to scale.

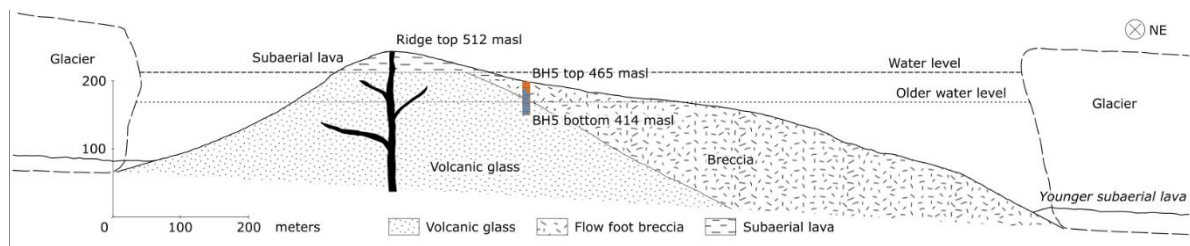


Figure 144 A schematic showing the theoretical internal structure of Lambafell through borehole BH5 (51 m deep). The samples in this borehole are glassy overall with mostly crystalline samples only in the top third or fourth of the borehole. This is taken to represent the boundary between the flow foot breccia (crystalline) and the volcanic glass (hyaloclastite). The topographic profile and borehole are to scale.

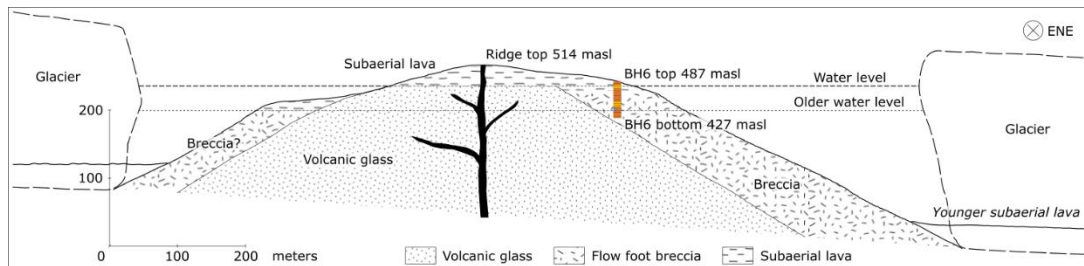


Figure 145 A schematic showing the theoretical internal structure of Lambafell through borehole BH6 (60 m deep), which is even more crystalline than BH4. Red oxidized samples throughout the borehole confirm that the borehole is situated entirely within the flow foot breccia. The topographic profile and borehole are to scale.

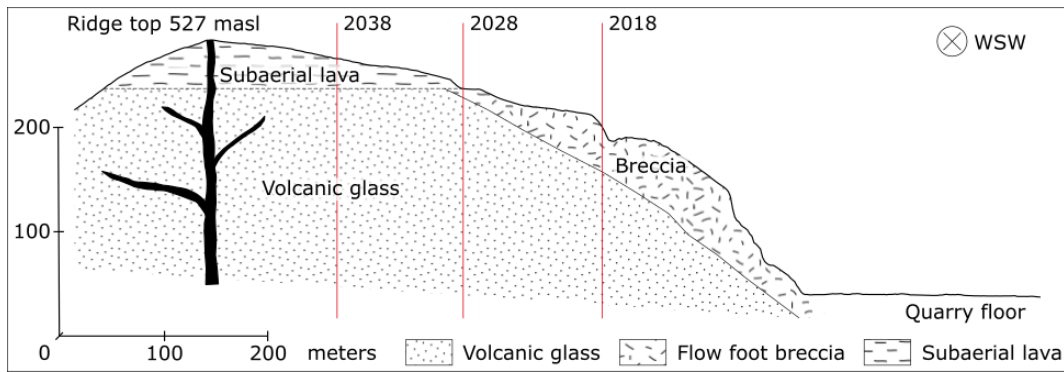


Figure 146 A schematic showing the theoretical internal structure of Lambafell through the Björgun quarry (taken from a DEM from the summer of 2022). Clearly, a large amount of the flow foot breccia has been excavated but it would have had a similar extent to those presented in the other schematics. However, some hyaloclastite is visible in the Björgun and ÍAV quarries (Figures 136-138). Presented are excavation estimates for the years 2018, 2028, and 2038 which are visible on the geological map below. The topographic profile is to scale.

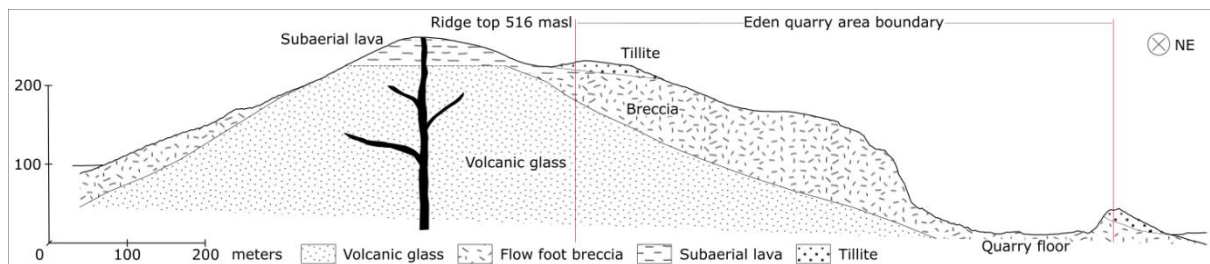


Figure 147 A schematic showing the theoretical internal structure of Lambafell through the Eden quarry (taken from a DEM from the summer of 2022). Some of the flow foot breccia has been excavated but no proper hyaloclastite formation is present in the quarry face yet. However, there are some glass sections present in the quarry that indicate that the proper volcanic glass formation is close (Figure 140). The topographic profile is to scale.

The profiles shown above indicate that a large volume of the eastern and northern slopes of Lambafell are made up of flow foot breccia that makes up the lava delta, i.e., crystalline brecciated material. Thus, a large volume of the brecciated material would need to be excavated before quarrying of the subglacial glassy unit of Lambafell's interior could begin.

Ground Penetrating Radar

In the summer of 2023, a ground penetrating radar (GPR) was applied to define the internal stratigraphy of different geological units making up Lambafell. Under normal

circumstances, the paired 100 MHz antenna used has good resolution down to about 60-70 m depth. However, an electric disturbance was present when the GPR was used in Lambafell which affected the instrument and data collected. Therefore, no radargrams are presented in this report. The plausible cause for the electric disturbance is the use of VHF radios in the quarries or bad grounding of the electric generators used for electricity production in the quarry area.

Geological map of Lambafell

Based on our observations, a new geological map is presented here (Figure 148). It is focused on the two quarries active in Lambafell. The geology of the mountain is formed by the fact that Lambafell is formed in a single eruption that began under an ice sheet. From our investigation the glacier ice in the area, at the time of eruption, was not more than 150-200 m thick. The main subglacial phase formed in this eruption can be observed in the northwestern slopes of Lambafell and it is starting to outcrop in the northern Björgun quarry. Eastern and the northeastern part of Lambafell is on the other hand made up of delta forming pillow lava breccia. The pillow breccia is interbedded at the base with subglacial hyaloclastite turbidity deposits. On top of the delta forming deposits, lava flows become dominant, with occasional interbedded layers of subaerial tuff rich deposits. Post eruptive deposits are observed sporadically, at the slopes and in the summit area. These deposits are made up of the same material as was erupted in the Lambafell eruption but have been transported by the glacier after the eruption ended. These deposits are characterized by brownish fine grained palagonite rich material with matrix supporting larger blocks of lava and pillow fragments. The delta forming flow foot breccia has by far the largest surface area out of the three main geological units that make up the mountain. However, the subglacial hyaloclastite makes up most of the mountain's volume.

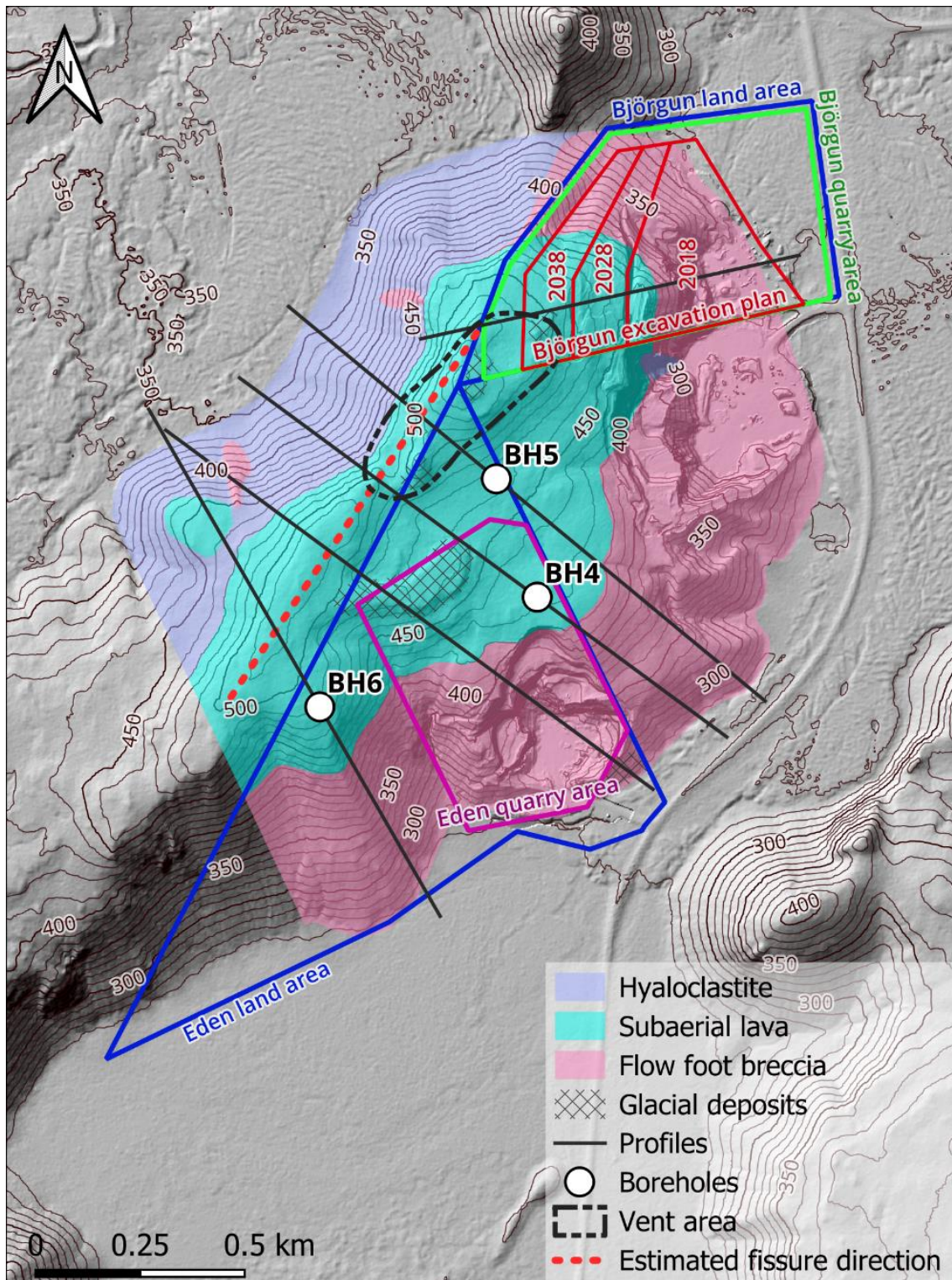


Figure 148 A geological map of the studied area of Lambafell. The purple area represents subglacial hyaloclastite (note a small area south of the Björgun quarry), pink represents flow foot breccia, and cyan represents subaerial lavas. Note the subaerial lava inside the hyaloclastite area. The hatched areas denote glacial deposits on the surface. Eden and Björgun quarrying areas are represented by labelled polygons of different colors. The DEM and contours are sourced from Landmælingar Íslands but supplemented by our lidar data of the quarries (from summer 2022).

7 Volume estimates of geological units in Lambafell

The volume of each geological unit in the studied area in Lambafell (Figure 146) was estimated from a combination of topographic modelling and interpretation of borehole samples supported by theoretical schematics of the mountain's inner stratigraphy.

Lambafell is surrounded by lava emplaced during at least three eruptions from the past 5200 years (Leitahraun, c. 5200 BP; Nesjahraun, c. 2000 BP; and Svínahraunsbruni, 1000 AD; Jónsson, 1978, Sæmundsson et al., 2016). The result of this is that the base of the mountain on the west side is at an elevation of around 400 masl whilst the southeast side is at around 250 masl. As a result of this, to measure the volume of the mountain a horizontal plane at an elevation of 253 masl was used. When measuring volumes restricted to the areas of the Björgun and Eden quarries, the quarry floors were used as the basal plane (283 and 269 masl respectively).

The volume of the studied area of Lambafell is 301 million m³ (Table 4). The volume of hyaloclastite within this area is 209 million m³. The lava and breccia (crystalline units) have a combined volume of 92 million m³ and the tillite a volume of 0.2 million m³. Figure 147 shows the configuration of the hyaloclastite under the cover of lava and flow foot breccia making up the delta.

The Eden quarry basal surface was set at 269 masl which gives the total volume of 31 million m³ when using our lidar model from the summer of 2022. The hyaloclastite within the area was calculated to be 12 million m³, the lava and breccia have a combined volume of 19 million m³, and the tillite has a volume of 0.1 million m³.

Based on our lidar model from summer 2022 and a basal surface of 283 masl, the Björgun quarry has a total volume of 28 million m³. Of that area, the excavation estimate area for the year 2018 has a volume of 5 million m³, the estimate area for 2028 has a volume of 7 million m³, and for 2038 the calculated volume is 9 million m³. The total hyaloclastite volume for the Björgun quarry is 21 million m³, and the 2018, 2028, and 2038 estimates have hyaloclastite volumes of 2, 5, and 8 million m³, respectively. The total volume of lava and breccia for the Björgun quarry is 6 million m³, and the 2018, 2028, and 2038 estimates have volumes of 3, 2, and 1 million m³, respectively. The tillite volumes are negligible. These results are best viewed in Table 4.

Table 4 Estimated volume of the geological units of Lambafell and the quarries therein.

	Volume (million m ³)					
	Studied area of Lambafell 253 masl base	Eden quarry 269 masl base	Björgun quarry 283 masl base	Björgun 2018 283 masl base	Björgun 2028 283 masl base	Björgun 2038 283 masl base
<i>Total</i>	301	31	28	5	7	9
<i>Hyaloclastite</i>	209	12	21	2	5	8
<i>Lava and breccia</i>	92	19	6	3	2	1
<i>Tillite</i>	0.2	0.1	0.0	0.0	0.0	0.0

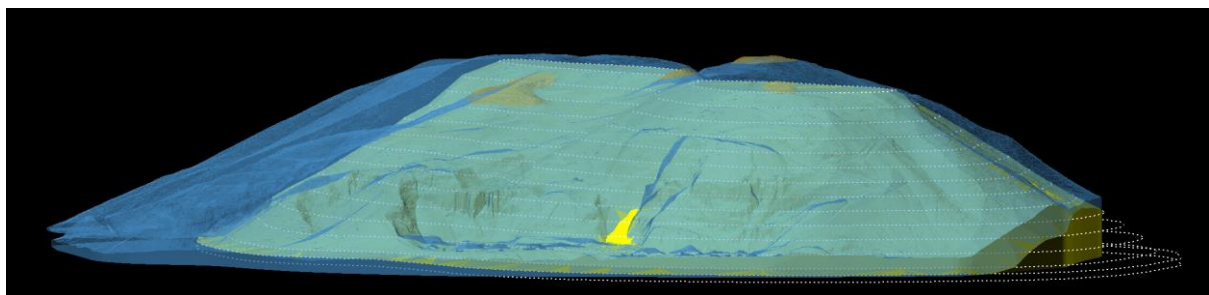


Figure 149 A view of the 3D model in Maptek Vulcan looking to the southwest showing the internal hyaloclastite model and contours. In front is the Björgun quarry. Note the small section of hyaloclastite (yellow) that is visible in the quarry.

8 Discussion and summary of results

The Lambafell mountain is formed in an eruption that began underneath a glacier during the latter stage of the Weichselian glaciation. Although the eruption might have begun along a short fissure, activity focused on one single vent. Remains of this vent are still detectable in the summit area of the mountain. Many dikes and dikelets with varying dip and strike, observed in the mountain's mining sections, manifest stress variations in the eruptive pile during eruption. Erupted material is piled up within a vault melted by the erupted magma inside the glacier. At the time of the eruption, the land's slope is towards the east and thus meltwater ponds towards the east of the melting vault, and the lake grows towards the east once the eruption reaches out of the glacier. Once the eruption becomes effusive and lava forms, the lava follows the same general slope in the land and flows into the intraglacial lake forming a delta of steeply dipping pillow lavas (flow foot breccia). Gradual decrease in the dipping of the pillow lava towards the surface represents the filling up of this intra glacial lake. At the time of the eruption, the glacier could not have been much thicker than about 150 m. This can be seen by the intersection of the low dipping lava and the steep dipping pillow breccia. The existence of the silty layer and the wet sediments in Björgun quarry represents the time when the eruption grew out of the water and the time that stirring of the lake water stopped, thus enabling the sedimentation of particles in suspension in the lake.

Aside from alteration observed within sections exposed to the elements from the time of glacier retreat, alteration is observed in the samples collected during the drilling of the three holes, BH4, BH5 and BH6. The alteration in the borehole samples is of two types. Firstly, alteration due to cooling of dikes and dikelets within the eruptive pile is commonly associated with the precipitation of calcite (hole BH5). And secondly, due to lava oxidation above the lake level, represented by red oxidized grains (hole BH6).

In summation, the geological mapping of the studied area of Lambafell reveals that a thick unit of flow foot breccia and lava covers the entire north, east and southeast sides of the mountain (Figure 146). This means that a large volume of crystalline material would need to be excavated before reaching the subglacial hyaloclastite tuff. However, on the west side, the mountain is almost entirely made up of subglacial hyaloclastite tuff since that side is uphill in the land.

Furthermore, mapping of the currently quarried areas reveals that large volumes of lava and pillow breccia make up the material being quarried. This is particularly important at the site of Eden quarry where 61% of the material to be quarried is made up of pillow lava breccia as defined in Figure 146 and Table 4.

Geological mapping of the Björgun quarry reveals, on the other hand, that quarrying has reached deeper into the mountain and subglacial hyaloclastite tuff is being

exposed. In the north face of Lambafell, mapping reveals that the lava and pillow lava breccia is not as massive and extends not as far away from the main subglacial tuff as on the Eden side. From our measurements up to present, the quarrying has been made up of about 61% of lava and pillow breccia. However, it has been difficult to separate the remaining subglacial hyaloclastite tuff from the brecciated material. Sectors defined in Figure 146 for future quarrying of the Björgun site indicate that the importance of the subglacial hyaloclastite tuff will steadily increase as the quarrying activity comes closer to the core of the mountain. Area to be quarried until 2028 is thus going to be made up of 71% subglacial hyaloclastite tuff and 29% lava and pillow lava breccia. The brecciated material being on top of the subglacial hyaloclastite tuff. The area to be quarried between 2028 and 2038 is on the other hand going to be made up of around 88% subglacial hyaloclastite tuff and about 12% lava and pillow breccia.

Quarrying strategy to maximize the yield of the subglacial hyaloclastite tuff in the Björgun quarry should be rethought. Since the lava and pillow lava breccia is set in place after the main subglacial eruptive phase, it is always on top of the subglacial hyaloclastite tuff. This suggests that before quarrying the subglacial hyaloclastite tuff, the lava and pillow lava breccia should be quarried out in the quarry. That would mean that about 3 million m³ of lava and pillow lava breccia would be excavated, leaving behind about 13 million m³ of subglacial hyaloclastite tuff. This strategy would mean that the sectors 2028 and sector 2038 would be mined at the same time for the lava and pillow lava breccia. Timing here would depend on the total volume mined in the Björgun quarry every year. This data we do not have at present and thus would be work worth doing in future analysis of the Björgun quarry.

References

- Allen, C. C. (1980). Icelandic Subglacial Volcanism: Thermal and Physical Studies. *The Journal of Geology*, 88(1), 108–117. <http://www.jstor.org/stable/30068485>
- Baker, P. E. (1969). A volcano erupts beneath the Antarctic ice. *Geographical Magazine*, 42 (2). 115-126.
- Barja, A. (2012). *Myndun Lambafells*. [Bachelor's thesis, University of Iceland]. Skemman. <http://hdl.handle.net/1946/10800>
- Best, J. L. (1992). Sedimentology and event timing of a catastrophic volcanoclastic mass flow, Volcan Hudson, Southern Chile. *Bulletin of Volcanology*, 54(4), 299-318. <https://doi.org/10.1007/BF00301484>
- Carlslaw H. S. (1959). *Conduction of heat in solids* (2d ed.). Clarendon Press.
- Geophysical Survey Systems, Inc. (2017). 100 MHz antenna: Model 3207. In *Antennas manual* (pp. 45-56).
- Geophysical Survey Systems, Inc. (2018, June 12). *What is GPR: A brief description by GSSI*. <https://www.geophysical.com/whatisgpr>
- Gudmundsson, M. T., & Bjornsson, H. (1991). Eruptions in Grimsvotn, Vatnajokull, Iceland, 1934-1991. *Jokull*, 41, 21-45.
- Habert, G., Choupay, N., Montel, J. M., Guillaume, D., & Escadeillas, G. (2008). Effects of the secondary minerals of the natural pozzolans on their pozzolanic activity. *Cement and Concrete Research*, 38(7), 963–975. doi:10.1016/j.cemconres.2008.02.005
- Höskuldsson, A., & Sparks, R. S. J. (1997). Thermodynamics and fluid dynamics of effusive subglacial eruptions. *Bulletin of Volcanology*, 59(3), 219-230. <https://doi.org/10.1007/s004450050187>
- Höskuldsson, Á., Hey, R., Kjartansson, E., & Guðmundsson, G. B. (2007). The Reykjanes Ridge between 63°10'N and Iceland. *Journal of Geodynamics*, 43(1), 73-86. <https://doi.org/https://doi.org/10.1016/j.jog.2006.09.003>
- Jones, J. G. (1969). Pillow lavas as depth indicators. *American Journal of Science*, 267(2), 181–195. <https://doi.org/10.2475/ajs.267.2.181>
- Jones, J. G. (1970). Intraglacial Volcanoes of the Laugarvatn Region, Southwest Iceland, II. *The Journal of Geology*, 78(2), 127–140. <http://www.jstor.org/stable/30063783>

- Jónsdóttir Blöndal, B. D. (2022). *Geological mapping of Litla Sandfell: a glaciovolcanic eruption*. [Bachelor's thesis, University of Iceland]. Skemman. <http://hdl.handle.net/1946/41337>
- Jónsson, J. (1971). Hraun í nágrenni Reykjavíkur. I. Leitahraun. *Náttúrufræðingurinn* 41(2): 49–63.
- Kjartansson, G. (1943). Geology of Árnessýsla. *Árnesingasaga I*, 1–250.
- Leica Microsystems. (n.d.). *DVM6 digital microscope*. <https://www.leica-microsystems.com/products/digital-microscopes/p/leica-dvm6/>
- Major, J. J., & Newhall, C. G. (1989). Snow and ice perturbation during historical volcanic eruptions and the formation of lahars and floods - A global review [Review]. *Bulletin of Volcanology*, 52(1), 1-27. <https://doi.org/10.1007/BF00641384>
- Moore, J. G., & Calk, L. C. (1991). Degassing and differentiation in subglacial volcanoes, Iceland. *Journal of Volcanology and Geothermal Research*, 46(1), 157-180. [https://doi.org/https://doi.org/10.1016/0377-0273\(91\)90081-A](https://doi.org/https://doi.org/10.1016/0377-0273(91)90081-A)
- Noe-Nygaard, A. (1940). Sub-glacial volcanic activity in ancient and recent times (studies in the palagonite system of Iceland, no. 1) [Article]. *Folia Geographica Danica*, 1(2), 1-67. <https://www.scopus.com/inward/record.uri?eid=2-s2.0-0002450790&partnerID=40&md5=bd0630c65a3f2b76c65e9374b30d2f3b>
- Pjetursson, H. (1900). The glacial palagonite-formation of Iceland. *Scottish Geographical Magazine*, 16(5), 265-293. <https://doi.org/10.1080/00369220008733153>
- Sigvaldason, G. E. (1968). Structure and products of subaquatic volcanoes in Iceland. *Contributions to Mineralogy and Petrology*, 18(1), 1–16. <https://doi.org/10.1007/BF00371983>
- SOLOMON, M. (1969). The nature and possible origin of the pillow lavas and hyaloclastite breccias of King Island, Australia. *Quarterly Journal of the Geological Society of London*, 124(1-4), 153-168. <https://doi.org/doi:10.1144/gsjgs.124.1.0153>
- Sæmundsson, K. (1970). Interglacial lava flows in the lowlands of southern Iceland and the problem of two-tiered columnar jointing. *Jökull* 20:62-77
- Sæmundsson, K., Sigurgeirsson, M. Á., Hjartarson, Á., Kaldal, I., Kristinsson, S. G., & Víkingsson, S. (2016). Geological map of the Reykjanes Peninsula (2nd ed.) [Geological]. Íslenskar Orkuránsóknir.
- Thorarinsson, S. (1974). *Vötnin stríð. Saga Skeiðarárhlaupa og Grímsvatnagosa (in Icelandic)*. Bókaútgáfa Menningarsjóðs, Reykjavík.

Thorarinsson, S. (1975). Katla og annáll Kötlugosa (in Icelandic). *Árbók Ferðafélags Íslands 1975*, 125-149.

Thordarson, T., & Hoskuldsson, A. (2008). Postglacial volcanism in Iceland. *Jökull*, 58. <https://doi.org/10.33799/jokull2008.58.197>

Appendix

Drill logs

A drill log from borehole 4 (BH4) in Lambafell is presented in Table 4. BH4 location is at 64.01370743766155°N, -21.46469165380078°W, 432 masl.

Table 5 Drill log from BH4 in Lambafell. Descriptions of the borehole material and additional comments of the samples and drilling conditions.

Sample	Depth (m)	Description of sample	Comments
BH4-1	0-3	Sample taken from 2-3 m. Topsoil and some rock and sandy-like material.	Dry sample.
BH4-2	3-6	Breccia, dark gray, low vesicularity, and loose material.	Dry sample, fairly dense but more loose in the end.
BH4-3	6-9	Similar but lighter color and more clay-like texture (light gray).	Dry sample, fluctuating dense and loose throughout.
BH4-4	9-12	Same as BH4-2, fine material coating the clasts, making them look rounded.	Dry sample.
BH4-5	12-15	Same.	Sample A wet, B + C dry. More difficulty drilling with longer exhaust tube.
BH4-6	15-18	Same.	Wet samples.
BH4-7	18-21	Looks the same.	A bit hard for the first 1.5 m, then better. Wet samples.
BH4-8	21-24	Same.	Wet samples.
BH4-9	24-27	Very similar, bigger pieces of rock, if anything. No coating on clasts, dark gray.	Not hard to drill but difficult to rinse material out of hole. Wet samples.
BH4-10	27-30	Similar but more of rocks than before.	Lost a part of sample because air pressure blew over two sample buckets, but there was enough left for each sample bag. Easier to drill than hole before. Wet samples.
BH4-11	30-33	Same but sample B had more dirty run-off water, thus more fines.	Wet samples.
BH4-12	33-36	Sample B had less clasts and C had more fines from dirty water. Sample A was rinsed of fines from excess water in bucket, otherwise similar to other samples.	Wet samples.
BH4-13	36-39	Again, sample B with less clasts, sample A rinsed a little of fines due to excess water in bucket, otherwise same. Sample C seemed to have more clasts than A and B.	Wet samples.
BH4-14	39-42	Coarser - more rocks, less fines (tuff).	Wet samples.
BH4-15	42-45	Coarser - more rocks, less fines (tuff).	Wet samples.
BH4-16	45-48	Same.	Wet samples.

BH4-17	48-51	Sample A similar. Sample B much coarser and muddy -> lava. Sample C same as B w/o mud -> lava.	Wet samples. Hard to drill.
BH4-18	51-54	Soft sandy sample w. some brown bits (first 50 cm).	Technical difficulties after ~50 cm, continuing later.
		Brown tuff for the rest.	Different drilling technique, no welded pipes. Wet drilling.
BH4-19	54-57	Samples A and B. A is brown tuff. B seems to have bigger grains, dark gray, some red grains.	Wet drilling.
BH4-20	57-60	Similar to sample BH4-19 B but finer. No obvious red grains.	Wet drilling.
BH4-21	60-63	Same.	Wet.
BH4-22	63-66	Same.	Wet.
BH4-23	66-69	Sample A brown and dark gray material in a mix, brown first. Sample B dark gray with some clasts ~4-5 cm.	Wet. Probably hit void space or softer material.
BH4-24	69-72	Brown muddy water ran off all samples. Samples A and C had clasts ~4-6 cm, sample B had smaller and some red grains.	Wet. Possibly looser material, so very fast drilling.
BH4-25	72-75	Brown run-off from A and C. A is probably some leftovers from prior drilling section, so very similar to last. B is scoria-like w/o big clasts. C is very similar to B but also has some bigger clasts.	Wet. Easy drilling.
BH4-26	75-78	Sample A w/o soap, very small sample. Sample B w. soap, a little bigger sample.	Very difficult to get material out of hole. Addition of soap helped.
BH4-27	78-81	Scoria-like samples, fairly homogeneous, some bigger clasts.	No addition of soap but still contaminated with soap.
BH4-28	81-84	No samples.	Difficult to get material out. Soap added. Drill got stuck, no samples because of that.
BH4-29	84-87	Samples might be a mix of other materials in the hole. Sample A was finest, like coarse sand. Samples B and C got gradually coarser, i.e., like breccia, but similar matrix.	Still plenty of soap in hole. Samples taken but then hole flushed out.

A drill log from borehole 5 (BH5) in Lambafell is presented in Table 5. BH5 location is at 64.01621163331627°N, -21.466916376091053°W, 465 masl.

Table 6 Drill log from BH5 in Lambafell. Comments from the drilling supervisor about samples and drilling conditions (translated from Icelandic).

Sample	Depth (m)	Comments
BH5-1	0-3	Soil and rock.
BH5-2	3-6	Rock for about 1 m, then looser material.
BH5-3	6-9	Seems rather layered and loose.
BH5-4	9-12	Rock, lava.
BH5-5	12-15	Rock at 13.5 m, soft
BH5-6	15-18	Soft
BH5-7	18-21	Soft
BH5-8	21-24	Soft
BH5-9	24-27	Soft
BH5-10	27-30	Soft
BH5-11	30-33	Drill bit tore loose. Soft.
BH5-12	33-36	Soft and difficult to get sample.
BH5-13	36-39	Soft and difficult to get sample.
BH5-14	39-42	Soft and difficult to get sample.
BH5-15	42-45	Soft and difficult to get sample.
BH5-16	45-48	Soft and difficult to get sample.
BH5-17	48-51	Soft and difficult to get sample.

A drill log from borehole 6 (BH6) in Lambafell is presented in Table 6. BH6 location is at 64.0111705385087°N, -21.475108789932403°W, 487 masl.

Table 7 Drill log from BH6 in Lambafell. Comments from the drilling supervisor about samples and drilling conditions (translated from Icelandic).

Sample	Depth (m)	Comments
BH6-1	0-3	Rock at 30 cm. Hard
BH6-2	3-6	Gravel at 4 m.
BH6-3	6-9	Soft.
BH6-4	9-12	Soft.
BH6-5	12-15	Dissimilarly hard.
BH6-6	15-18	Dissimilarly hard.
BH6-7	18-21	Easy to go through but difficult to get samples.
BH6-8	21-24	Easy to go through but difficult to get samples.
BH6-9	24-27	Very soft, easy to go through.
BH6-10	27-30	Very soft, easy to go through.
BH6-11	30-31	Drill bit tore loose at 31 m, the pipe was loose; pushed it down to 33 m.
	31-33	Soft. Sand.
BH6-12	33-36	Soft.
BH6-13	36-39	Soft. Brown filings in the last meter.
BH6-14	39-42	Soft. Brown filings.
BH6-15	42-45	Soft. Brown filings.
BH6-16	45-48	Soft. Brown filings.
BH6-17	48-51	Harder.
BH6-18	51-54	Harder. Difficult to get samples.
BH6-19	54-57	Soft. 1 m crevice.
BH6-20	57-60	Soft. The drill fell down as drilling through air.